

**Surface Water and Groundwater Hydraulics, Exchange, and Transport during Simulated
Overbank Floods along a Third-Order Stream in Southwest Virginia**

Christopher R. Guth

Thesis submitted to the faculty of the Virginia Polytechnic Institute
and State University in partial fulfillment of the requirements for the
degree of

Master of Science
In
Environmental Engineering

Erich T. Hester, Chair
Durelle T. Scott
Mark A. Widdowson

April 30, 2014
Blacksburg, VA

Keywords: surface water-groundwater exchange, hydrologic connectivity, floodplain,
hydraulics, overbank flooding, stream restoration

Copyright © 2014 Christopher R. Guth

Surface Water and Groundwater Hydraulics, Exchange, and Transport during Simulated Overbank Floods along a Third-Order Stream in Southwest Virginia

Christopher R. Guth

Abstract

Restoring hydrologic connectivity between the channel and floodplain is a common practice in stream and river restoration. Floodplain hydrology and hydrogeology impact biogeochemical processing and potential nutrient removal, yet rigorous field evaluations of surface and groundwater flows during overbank floods are rare. We conducted five sets of experimental floods to mimic floodplain reconnection. Experimental floods entailed pumping stream water onto an existing floodplain swale, and were conducted throughout the year to capture seasonal variation. Each set of experimental floods entailed two replicate floods occurring on successive days to test the effect of varying antecedent moisture. Water levels and specific conductivity were measured in surface water, shallow soils, and deep soils, along with surface flow into and out of the floodplain. Total flood water storage increased as vegetation density increased and or antecedent moisture decreased. Hydrologic flow mechanisms were spatially and temporally heterogeneous in surface water, in groundwater, as well as in exchange between the two and appeared to coexist in small areas. Immediate propagation of hydrostatic pressure into deep soils was suggested at some locations. Preferential groundwater flow was suggested in locations where the pressure and electrical conductivity signals propagated too fast for bulk Darcy flow through porous media. Preferential flow was particularly obvious where the pressure signal bypassed an intermediate depth but was observed at a deeper depth. Bulk Darcy flow in combination with preferential flow was suggested at locations where the flood pressure and electrical conductivity signal propagated more slowly yet arrived too quickly to be described using Darcy's Law. Finally, other areas exhibited no transmission of pressure or conductivity signals, indicating a complete lack of groundwater flow. Antecedent moisture affected the flood pulse arrival time and in some cases vertical connectivity with deeper sediments while vegetation density altered surface water storage volume. Understanding the variety of exchange mechanisms and their spatial variability will help understand the observed variability of floodplain impacts on water quality, and ultimately improve the effectiveness of floodplain restoration in reducing excess nutrient in river basins.

Acknowledgements

I thank the National Science Foundation for support of my thesis research, under grant ENG-CBET-1066817. Views expressed in this thesis are those of the authors and not necessarily those of the NSF. I thank Laura Lehmann and Cully Hession for access to the equipment and resources at the Virginia Tech BSE StREAM Lab (<http://www.bse.vt.edu/site/streamlab>). I would also like to thank C. Nathan Jones for assistance with experimental setup and analysis and my research group for their substantial help and support. Lastly, I would like to thank my advisor Erich Hester and my committee members Durelle Scott and Mark Widdowson. All photographs of the experimental setup and experiment site conditions were taken by the co-authors of the journal article and are not to be used for any other purpose.

Attribution

Several colleagues aided in the writing and research leading to the completion of this thesis. A brief description of each of their contributions is included here.

Thesis Topic: Surface Water and Groundwater Hydraulics, Exchange, and Transport during Simulated Overbank Floods along a Third-Order Stream in Southwest Virginia

Erich T. Hester, PhD Assistant Professor in the Department of Civil and Environmental Engineering at Virginia Polytechnic and State University. Dr. Hester is a co-author on this paper and provided assistance using his experiences examining surface water-groundwater exchange in many environments.

Durelle T. Scott, PhD Assistant Professor in the Department of Biological Systems Engineering at Virginia Polytechnic and State University. Dr. Scott is a co-author on this thesis and provided assistance with the completion of this thesis using his knowledge of nutrient processing to better understand the implications of the flood hydraulics on floodplain nutrients.

C. Nathan Jones, PhD Candidate in the Department of Biological Systems Engineering at Virginia Polytechnic and State University. Nathan Jones is a co-author on this thesis and provided extensive help with the setup of the field site and knowledge of commonly implemented field techniques.

Table of Contents

Abstract	ii
Acknowledgements	iii
Attribution	iv
List of Figures	vii
List of Tables	x
List of Abbreviations	xi
1 Introduction.....	1
1.1 Literature Review.....	1
1.1.1 Natural Floodplain Functioning	1
1.1.2 Human Impacts.....	3
1.1.3 Restoration.....	4
1.2 Research Objectives	5
1.3 Organization of Thesis	6
1.4 References	6
2 Surface Water and Groundwater Hydraulics, Exchange, and Transport during Simulated Overbank Floods along a Third-Order Stream in Southwest Virginia	11
2.1 Introduction	12
2.1.1 Natural Floodplain Functioning	12
2.1.2 Human Impacts.....	13
2.1.3 Restoration.....	13
2.1.4 Purpose of Study.....	14
2.2 Methods	15
2.2.1 Site Description	15
2.2.2 Field Methods.....	15
2.2.3 Data Analysis.....	21
2.3 Results	25
2.3.1 Site Characteristics	25
2.3.2 Background Data Collected Throughout the Year	26
2.3.3 Data Collected During Experimental Floods	29
2.4 Discussion	37
2.4.1 Background Hydraulics	37
2.4.2 Spatial and Temporal Variation in Types of Vertical Connectivity	37
2.4.3 Seasonal Effects.....	40
2.4.4 Antecedent Moisture Effects	41
2.4.5 Implications of Heterogeneous Flow Mechanisms	42
2.4.6 Limitations of Study	43
2.5 Conclusions	44
2.6 Acknowledgements	45
2.7 References	45
3 Engineering Applications.....	52
Appendix A: Experiment Site Setup and Maintenance	55
A.1 Site Configuration	55
A.2 Piezometer Installation	55
A.3 Instrumentation.....	57
A.3.1 Soil Moisture Probes	57
A.3.2 Onset HOBO U20 Pressure Transducers.....	58

A.3.3 Solinst LTC Levellogger Junior	58
A.3.4 Instrument Configuration Along Flood Centerline	59
Appendix B: Additional (Complete) Data Not Included In Journal Article	61
B.1 Background Data Collected Throughout the Year	61
B.1.1 Surface Water and Groundwater Elevation	61
B.1.2 Electrical Conductivity in Surface Water and Groundwater	63
B.1.3 Temperature in Surface Water, Groundwater, and Soil.....	65
B.1.4 Soil Moisture Content.....	67
B.1.5. Rising Head Tests	68
B.2 Data Collected During Flood Experiments	72
B.2.1 Surface Water and Groundwater Levels Along Centerline	72
B.2.2 Groundwater Levels in Transverse Piezometers	72
B.2.3 Vertical Head Gradients.....	74
B.2.4 Horizontal Head Gradients	76
B.2.5 Soil Moisture Content.....	79
B.2.6 Electrical Conductivity in Surface Water and Groundwater	80
B.2.7 Water Temperature During Floods.....	85
B.2.8 Air Temperature During Floods	86
B.3 Data From Rising Head Tests.....	87
Appendix C: Supplemental Analyses Not Included in Journal Article	88
C.1 Site Characteristics	88
C.2 Storage of Flood Water.....	89

List of Figures

Figure 1: Layout of study location. We used ArcGIS to derive contour lines using survey data obtained during site setup. Dotted line represents the pipe network routing water from Stroubles Creek to the swale and the dashed line represents the approximate flood centerline.....	17
Figure 2: Soil cores extracted along site centerline	25
Figure 3: (a) Background surface water and groundwater levels measured at upgradient and downgradient piezometers (100 cm BGS), XS1-Center-Surface, XS1-Center-30 cm (piezometer 30 cm BGS) and XS1-Center-100 cm (piezometer 100 cm BGS) and (b) precipitation at study site from March 2013 through March 2014. Vertical dashed lines signify flood artificial flood events and the vertical solid line signifies the time when rising head tests were performed.	27
Figure 4: Background moisture content throughout floodplain. Data were not collected from XS1-R for the second half of the year due to malfunction of the data logger being used. ...	28
Figure 5: Inflow and outflow of surface water at flood site. Flow rates are shown for both days of each flood, although in some cases similar values make the lines overlap. Flume data were not recorded during the Winter flood due to a malfunction in the HOBO at that location.....	30
Figure 6: (a) Percent of total water applied to site which drained out of site following the end of each flood, (b) change in groundwater elevation normalized to change in surface water elevation at XS1 and XS2, (c) arrival time of flood pulse at parshall flume following the beginning of each flood, (d) the average lag time between surface water peak elevation and groundwater peak elevation being observed, and (e) total storage as a percent of flood water pumped onto the site during the first day of flooding.	31
Figure 7: Seasonal variation in floodplain vegetation.	32
Figure 8: Types of observed pressure responses resulting from the artificial flood events. These data showing the three types of pressure responses were recorded during the Spring flood with floods occurring on April 8, 2013 and April 9, 2013.	32
Figure 9: Percent saturation in shallow subsurface during Late Summer flood event. Soil moisture content at XS2 is representative to other soil moisture data collected during the Late Summer. These floods were completed on August 30, 2013 and August 31, 2013.	34
Figure 10: Moisture front at XS2 centerline during Late Summer and Fall floods.....	35
Figure 12: Observed responses in surface water and groundwater electrical conductivity during artificial flood events. Response type (a) was recorded during the Early Summer flood (June 29, 2013) and response types (b) and (c) were observed during the Late Summer flood where flooding began on August 30, 2013. Red vertical line signifies a flood event where a malfunction occurred and repeating the flood was necessary.....	36
Figure 12: Water level and SC normalized to peak values during Late Summer.....	39
Figure A-1: (a) Pump outlet structure used to disperse flow, (b) typical cross section construction method used throughout the site, and (c) site outflow point through 3" parshall flume.....	55
Figure A-2: Piezometer construction method used for all piezometers throughout the site. The screen length was kept constant at 10 cm with the screened interval being between 4 and 14 cm from the piezometer base for each piezometer constructed.	56

Figure A-3: Example of the method used to visually classify soils during the installation of piezometers 100 cm BGS.....	56
Figure A-4: (a) Decagon Devices 5TM soil moisture probes and (b) Decagon Devices GS3 soil moisture probes (<i>www.decagon.com</i> , used under fair use, 2014).....	57
Figure A-5: Campbell Scientific CR200 data logger used for each pair of soil moisture probes (left, <i>www.campbellsci.com</i> , used under fair use, 2014). The method for housing the data loggers at the site for the entire experiment duration while charging with solar panels (right).....	57
Figure A-6: Onset HOBO pressure transducer (<i>www.onsetcomp.com</i> , used under fair use, 2014).	58
Figure A-7: 3001 Solinst LTC Levelogger used throughout the floodplain (<i>www.solinst.com</i> , used under fair use, 2014).	58
Figure A-8: Instrumentation located at flood centerline locations.	60
Figure B-1: Background water elevations along centerline. Data recorded during times when measuring point on device was not submerged were omitted. Decreases in groundwater levels experienced on June 12, 2013 were a result of rising head tests being conducted. The sharp increases in groundwater levels in XS3-Center-30 cm and XS3-Center-100 cm that occur on July 3, 2013 are a result of an overbank storm event in which surface water levels increased to a stage that exceeded the TOC elevation.....	62
Figure B-2: Background electrical conductivity along centerline. Conditions in which the monitoring devices were not fully submerged in water were present occasionally over the deployment year for all probes. In these instances readings were altered resulting in either values of zero or values far greater than what would be expected and for this reason these outliers were removed.....	64
Figure B-3: Temperature recorded in surface water, soil 5 cm BGS, soil 10 cm BGS, groundwater 30 cm BGS, and groundwater 100 cm BGS at each cross section centerline location.....	66
Figure B-4: Percent saturation in shallow sediments for Spring and Early Summer floods. Variability in moisture probe measurements caused values exceeding 100% saturation to be calculated at some points when converting the probe output (volumetric moisture content) to percent saturation.....	67
Figure B-5: Results obtained from the initial rising head tests performed throughout the site using the Hvorslev method. Tests were started on June 12, 2013.	69
Figure B-6: Results obtained from the second set of rising head tests performed throughout the inundated using the Hvorslev method. Tests were started on March 8, 2014.	71
Figure B-7: Surface water and groundwater elevations recorded along the flow centerline during each flood	73
Figure B-8: Flood event water levels in in groundwater 30 cm BGS at the transverse piezometers.	74
Figure B-9: Vertical head gradients calculated along the floodplain centerline during each flood. Water elevations from the floodplain surface, 30 cm BGS (shallow), and 100 cm BGS (deep) were used in the calculation	75
Figure B-10: Horizontal head gradients calculated between piezometers of equivalent depth BGS between centerline locations.	77
Figure B-11: Floodplain piezometric surfaces created using pre-event water levels and water levels two hours after the flood began. The piezometric surface domain is bounded by XS3 (bottom) and XS1-L (top).	78

Figure B-12: Percent saturation in shallow subsurface during Late Summer flood event.	79
Figure B-13: Percent saturation in shallow subsurface during Fall flood event.	80
Figure B-14: Flood event electrical conductivity. The decrease in SC measured at XS2- Center-30 cm immediately preceding the first day of the Winter flood was due to changing logging intervals for the probe at that location. Lower water table elevations during the Fall flood prevented the measurement of SC in the shallow piezometer at XS3.	82
Figure B-15: Electrical conductivity measured in the bypass region.	83
Figure B-16: Centerline Aquatroll Data.	83
Figure B-17: Steady state residence time calculated by measuring the time required to observe the peak in electrical conductivity in surface water at XS3 following the pulse injection. Pump flow rates measured at the inlet are also included for comparison.	84
Figure B- 18: Water temperature recorded during flood events	85
Figure B-19: Air temperature recorded at the StREAM Lab weather station during floods.	86
Figure C-1: Floodplain elevation along the flow centerline.	88
Figure C-2: Percent of the time that each cross section centerline location was inundated over the course of the year.	88
Figure C-3: Aerial photo of the flood site showing changes in vegetation throughout our study site and showing that our site is likely an old meander bend of Stroubles Creek.	89
Figure C-4: Comparison of the recession constant calculated using the flow through flume following the second day of each flood (not including the Winter flood due to equipment malfunction) to the corresponding average pump flow rate.	90
Figure C-5: Total percent of flood water stored on the first day of flooding minus the total volume of flood water stored on the second day for each flood with the exception being the Winter flood when outlet flows were not measured.	91

List of Tables

Table 1: Details of pumping during simulated floods 19

Table 2: Hydraulic conductivity (K) results using the Hvorslev method in each of the piezometers located throughout the study site. 26

Table 3: Darcy travel times between surface and centerline piezometers. The average hydraulic conductivity was used from the two rising head tests performed at the site. The theoretical arrival times were compared to the actual arrival times calculated using the pressure data obtained from the first day of flooding during the Winter flood. 33

Table 4: SW-GW Vertical Connectivity Classifications 38

Table B-1: Temperature and SC that the groundwater approached during rising head tests compared to the surface water temperature and SC..... 87

List of Abbreviations

BGS	Below Ground Surface
EC	Electrical Conductivity
N ₂	Dinitrogen Gas
NO ₃ ⁻	Nitrate
PFP	Preferential Flow Path
SC	Specific Conductivity
TOC	Top of Casing

1 Introduction

1.1 Literature Review

1.1.1 Natural Floodplain Functioning

Hydrologic connectivity between a stream or river and adjacent floodplains (“floodplain connectivity”) can benefit water quality and ecosystem health [*Pringle, 2003; Ward, 1997*]. When coupled with natural variability in stream stage, inundation frequency, and floodplain temperature, floodplain connectivity can directly influence ecosystem biodiversity [*Poff et al., 1997; Tockner et al., 2000*]. This increase in diversity stems from the connection between landscape patches and biological processes that occur at different spatial and temporal scales [*Amoros and Bornette, 2002*]. Examples of the ecological benefits are pervasive throughout the literature and include the lateral exchange of organic matter and nutrients increasing aquatic and terrestrial productivity [*Junk et al., 1989*], changes in egg development rates of macroinvertebrates [*Knispel et al., 2006*] and changes in leaf decomposition rates on the floodplain surface [*Langhans and Tockner, 2006*].

The ecological benefits that exist due to floodplain inundation are largely dependent on flood duration and frequency. These characteristics are strongly influenced by watershed area, with larger watersheds typically having longer and more predictable flooding periods when compared to smaller watersheds [*Dunne, 1978*]. In addition to the ecological benefits listed above, floodplains can also act as a natural hotspot for nutrient removal. The relationships between surface water hydraulics during overbank floods in streams and water quality have been examined in great detail. Increasing sinuosity of a once channelized stream and/or reconnecting it to its floodplain can reduce the average surface water velocity and result in a net removal of nutrients [*Bukaveckas, 2007; Kronvang et al., 2007*]. Also, while floodplain topography can dictate surface water storage and mixing [*Mertes, 1997*], floodplain sediment properties can have a high degree of impact on surface water and groundwater flow characteristics as well as the exchange between both domains [*Doble et al., 2012; Helton et al., 2014; Krause and Bronstert, 2007*]. During analysis of the potential for nutrient removal in floodplain systems, the sources of surface water become very important due to varying concentrations of pollutants. Floodplain surface water can originate from local overland flow from an adjacent hillslope, direct precipitation, overbank flow and/or high water tables intersecting depressions in the ground surface [*Mertes, 1997*]. The contribution from each of these sources is largely dependent on the topographic conditions present. For example, ponding of direct precipitation and hillslope runoff would likely be minimal in flat environments while in environments where terrain is complex and topographic undulations are present there is greater potential for surface water storage. Although the correlation between surface water

hydraulics and water quality have been well documented, the methods in which seasonal variation and moisture conditions independently alter these processes are not yet as well understood.

Understanding controls on nutrient removal via biogeochemical reactions during overbank floods requires fully understanding floodplain groundwater flow paths [Helton *et al.*, 2012] and floodplains are often simplified to being homogeneous for the sake of simplicity or due to the lack of necessary data [Bates *et al.*, 2000; Krause *et al.*, 2007]. Floodplain groundwater hydraulics must be evaluated in response to both short term storm events and seasonal variations. For storms, the characteristics associated with groundwater recharge during overbank flood events have been evaluated extensively in different floodplain environments [Dahan *et al.*, 2008; Doble *et al.*, 2011a; Doble *et al.*, 2012]. The rate at which surface water infiltrates into the floodplain subsurface can be heavily impacted by low hydraulic conductivity sediments [Andersen, 2004; Doble *et al.*, 2011b; Jolly *et al.*, 1994] and local ponding on the floodplain surface [Jung *et al.*, 2004]. In addition, heterogeneity within the floodplain resulting from the presence of abandoned channels (or paleochannels), can increase the average hydraulic conductivity and therefore increase the infiltration and groundwater flow rates [Heeren *et al.*, 2010; Poole *et al.*, 2002]. Annual groundwater level changes can result from seasonal differences in precipitation and evapotranspiration. As stream stage increases during wet seasons, a reversal in hydraulic head gradient between riparian groundwater and the stream can occur resulting in groundwater elevation changes in the floodplain [Burt *et al.*, 2002; Jung *et al.*, 2004; Sawyer *et al.*, 2009]. This can also occur to some extent in areas without seasonal variations in precipitation. Increased evaporation in shallow sediments and transpiration by plants during the warm season can lead to a drop in floodplain groundwater elevation [Bear, 2012]. With the main sources of groundwater being lateral flow from an adjacent hillslope and/or vertical infiltration, this reversal in head gradient can alter water properties by changing the source location.

As channel stage fluctuates during a storm event, the groundwater response is often delayed with the main hydrologic flow mechanisms between the channel and bank being preferential flow and/or Darcy flow [Menichino *et al.*, 2014]. Darcy flow is laminar flow through a porous media where viscous forces dominate while preferential flow paths occur in localized areas where high K sediments or large void spaces are present. However, observed increases in pressure head that occur too quickly based on the hydraulic conductivity and travel distance (i.e. pressure waves, or kinematic waves) in response to an increase in stream stage have also been recorded at greater distances into the floodplain [Käser *et al.*, 2009; Vidon, 2012], although the mechanisms and associated impacts of this phenomenon are not well understood [Singh, 2002]. While the effects

of pressure waves propagating into the floodplain are not well known, there is no evidence of solute transfer in such cases. Fully understanding the mechanisms behind pressure waves is important because increasing groundwater levels can increase the soil moisture content in the vadose zone and potentially increase surface water infiltration rates [*Pirastru and Niedda, 2013*]. Fully understanding when and where particular transport mechanisms dominate in floodplain systems would help better characterize the hydraulics during overbank events.

Efforts to quantify the effect of moisture conditions on floodplain hydraulics have largely coincided with changes in season. Seasonal variations can bring significant changes in vegetative cover and evapotranspiration (ET) rates at the floodplain surface, although the magnitude of these changes is heavily dependent on geographic region. Water velocities during overbank events can be altered by the vegetation density and affect the residence time on the floodplain surface [*Luhar and Nepf, 2013*]. Not only are surface water residence times affected by the vegetation density, but infiltration rates in vegetated areas can be much greater than areas lacking vegetation [*Bramley et al., 2003*]. This increase in infiltration rate can have a direct impact on potential water quality benefits [*Nieber, 2000*] while the mechanism in which surface water is transported into the subsurface can impact nutrient removal rates [*Fuchs et al., 2009*] along with infiltration rates into shallow groundwater [*Heeren et al., 2010*]. Separating the effects associated with seasonal and moisture variations on SW-GW exchange during overbank storm events in hydrologically connected streams would lead to a better understanding of why floodplain hydraulic properties, and therefore biogeochemical processing, are highly variable.

1.1.2 Human Impacts

Alterations of the landscape have led to the deterioration of water quality and a loss of the natural flow regime in river systems [*Poff et al., 1997*]. Dam construction is common due to its potential for energy production although this regulates downstream flow rates and therefore decreases variability in discharge rates. Increases in impervious land cover coinciding with urbanization also affect the response in stream discharge to rainfall events. As impervious area increases and storm water managements systems such as storm sewers are implemented, rainfall is routed directly to local stream networks, reducing the potential for evapotranspiration and infiltration to occur [*Leopold, 1968; O'Driscoll et al., 2010*]. This often leads to a reduction in baseflow and increase in storm peak flow, although in some urban environments increases in baseflow have been recorded due to leakage from water infrastructure [*Lerner, 2002*].

Higher peak flow discharge during storms resulting from land use changes within a catchment area can increase stream instability and channel dimensions [Booth, 1990; Doll *et al.*, 2002; Graf, 1975] by increasing the streams capacity to carry sediment [Lane, 1955]. This degradation of the stream bank can therefore decrease hydrologic connectivity between the stream and floodplain and reduce the potential for the benefits listed above to occur [Craig *et al.*, 2008] and the extent of the hyporheic zone [Wondzell and Swanson, 1999]. As streams become deeply incised, sediment loads within the water column typically increase due to the reshaping of the channel profile and/or increases in subaerial processes on the exposed stream bank surface [Prosser *et al.*, 2000]. Particularly in the Mid-Atlantic region, the effect of this incision on channel depth and overbank flooding is often exacerbated by the construction of milldams between the 17th and 19th century which resulted in increased floodplain sedimentation and burial of natural wetlands [Walter and Merritts, 2008].

1.1.3 Restoration

In order to mitigate the degradation of streams, restoration practices are commonly implemented. Stream restoration is the act of returning a stream to its natural conditions and restoring stream functions [Hester and Gooseff, 2010; Landers, 2010; Simon *et al.*, 2011; Wohl *et al.*, 2005]. The most common goals when restoring streams in the United States are to improve water quality, alter riparian zones (i.e. riparian buffers), allow for improvement of aquatic habitat, allow unobstructed fish travel and migration, and increase bank stability [Bernhardt *et al.*, 2005]. Additionally, the attenuation of flood water during overbank events can also help in remediating downstream flooding by reducing the flood pulse [Sholtes and Doyle, 2010]. Restoring floodplain connectivity is therefore a common action taken due to its many potential benefits and has increased in frequency as the importance of lateral connectivity within a stream system became more evident [Boon, 1998]. This restored lateral connection is the main purpose for floodplain restoration with the idea that floodplain forest growth [Rood *et al.*, 2005], increased biodiversity [Pringle, 2003; Ward, 1997] and improved water quality [Klocker *et al.*, 2009] will all occur as a direct result of this action.

The potential benefits stemming from stream restoration are diverse, but of particular interest in the Chesapeake Bay watershed is the reduction of nutrient loads [USEPA, 2010]. Excess nutrients in river systems caused by excess fertilizer application and urbanization [Vitousek *et al.*, 1997] can lead to accelerated eutrophication in large water bodies, which results in the depletion of dissolved oxygen (DO) and the subsequent loss of ecosystem function. Rates of biogeochemical

processing, including denitrification, can be altered during exchange between surface water and groundwater (SW-GW exchange) beneath the channel [Moser *et al.*, 2003; Zarnetske *et al.*, 2011; Zarnetske *et al.*, 2012] through the induction of SW-GW exchange by installing in-stream structures such as weirs or J-hooks [Hester and Doyle, 2008]. Increased contact between stream water and both riparian zones [Mayer *et al.*, 2007; Osborne and Kovacic, 1993; Peter *et al.*, 2012] and floodplains [Harrison *et al.*, 2011; Klocker *et al.*, 2009; Roley *et al.*, 2012; Welte *et al.*, 2012] can also result in a net reduction of nutrient loads from increased contact with vegetation and redox conditions that encourage denitrification. Many studies label floodplains as being a nutrient sink either from sedimentation of phosphorus rich particulates [Kronvang *et al.*, 2007], uptake by terrestrial plants [Lewandowski and Nützmann, 2010] or biogeochemical reactions [Kaushal *et al.*, 2008]. However, many results show insignificant nutrient removal and at times show floodplains being a nutrient source [Noe and Hupp, 2007; Orr *et al.*, 2007; Valett *et al.*, 2005]. Despite a high degree of variability in nutrient cycling stemming from floodplain reconnection, new policies are awarding credits for reducing nutrient loads from these actions [Berg *et al.*, 2014]. Through a better understanding of the transport mechanisms of flood water during overbank flood events coupled with accepted knowledge regarding how these mechanisms affect solute transport we may be able to better comprehend why such variability exists.

1.2 Research Objectives

The objectives of this study were to characterize 1) surface water flow, 2) groundwater flow, and 3) the exchange between surface water and groundwater during simulated overbank flood events along a controlled floodplain reach of Stroubles Creek. We aimed to examine the effect of seasons and antecedent moisture conditions by conducting multiple simulated floods over the course of the year and conducting floods on consecutive days in each season. Our goal was to replicate natural conditions typical of an overbank event while not only having greater control over timing and inflow/outflow parameters, but also recording hydraulic parameters at a greater spatial and temporal scale than has been done in the past. In addition to times at which floods were conducted, data were recorded continuously over the course of one year to evaluate any effects the periodic application of surface water had on the natural seasonal variations in groundwater elevations. Hydraulic properties were determined by monitoring electrical conductivity (EC), temperature, pressure, inflow and outflow with a network of both surface and subsurface monitoring locations. By better understanding the hydraulics during overbank flood events, we

may be able to determine why such variability in nutrient retention exists in floodplain environments.

1.3 Organization of Thesis

This document is organized around a journal article that will be submitted for publication in *Hydrological Processes*. This article is located in Section 2 of this thesis. A summary of the engineering significance associated with this study is included in Section 3. Appendices are included at the end of the document and include additional data and experiment methodology used for this research.

1.4 References

- Amoros, C., and G. Bornette (2002), Connectivity and biocomplexity in waterbodies of riverine floodplains, *Freshw. Biol.*, 47(4), 761-776.
- Andersen, H. E. (2004), Hydrology and nitrogen balance of a seasonally inundated Danish floodplain wetland, *Hydrological Processes*, 18(3), 415-434.
- Bates, P. D., M. D. Stewart, A. Desitter, M. G. Anderson, J. P. Renaud, and J. A. Smith (2000), Numerical simulation of floodplain hydrology, *Water Resources Research*, 36(9), 2517-2529.
- Bear, J. (2012), *Hydraulics of groundwater*, Courier Dover Publications.
- Berg, J., J. Burch, D. Cappuccitti, S. Filoso, L. Fraley-McNeal, D. Goerman, N. Hardman, S. Kaushal, D. Medina, and M. Meyers (2014), Recommendations of the Expert Panel to Define Removal Rates for Individual Stream Restoration Projects *Rep.*
- Bernhardt, E. S., et al. (2005), Ecology - Synthesizing US river restoration efforts, *Science*, 308(5722), 636-637.
- Boon, P. J. (1998), River restoration in five dimensions, *Aquatic Conservation: Marine and Freshwater Ecosystems*, 8(1), 257-264.
- Booth, D. B. (1990), Stream-channel incision following drainage-basin urbanization, *JAWRA Journal of the American Water Resources Association*, 26(3), 407-417.
- Bramley, H., J. Hutson, and S. D. Tyerman (2003), Floodwater infiltration through root channels on a sodic clay floodplain and the influence on a local tree species *Eucalyptus largiflorens*, *Plant and Soil*, 253(1), 275-286.
- Bukaveckas, P. A. (2007), Effects of channel restoration on water velocity, transient storage, and nutrient uptake in a channelized stream, *Environmental Science & Technology*, 41(5), 1570-1576.
- Burt, T. P., P. D. Bates, M. D. Stewart, A. J. Claxton, M. G. Anderson, and D. A. Price (2002), Water table fluctuations within the floodplain of the River Severn, England, *Journal of Hydrology*, 262(1), 1-20.
- Craig, L. S., et al. (2008), Stream restoration strategies for reducing river nitrogen loads, *Frontiers in Ecology and the Environment*, 6(10), 529-538.

- Dahan, O., B. Tatarsky, Y. Enzel, C. Kull, M. Seely, and G. Benito (2008), Dynamics of flood water infiltration and ground water recharge in hyperarid desert, *Ground Water*, 46(3), 450-461.
- Doble, R. C., R. S. Crosbie, and B. D. Smerdon (2011a), Aquifer recharge from overbank floods, *IAHS-AISH publication*, 169-174.
- Doble, R. C., R. S. Crosbie, B. D. Smerdon, L. Peeters, and F. J. Cook (2012), Groundwater recharge from overbank floods, *Water Resources Research*, 48, 14.
- Doble, R. C., R. S. Crosbie, B. D. Smerdon, L. Peeters, F. Chan, D. Marinova, and R. S. Andersson (2011b), Examining the controls on overbank flood recharge for improved estimates of national water accounting.
- Doll, B. A., D. E. Wise-Frederick, C. M. Buckner, S. D. Wilkerson, W. A. Harman, R. E. Smith, and J. Spooner (2002), Hydraulic geometry relationships for urban streams throughout the piedmont of north carolina, *JAWRA Journal of the American Water Resources Association*, 38(3), 641-651.
- Dunne, T. (1978), *Water in environmental planning*, Macmillan.
- Fuchs, J. W., G. A. Fox, D. E. Storm, C. J. Penn, and G. O. Brown (2009), Subsurface transport of phosphorus in riparian floodplains: Influence of preferential flow paths, *Journal of environmental quality*, 38(2), 473-484.
- Graf, W. L. (1975), The impact of suburbanization on fluvial geomorphology, *Water Resources Research*, 11(5), 690-692.
- Harrison, M. D., P. M. Groffman, P. M. Mayer, S. S. Kaushal, and T. A. Newcomer (2011), Denitrification in alluvial wetlands in an urban landscape, *Journal of environmental quality*, 40(2), 634-646.
- Heeren, D. M., R. B. Miller, G. A. Fox, D. E. Storm, T. Halihan, and C. J. Penn (2010), Preferential flow effects on subsurface contaminant transport in alluvial floodplains.
- Helton, A. M., G. C. Poole, R. A. Payn, C. Izurieta, and J. A. Stanford (2012), Scaling flow path processes to fluvial landscapes: An integrated field and model assessment of temperature and dissolved oxygen dynamics in a river-floodplain-aquifer system, *Journal of Geophysical Research-Biogeosciences*, 117, 13.
- Helton, A. M., G. C. Poole, R. A. Payn, C. Izurieta, and J. A. Stanford (2014), Relative influences of the river channel, floodplain surface, and alluvial aquifer on simulated hydrologic residence time in a montane river floodplain, *Geomorphology*, 205, 17-26.
- Hester, E. T., and M. W. Doyle (2008), In-stream geomorphic structures as drivers of hyporheic exchange, *Water Resources Research*, 44(3).
- Hester, E. T., and M. N. Gooseff (2010), Moving Beyond the Banks: Hyporheic Restoration Is Fundamental to Restoring Ecological Services and Functions of Streams, *Environmental Science & Technology*, 44(5), 1521-1525.
- Jolly, I. D., G. R. Walker, and K. A. Narayan (1994), Floodwater recharge processes in the Chowilla anabranch system, South Australia, *Soil Research*, 32(3), 417-435.
- Jung, M., T. P. Burt, and P. D. Bates (2004), Toward a conceptual model of floodplain water table response, *Water Resources Research*, 40(12), 13.

- Junk, W. J., P. B. Bayley, and R. E. Sparks (1989), The flood pulse concept in river-floodplain systems, *Canadian special publication of fisheries and aquatic sciences*, 106(1), 110-127.
- Käser, D. H., A. Binley, A. L. Heathwaite, and S. Krause (2009), Spatio-temporal variations of hyporheic flow in a riffle-step-pool sequence, *Hydrological Processes*, 23(15), 2138-2149.
- Kaushal, S. S., P. M. Groffman, P. M. Mayer, E. Striz, and A. J. Gold (2008), Effects of stream restoration on denitrification in an urbanizing watershed, *Ecological Applications*, 18(3), 789-804.
- Klockner, C. A., S. S. Kaushal, P. M. Groffman, P. M. Mayer, and R. P. Morgan (2009), Nitrogen uptake and denitrification in restored and unrestored streams in urban Maryland, USA, *Aquatic Sciences*, 71(4), 411-424.
- Knispel, S., M. Sartori, and J. E. Brittain (2006), Egg development in the mayflies of a Swiss glacial floodplain, *Journal of Insect Conservation*, 25(2).
- Krause, S., and A. Bronstert (2007), The impact of groundwater–surface water interactions on the water balance of a mesoscale lowland river catchment in northeastern Germany, *Hydrological Processes*, 21(2), 169-184.
- Krause, S., A. Bronstert, and E. Zehe (2007), Groundwater–surface water interactions in a North German lowland floodplain—Implications for the river discharge dynamics and riparian water balance, *Journal of hydrology*, 347(3), 404-417.
- Kronvang, B., I. K. Andersen, C. C. Hoffmann, M. L. Pedersen, N. B. Ovesen, and H. E. Andersen (2007), Water exchange and deposition of sediment and phosphorus during inundation of natural and restored lowland floodplains, *Water Air and Soil Pollution*, 181(1-4), 115-121.
- Landers, J. (2010), Entering the Mainstream, *Civil Engineering*, 80(8), 58-+.
- Lane, E. W. (1955), Design of stable channels, *Transactions of the American Society of Civil Engineers*, 120(1), 1234-1260.
- Langhans, S. D., and K. Tockner (2006), The role of timing, duration, and frequency of inundation in controlling leaf litter decomposition in a river-floodplain ecosystem (Tagliamento, northeastern Italy), *Oecologia*, 147(3), 501-509.
- Leopold, L. B. (1968), Hydrology for urban land planning: A guidebook on the hydrologic effects of urban land use.
- Lerner, D. N. (2002), Identifying and quantifying urban recharge: a review, *Hydrogeology Journal*, 10(1), 143-152.
- Lewandowski, J., and G. Nützmann (2010), Nutrient retention and release in a floodplain's aquifer and in the hyporheic zone of a lowland river, *Ecological Engineering*, 36(9), 1156-1166.
- Luhar, M., and H. M. Nepf (2013), From the blade scale to the reach scale: A characterization of aquatic vegetative drag, *Advances in Water Resources*, 51, 305-316.
- Mayer, P. M., S. K. Reynolds, M. D. McCutchen, and T. J. Canfield (2007), Meta-analysis of nitrogen removal in riparian buffers, *Journal of Environmental Quality*, 36(4), 1172-1180.
- Menichino, G. T., A. S. Ward, and E. T. Hester (2014), Macropores as preferential flow paths in meander bends, *Hydrological Processes*, 28(3), 482-495.
- Mertes, L. A. K. (1997), Documentation and significance of the perirheic zone on inundated floodplains, *Water Resources Research*, 33(7), 1749-1762.

- Moser, D. P., J. K. Fredrickson, D. R. Geist, E. V. Arntzen, A. D. Peacock, S. M. W. Li, T. Spadoni, and J. P. McKinley (2003), Biogeochemical processes and microbial characteristics across groundwater-surface water boundaries of the Hanford Reach of the Columbia River, *Environmental Science & Technology*, 37(22), 5127-5134.
- Nieber, J. L. (2000), The relation of preferential flow to water quality, and its theoretical and experimental quantification, *Preferential Flow: Water Movement and Chemical Transport in the Environment*, 1-10.
- Noe, G. B., and C. R. Hupp (2007), Seasonal variation in nutrient retention during inundation of a short-hydroperiod floodplain, *River Research and Applications*, 23(10), 1088-1101.
- O'Driscoll, M., S. Clinton, A. Jefferson, A. Manda, and S. McMillan (2010), Urbanization effects on watershed hydrology and in-stream processes in the southern United States, *Water*, 2(3), 605-648.
- Orr, C. H., E. H. Stanley, K. A. Wilson, and J. C. Finlay (2007), Effects of restoration and reflooding on soil denitrification in a leveed Midwestern floodplain, *Ecological Applications*, 17(8), 2365-2376.
- Osborne, L. L., and D. A. Kovacic (1993), Riparian vegetated buffer strips in water-quality restoration and stream management, *Freshw. Biol.*, 29(2), 243-258.
- Peter, S., R. Rechsteiner, M. F. Lehmann, R. Brankatschk, T. Vogt, S. Diem, B. Wehrli, K. Tockner, and E. Durisch-Kaiser (2012), Nitrate removal in a restored riparian groundwater system: functioning and importance of individual riparian zones, *Biogeosciences*, 9(11), 4295-4307.
- Pirastu, M., and M. Niedda (2013), Evaluation of the soil water balance in an alluvial flood plain with a shallow groundwater table, *Hydrological Sciences Journal-Journal Des Sciences Hydrologiques*, 58(4), 898-911.
- Poff, N. L., J. D. Allan, M. B. Bain, J. R. Karr, K. L. Prestegard, B. D. Richter, R. E. Sparks, and J. C. Stromberg (1997), The Natural Flow Regime, *Bioscience*, 47(11), 12.
- Poole, G. C., J. A. Stanford, C. A. Frissell, and S. W. Running (2002), Three-dimensional mapping of geomorphic controls on flood-plain hydrology and connectivity from aerial photos, *Geomorphology*, 48(4), 329-347.
- Pringle, C. (2003), What is hydrologic connectivity and why is it ecologically important?, *Hydrological Processes*, 17(13), 2685-2689.
- Prosser, I. P., A. O. Hughes, and I. D. Rutherford (2000), Bank erosion of an incised upland channel by subaerial processes: Tasmania, Australia, *Earth Surface Processes and Landforms*, 25(10), 1085-1101.
- Roley, S. S., J. L. Tank, and M. A. Williams (2012), Hydrologic connectivity increases denitrification in the hyporheic zone and restored floodplains of an agricultural stream, *Journal of Geophysical Research-Biogeosciences*, 117, 16.
- Rood, S. B., G. M. Samuelson, J. H. Braatne, C. R. Gourley, F. M. R. Hughes, and J. M. Mahoney (2005), Managing river flows to restore floodplain forests, *Frontiers in Ecology and the Environment*, 3(4), 193-201.
- Sawyer, A. H., M. B. Cardenas, A. Bomar, and M. Mackey (2009), Impact of dam operations on hyporheic exchange in the riparian zone of a regulated river, *Hydrological processes*, 23(15), 2129-2137.

- Sholtes, J. S., and M. W. Doyle (2010), Effect of channel restoration on flood wave attenuation, *Journal of Hydraulic Engineering*, 137(2), 196-208.
- Simon, A., S. J. Bennett, and J. M. Castro (Eds.) (2011), *Stream Restoration in Dynamic Fluvial Systems: Scientific Approaches, Analyses, and Tools*, 1 ed., Wiley, John & Sons, Incorporated.
- Singh, V. P. (2002), Is hydrology kinematic?, *Hydrological processes*, 16(3), 667-716.
- Tockner, K., F. Malard, and J. V. Ward (2000), An extension of the flood pulse concept, *Hydrological processes*, 14(16-17), 2861-2883.
- USEPA (2010), Chesapeake Bay Total Maximum Daily Load for Nitrogen, Phosphorus and Sediment.
- Valett, H. M., M. A. Baker, J. A. Morrice, C. S. Crawford, M. C. Molles Jr, C. N. Dahm, D. L. Moyer, J. R. Thibault, and L. M. Ellis (2005), Biogeochemical and metabolic responses to the flood pulse in a semiarid floodplain, *Ecology*, 86(1), 220-234.
- Vidon, P. (2012), Towards a better understanding of riparian zone water table response to precipitation: surface water infiltration, hillslope contribution or pressure wave processes?, *Hydrological Processes*, 26(21), 3207-3215.
- Vitousek, P. M., J. D. Aber, R. W. Howarth, G. E. Likens, P. A. Matson, D. W. Schindler, W. H. Schlesinger, and D. Tilman (1997), Human alteration of the global nitrogen cycle: Sources and consequences, *Ecological Applications*, 7(3), 737-750.
- Walter, R. C., and D. J. Merritts (2008), Natural streams and the legacy of water-powered mills, *Science*, 319(5861), 299-304.
- Ward, J. V. (1997), An expansive perspective of riverine landscapes: pattern and process across scales, *GAIA-Ecological Perspectives for Science and Society*, 6(1), 52-60.
- Welti, N., E. Bondar-Kunze, G. Singer, M. Tritthart, S. Zechmeister-Boltenstern, T. Hein, and G. Pinay (2012), Large-scale controls on potential respiration and denitrification in riverine floodplains, *Ecological Engineering*, 42, 73-84.
- Wohl, E., P. L. Angermeier, B. Bledsoe, G. M. Kondolf, L. MacDonnell, D. M. Merritt, M. A. Palmer, N. L. Poff, and D. Tarboton (2005), River restoration, *Water Resources Research*, 41(10).
- Wondzell, S. M., and F. J. Swanson (1999), Floods, channel change, and the hyporheic zone, *Water Resources Research*, 35(2), 555-567.
- Zarnetske, J. P., R. Haggerty, S. M. Wondzell, and M. A. Baker (2011), Dynamics of nitrate production and removal as a function of residence time in the hyporheic zone, *Journal of Geophysical Research-Biogeosciences*, 116, 12.
- Zarnetske, J. P., R. Haggerty, S. M. Wondzell, V. A. Bokil, and R. Gonzalez-Pinzon (2012), Coupled transport and reaction kinetics control the nitrate source-sink function of hyporheic zones, *Water Resources Research*, 48, 15.

2 Surface Water and Groundwater Hydraulics, Exchange, and Transport during Simulated Overbank Floods along a Third-Order Stream in Southwest Virginia

In Preparation for Hydrological Processes

Christopher R. Guth, Erich T. Hester*, Charles N. Jones, and Durelle T. Scott

**Corresponding Author:*

Erich T. Hester
The Charles E. Via, Jr. Department of Civil and Environmental Engineering
Virginia Polytechnic and State University
220-D Patton Hall
Blacksburg, VA 24061

Email: ehester@vt.edu
Phone: 540-231-9758

Other Authors:

Christopher R. Guth
The Charles E. Via, Jr. Department of Civil and Environmental Engineering
Virginia Polytechnic and State University
220-D Patton Hall
Blacksburg, VA 24061

C. Nathan Jones
Department of Biological Systems Engineering
Virginia Polytechnic and State University
200 Seitz Hall
Blacksburg, VA 24061

Durelle T. Scott
Department of Biological Systems Engineering
Virginia Polytechnic and State University
305 Seitz Hall
Blacksburg, VA 24061

2.1 Introduction

2.1.1 Natural Floodplain Functioning

Hydrologic connectivity between a stream or river and adjacent floodplains (“floodplain connectivity”) can have many benefits for water quality and ecosystem health [Pringle, 2003; Ward, 1997]. When coupled with natural variability in stream stage, inundation frequency, and floodplain temperature, floodplain connectivity can directly influence ecosystem biodiversity [Poff et al., 1997; Tockner et al., 2000]. Examples of the ecological impacts are pervasive throughout the literature [Junk et al., 1989; Knispel et al., 2006; Langhans and Tockner, 2006] and can be directly attributed to the connection between landscape patches and biological processes that occur at different spatial and temporal scales [Amoros and Bornette, 2002].

The ecological benefits that exist due to floodplain inundation are largely dependent on flood duration and frequency. In addition to the many ecological benefits, floodplains can also naturally act as a hotspot for nutrient removal. During overbank floods surface water velocity decreases resulting in the potential net removal of nutrients [Bukaveckas, 2007; Kronvang et al., 2007]. Also, while floodplain topography can dictate surface water storage and mixing [Mertes, 1997], floodplain soil properties can have a high degree of impact on surface water and groundwater flow characteristics as well as the exchange between both domains [Doble et al., 2012; Helton et al., 2014; Krause and Bronstert, 2007].

Understanding controls on nutrient removal via biogeochemical reactions during overbank floods requires fully understanding floodplain groundwater flow paths [Helton et al., 2012] but in many cases floodplain soils are often simplified to being homogeneous for the sake of simplicity or due to the lack of necessary data [Bates et al., 2000; Krause et al., 2007]. For storms, the characteristics associated with groundwater recharge during overbank flood events have been evaluated extensively in different floodplain environments [Dahan et al., 2008; Doble et al., 2011a; Doble et al., 2012]. The rate at which surface water infiltrates into the floodplain subsurface can be heavily impacted by low hydraulic conductivity sediments [Andersen, 2004; Doble et al., 2011b; Jolly et al., 1994] and local ponding on the floodplain surface [Jung et al., 2004]. In addition, the presence of paleochannels [Poole et al., 2002] and preferential flow paths [Bramley et al., 2003; Heeren et al., 2010] can increase average infiltration rates. Increased infiltration rates along preferential flow paths reduce residence time and contact with floodplain sediments therefore reducing the potential for nutrient removal [Fuchs et al., 2009; Heeren et al., 2010; Nieber, 2000]. The response to changing stream stage and surface inundation in groundwater elevation has been observed to be dependent on both preferential flow and Darcy flow [Menichino

et al., 2014]. Groundwater elevations have also been shown to increase in response to an elevated stream stage with a response time too quick to be explained using the hydraulic conductivity and travel distance [Käser *et al.*, 2009; Vidon, 2012]. These responses (i.e. pressure waves, or kinematic waves) are commonly observed but well understood [Singh, 2002]. Analysis of overbank floods in a more controlled environment would allow for the independent effects of seasonal and moisture variations on floodplain hydraulics to be quantified.

2.1.2 Human Impacts

Alterations of the landscape have led to the deterioration of water quality and a loss of the natural flow regime in river systems [Poff *et al.*, 1997]. For example, urbanization and the implementation of storm water management systems such as storm sewers has reduced the potential for evapotranspiration and infiltration [Leopold, 1968; O'Driscoll *et al.*, 2010] and altered baseflow discharge in many areas [Lerner, 2002]. These changes typically result in higher peak discharge during storms therefore increasing the streams capacity to carry sediment [Lane, 1955] and increasing channel instability and dimensions [Booth, 1990; Doll *et al.*, 2002; Graf, 1975]. This degradation of the stream bank then decreases floodplain connectivity and reduces the potential for the benefits listed above to occur [Craig *et al.*, 2008]

2.1.3 Restoration

In order to mitigate the degradation of streams, restoration practices are commonly implemented. Stream restoration is the act of returning a stream to its natural conditions and restoring stream functions [Hester and Gooseff, 2010; Landers, 2010; Simon *et al.*, 2011; Wohl *et al.*, 2005]. The most common goals when restoring streams in the United States are to improve water quality, alter riparian zones (i.e. riparian buffers), allow for improvement of aquatic habitat, allow unobstructed fish travel and migration, and increase bank stability [Bernhardt *et al.*, 2005]. Floodplain reconnection as a means of stream restoration increased in frequency as the importance of lateral connectivity within a stream system became more evident [Boon, 1998].

The potential benefits stemming from stream restoration are diverse, but of particular interest in the Chesapeake Bay watershed is the reduction of nutrient loads [USEPA, 2010]. Excess nutrients in river systems caused by excess fertilizer application and urbanization [Vitousek *et al.*, 1997] can lead to accelerated eutrophication and the subsequent loss of ecosystem function in large water bodies. The reduction of nitrate to unreactive nitrogen through the process of denitrification can permanently remove nutrients from the system. Rates at which this occurs can be altered through exchange between surface water and groundwater (SW-GW exchange) beneath the channel [Moser *et al.*, 2003; Zarnetske *et al.*, 2011; Zarnetske *et al.*, 2012] through the induction

of SW-GW exchange by installing in-stream structures such as weirs or J-hooks [Hester and Doyle, 2008]. Increased contact between stream water and both riparian zones [Mayer et al., 2007; Osborne and Kovacic, 1993; Peter et al., 2012] and floodplains [Harrison et al., 2011; Klocker et al., 2009; Roley et al., 2012; Welte et al., 2012] can also result in a net reduction of nutrient loads from increased contact with vegetation and redox conditions that encourage denitrification. Contact with floodplain sediments and soils and interaction between surface water and groundwater play key roles in water quality [Haycock and Burt, 1993]. While floodplains are typically thought of as a hotspot for these reactions and have been shown to act as a nutrient sink [Kaushal et al., 2008; Kronvang et al., 2007; Lewandowski and Nützmann, 2010], it has also been shown that floodplains can exhibit no significant nutrient retention and at times act as a nutrient source [Noe and Hupp, 2007; Orr et al., 2007; Valett et al., 2005]. Despite a high degree of variability in nutrient cycling stemming from floodplain reconnection, new policies are awarding credits for reducing nutrient loads when floodplain connectivity is restored [Berg et al., 2014]. Through a better understanding of the transport mechanisms of flood water during overbank flood events coupled with accepted knowledge regarding how these mechanisms effect solute transport we may be able to better comprehend why such variability exists.

2.1.4 Purpose of Study

The objectives of this study were to characterize surface water flow, groundwater flow and the exchange between the two during simulated overbank flood events conducted seasonally and with varying antecedent moisture conditions at a field site. Our aim was to replicate natural conditions typical of an overbank event while not only having greater control over timing and inflow/outflow parameters, but also recording hydraulic parameters at a greater spatial and temporal scale than what has been done in past studies by others. In addition to periods at which simulated floods were conducted, background data were recorded continuously over the course of one year to evaluate any effects the periodic application of surface water had on the natural seasonal variations in groundwater elevations. Hydraulic properties were determined by monitoring electrical conductivity (EC), temperature, pressure, inflow, and outflow with a network of both surface and subsurface monitoring locations. The effects of overbank flood events on water quality were quantified through the completion of a separate study [Jones et al., In Preparation] run in parallel with the study the study we present here. The findings from each were used to reinforce the processes occurring throughout the floodplain. By better understanding the

hydraulics associated with overbank events and knowing the corresponding impacts on water quality we can better understand why nutrient cycling is highly variable in floodplain systems.

2.2 Methods

2.2.1 Site Description

The study site is located along a floodplain reach of Stroubles Creek, a third-order alluvial stream in Southwest Virginia with average discharge of 0.22 m³ and approximate bankfull depth of 0.7 m. The catchment area is approximately 15 km² and is predominantly urban and/or residential land use (84%), largely due to the Virginia Tech campus immediately upstream. Agricultural land use (13%) and forest (3%) are also present. The site is within the Stream Research, Education, and Management Lab (StREAM Lab, <http://www.bse.vt.edu/site/streamlab>), which is an extensively monitored reach of Stroubles Creek that began as part of a stream restoration project in 2008 [Thompson *et al.*, 2012]. Motivation for the restoration was in part the 2002 Total Maximum Daily Load (TMDL) identifying sediment loads, nutrients, and organic matter as potential stressors that caused benthic impairment [Mostaghimi *et al.*, 2003]. As part of the TMDL Implementation Plan (IP), cattle access to the stream was prevented and inset floodplains were constructed [Yagow *et al.*, 2006]. Reed canary grass, a nonnative grass, is prevalent throughout the floodplain. We chose this site for our field study because (1) it already had extensive stream and hydrologic monitoring as part of the StREAM Lab, (2) it was the site of a past stream restoration project, and (3) was in an urban environment with land cover typical of areas where floodplain reconnection would be a common stream restoration method.

2.2.2 Field Methods

2.2.2.1 Artificial Flood Experiments

We conducted a series of five flood events over the course of approximately one year. This number of floods was completed in order to account for seasonal differences in evapotranspiration rates, soil moisture, vegetative density, baseflow, and groundwater elevations. The five floods were conducted on April 8, 2013 (Spring), June 29, 2013 (Early Summer), August 30, 2013 (Late Summer), November 11, 2013 (Fall) and February 7, 2014 (Winter). Each flood consisted of pumping surface water from Stroubles Creek onto the floodplain for a total of three hours with inflow and outflow rates of surface water being measured during the entire flood duration. During the second hour of each flood a pulse of NaCl was injected onto the floodplain and used as a tracer. In order to quantify the effect of antecedent moisture conditions on the hydraulics, separate floods

occurred on two or more consecutive days. When possible, the first day of pumping for each flood was preceded by at least two days with no precipitation to ensure that the observed hydraulic responses were a result of the simulated flood rather than a natural rainfall event. The second flood then occurred with wet conditions, allowing comparison to the drier first flood. In addition to monitoring during each of these five floods we also evaluated background conditions by continuously monitoring surface water and groundwater throughout the time that instruments were deployed. We also used these data to examine how a short term event (i.e. overbank flood) affects long term variations impacted by wet and dry seasons.

2.2.2.2 Piezometers and Stilling Wells

We constructed piezometers to monitor groundwater using schedule 40 polyvinyl chloride (PVC) with an internal diameter of 3.81 cm. All piezometers had a total screen length of 10 cm with the screened area located between 4 and 14 cm (10 cm total) from the piezometer base in each case. A series of 0.635 cm holes were created to form the screened area of each piezometer. To prevent the presence of stagnant water between the piezometer base and the screen bottom (4 cm from base) a 3.81 cm washer was installed at the bottom opening to allow for vertical drainage to occur. The washer was attached using a combination of liquid nail adhesive and all-weather electrical tape. Nylon mesh filter fabric was added to the piezometer base and screened interval to prevent sediment from entering. All filter fabric was attached to the piezometer casing using all-weather electrical tape.

Stilling wells for monitoring surface water were constructed similar to the piezometers but no filter fabric was used and the screened length was much greater. The stilling wells prevented debris from interfering with sensors located inside (see Section 2.2.2.7).

In order to install the piezometers, we constructed bore holes using a hand auger with 3.8 cm diameter auger bit. Earlier analysis of the site showed evidence of a clay lens present in the subsurface [*Hofmeister et al.*, 2012]. We estimated the flow centerline through our site prior to installation and placed piezometers according to those estimations to form three monitoring transects (Figure 1). For this reason we placed piezometers at two depths, with shallow piezometers approximately 30 cm below ground surface (BGS) typically in the clay layer and deep piezometers approximately 100 cm BGS typically in a layer of gravel mixed with silts. We packed bentonite clay between the sediment and piezometer at and directly below the ground surface to prevent artificial connection between surface water and the subsurface. We used boreholes with diameters equivalent to the piezometers in order to minimize the potential for short circuiting of

surface water into the subsurface and reduce the impact on the natural floodplain soil structure. This prevented the need to fill the annulus surrounding the piezometer due to the continuous contact between the installed piezometer and the surrounding natural soils. The depth to ground surface and depth to well bottom were measured from the top of well casing (TOC) to determine the measuring point elevation of each probe and to verify the soil core depths with the actual depth of soil extracted.

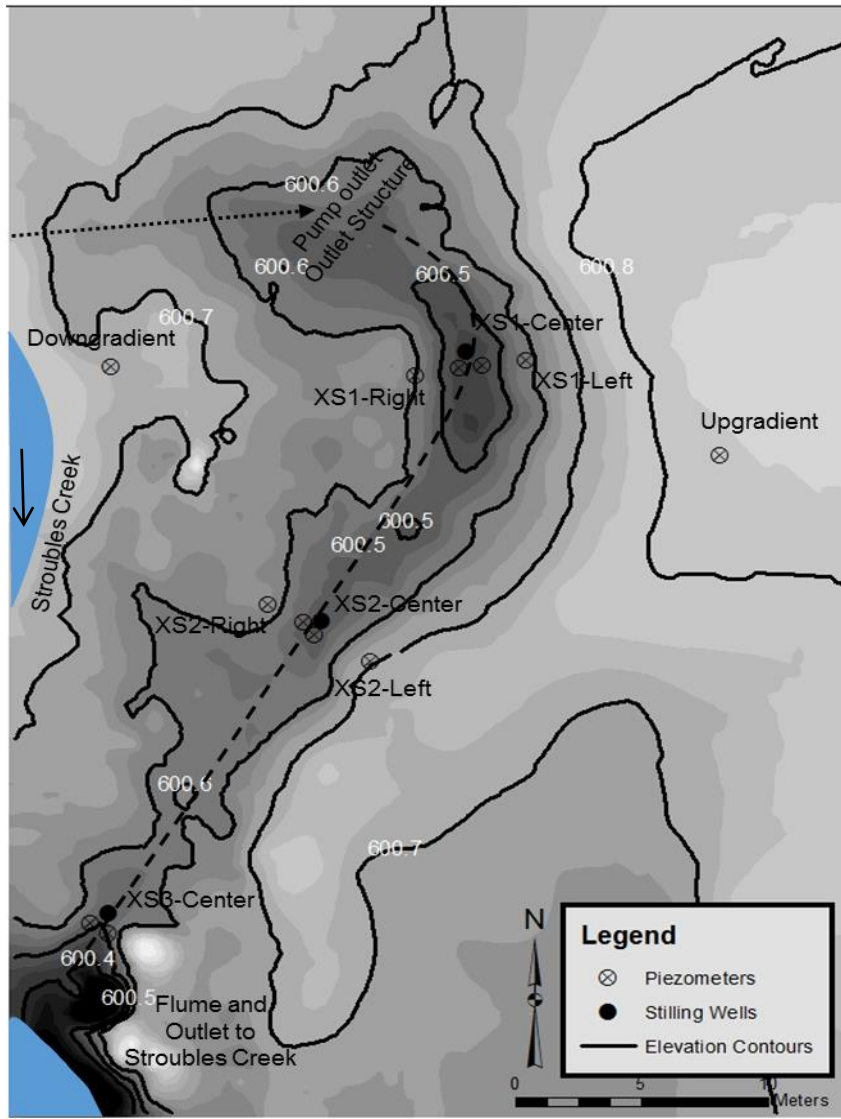


Figure 1: Layout of study location. We used ArcGIS to derive contour lines using survey data obtained during site setup. Dotted line represents the pipe network routing water from Stroubles Creek to the swale and the dashed line represents the approximate flood centerline.

We installed nested piezometer pairs along the centerline while only shallow piezometers were placed to the left and right of the thalweg (Figure 1). We used only one monitoring location at cross section 3 (XS3-Center) due to convergence of surface flow near that location. We installed

one deep piezometer (100 cm BGS) upgradient of the study site and one downgradient of the site near Stroubles Creek to measure larger scale EC and head gradients at the site. Lastly, we installed stilling wells on the floodplain surface at each of the three cross sections centerline locations to measure surface water properties.

We routinely repacked bentonite next to the piezometers throughout the study duration to prevent preferential flow paths (PFPs) from forming artificially down the piezometer bore holes. We monitored this maintenance work by performing rising head tests at the beginning and end of the study where surface inundation was most common (i.e. XS1 and XS2 groundwater monitoring network).

2.2.2.3 Soil Cores

We classified soils from borehole cores along the site centerline during the installation of the deep piezometers. Soils were classified as organic, clay, or sand/gravel using both visual and textural characteristics. Classification of gravel sediments was clear due to its coarse nature. Clay and organic soil layers were distinguished from each other through the analysis of ribbon lengths and the use of the “feel method”, which is commonly used for a quick classification in the field [Thien, 1979].

2.2.2.4 Pump (Flow Entering Floodplain)

We used a Berkeley B3-ZRMS pump with a Briggs and Stratton Vanguard gas motor to inundate the floodplain. Pump flow rates were manually recorded during each flood and were measured using a Fuji M-flow meter during the Spring, Early Summer, Late Summer, and Fall floods. Due to malfunction of the Fuji M-Flow meter during the Winter flood, flow entering the floodplain was measured using a Sensus 1125-W fire hydrant flow meter. Flow rates entering the site averaged 23.9 L s^{-1} across all five floods, with a standard deviation of 1.6 L s^{-1} (Table 1). The pump discharged to a 4.9 meter segment of 7.62 cm internal diameter schedule 40 PVC pipe to reduce turbulence and increase accuracy of the M-flow meter. The PVC pipe discharged to a standard fire hose that directed flow to the desired location. The fire hose discharged water into a large corrugated 23 cm diameter irrigation pipe to reduce water velocities. The irrigation pipe then discharged to a 6.1 m x 3.7 m tarp to prevent erosion of the floodplain surface. Cinder blocks were placed on the tarp to disperse flow and further reduce water velocities to allow for a more accurate representation of natural overbank flow conditions.

Table 1: Details of pumping during simulated floods

Flood Event	Date of Flooding	Time of Flooding	Average Flow Rate (L s ⁻¹)
Spring	April 8, 2013	12:18-3:18 PM	23.36
	April 9, 2013	12:01-3:01 PM	*23.36
Early Summer	June 29, 2013	9:42 AM-12:42 PM	21.82
	June 30, 2013	**9:42 AM-1:06 PM	21.55
	July 1, 2013	9:13 AM-12:13 PM	*21.82
Late Summer	August 30, 2013	12:15-3:15 PM	24.64
	August 31, 2013	12:00 -3:00 PM	*24.64
Fall	November 11, 2013	1:01-3:01 PM	26.35
	November 12, 2013	1:39-4:49 PM	25.36
Winter	February 7, 2014	1:14-4:14 PM	23.26
	February 8, 2014	12:50-3:50 PM	22.47

* Flow meter malfunctioned on second day and flows from first day were used

** The pump piping system became detached and required the pump to be turned off briefly. Three total hours of pumping surface water onto the floodplain were completed, although this time was not continuous and instead occurred off-and-on over the timeframe listed. This interruption in inflow resulted in the need for a third day of flooding to be completed during the Early Summer.

2.2.2.5 Flume (Flow Existing Floodplain)

We measured the discharge rate of surface water leaving the flood site using a 7.62 cm fiberglass parshall flume (Engineered Fiberglass Composites, Inc.) installed at the downstream end of the swale (Figure 1). Plywood was used to taper flow into the flume and was inserted into the ground to a depth of approximately 20 cm BGS to reduce the potential for water leaving the site via groundwater flow. Leaks between the flume and plywood were sealed using a combination of a flexible aluminum sheeting and heavy duty duct tape sealed with PC-11 Marine Epoxy (Protective Coating Company). We minimized surface water leaks in other areas using sandbags. Constant monitoring of the flood site occurred during each flood event and leaks were fixed as needed. We installed an Onset HOBO Pressure Transducer to measure the water column depth in the flume (See Section 2.2.2.7).

2.2.2.6 Rising Head Tests

We used rising head tests (bail tests) to measure the hydraulic conductivity of soil near each piezometer [Landon *et al.*, 2001]. We did this near the beginning (June 12, 2013) and end (March

8, 2014) of the study to track potential changes in hydraulic conductivity over time. We used instrumentation already installed in each piezometer but reset the logging interval to 15 seconds. Once an initial water depth measurement was recorded at each location we extracted water from each piezometer using a Geotech Geopump

We changed logging frequencies back to 15 minute intervals approximately 48 hours into the rising head test. XS2-R, XS3-Center-30 cm, XS3-Center-100 cm, Upgradient, and Downgradient piezometers (those in very low K soils) had not returned to background levels by this time.

2.2.2.7 Instrumentation

Instrument locations were labelled based on the transect in which they were installed (i.e. XS1, XS2, or XS3), their location relative to the flow centerline (i.e. left, center, or right), and their measurement depth (e.g. surface, 30 cm BGS, etc.). For example, the piezometer located to the left of the flow centerline at XS1 at a depth of 30 cm BGS is labelled as XS1-Left-30 cm.

We installed a variety of instruments to measure and log pressure (water levels), soil moisture, electrical conductivity, and temperature (Figure 1). We installed a total of 11 Solinst LTCs that measure pressure, electrical conductivity, and temperature along the centerline of XS1 and XS2 in surface water (2 total), in each of the nested piezometers along the centerline (6 total), in the Upgradient piezometer (1 total), and in the transverse piezometers (i.e. piezometers 30 cm BGS located within the flooded area but not along the flow centerline) at XS2 (2 total). Additionally, 6 Onset HOBO Pressure Transducers that measure pressure and temperature were placed in open air to measure barometric pressure (1 total), in the parshall flume stilling well (1 total), in surface water at XS3 centerline (1 total), in transverse piezometers at XS1 (2 total), and in the Downgradient piezometer near Stroubles Creek (1 total). Beginning with the Early Summer flood, the LTC located at XS2-Left-30 cm (part of the XS2 groundwater monitoring network) was switched with the HOBO located at XS3-Center-Surface. All other instrumentation was kept constant between flood events.

We measured moisture content and temperature in shallow soils (5 cm BGS and 10 cm BGS) with moisture probes at each piezometer in the flooded area. We placed Decagon Devices GS3 soil moisture probes which measure volumetric moisture content, temperature, and electrical conductivity along the centerline (6 probes total) and Decagon Devices 5TM soil moisture probes which measure volumetric moisture content and temperature at the other four locations (8 probes total). We used Campbell Scientific CR200 loggers to log and store data during probe deployment.

During the Spring flood we set logging frequencies for the LTCs and HOBOS measuring surface water properties to 5 minutes while the subsurface instruments recorded data every 15 minutes. All soil moisture probes were also set at a logging interval of 5 minutes. Water depth in the flume was recorded every 2 minutes during the Spring flood. Logging intervals for the Early Summer flood were identical to Spring except that the flume logging interval was reduced to every minute. The logging interval for all LTCs and HOBOS (surface, subsurface, and parshall flume) was set at 2 minutes for the Late Summer, Fall, and Winter floods. Changes in logging intervals allowed for greater temporal resolution of data during floods. We kept all instrumentation installed on the flood site between flood events with a programmed logging interval of 15 minutes. We obtained hourly precipitation and air temperature from a weather station located approximately 80 m to the north of the swale that is part of the Virginia Tech StREAM Lab.

2.2.3 Data Analysis

2.2.3.1 Water Balance

Surface water flow rates entering and leaving the site were measured by the pump flow meter and parshall flume, respectively. We calculated total storage (i.e. surface storage and subsurface storage) of flood water as the difference in the volume of water applied to the site and the volume of water leaving the site (Equations 1 and 2) from the time the pump was turned on until the time when flow through the flume stopped.

$$\sum V_{in} - \sum V_{out} = V_{surface} + V_{subsurface} + V_{error} \quad (1)$$

$$V_{surface} + V_{subsurface} = V_{total\ storage} \quad (2)$$

We calculated the volume of water that drained from the flood site after each flood by integrating the flume flow rate over time from when the pump was turned off to when flow through the flume stopped. The drained volume was then normalized to the total volume of surface water applied to the site to account for variations in inflow discharge rates. We conducted this analysis following the second day of flooding for each season assuming antecedent soil moisture and water levels were equivalent for each case. Observed differences could then be attributed to seasonal changes rather than differences in moisture.

We estimated the storage volume of flood water in the subsurface using Equation 3 in order to estimate the fraction of total storage that is due to subsurface storage where S is the average percent saturation (%), n is the total porosity of the soil ($m^3\ m^{-3}$), w is the plan view width of the

control volume (m), L is the plan view length of the control volume (m), and h is the average depth to water table (m).

$$\text{Subsurface Storage Volume} = [(1 - S) * n] * wLh \quad (3)$$

The water table depth BGS at XS1 was assumed as a constant throughout the floodplain at 0.55 m. Average soil moisture content at 5 cm and 10 cm BGS along the centerline was approximately 90% saturated prior to flooding during dry periods. We assumed this to be constant throughout the sediment control volume although actual moisture content may be higher due to the capillary fringe. We assumed a porosity of 0.3 along with an estimated plan view inundation extent of 35 m by 15 m. We estimated the storage volume of surface water on the floodplain surface by taking the difference between the total volume of water added to the site and the total volume that exited the site during the first day of the Late Summer (low antecedent soil moisture and groundwater levels) and subtracting out the estimated volume of subsurface storage.

2.2.3.2 Hydraulic Comparisons Between Floods

We made many direct comparisons between seasons and between consecutive floods conducted each season. We took the elapsed time between the point when the application of surface water began to the point when the flume began experiencing flow as the arrival time of the flood pulse. This allowed for a quantification of how antecedent moisture affects the arrival time and how the arrival time changes between seasons.

We compared the magnitude of increase in groundwater elevation compared to surface water elevation during each flood. This analysis was only valid during floods which had high antecedent water levels because water levels below the measuring points cannot be recorded and therefore the change in water level cannot be calculated. After we measured the pre-event water levels for surface water and groundwater, the maximum water elevation over the 24 hours following the flood beginning was recorded. We then calculated the change in elevation based on this value. If another flood event started within the 24 hour window we took the maximum elevation up to the point when the pump was turned on for the flood on the following day. We normalized the elevation change in groundwater to the elevation change in the corresponding surface water measuring point (e.g. XS1 groundwater normalized to XS1 surface water) and averaged the four values obtained from XS1 and XS2. This analysis was not completed for water levels in XS3.

In order to quantify the average time for the peaks in groundwater elevation to occur we used the elapsed time between the time that the flood started to the time that the peak elevations were observed. The time between the surface water peak elevation and groundwater peak elevation was calculated for each piezometer in XS1 and XS2. The four values obtained from each cross section were averaged to give a representative lag time between surface water and groundwater during each flood.

The travel time required for surface water to reach the measuring points in each piezometer was calculated using Darcy's Law along with the depth BGS for each centerline location. Equation 4 was used where v is the average linear water velocity (m s^{-1}), K is the hydraulic conductivity surrounding each centerline piezometer (m s^{-1}), i is the maximum vertical head gradient recorded between the surface and each centerline piezometer (m m^{-1}), and n is the effective porosity of the soil which was assumed as being 0.3 ($\text{m}^3 \text{m}^{-3}$). The travel time, t (sec), indicative of Darcy flow was then calculated using the depth BGS of each centerline monitoring point, d (m), in Equation 5.

$$v = \frac{Ki}{n} \quad (4)$$

$$t = \frac{d}{v} \quad (5)$$

2.2.3.3 Hydraulic Conductivity

The Hvorslev method (Equation 6) was used to calculate the horizontal hydraulic conductivity in each case where K is the hydraulic conductivity (m s^{-1}), r_c is piezometer diameter (m), L is screen length (m), R is diameter of screened portion of piezometer (m), and T_o is the time required for 63% recovery of the water depth (s) [Hvorslev, 1951].

$$K = \frac{r_c^2 \ln\left(\frac{L}{R}\right)}{2LT_o} \quad (6)$$

2.2.3.4 Hydraulic Head Gradients

We calculated vertical groundwater head gradients along the flood centerline during each flood event using Equation 7 where h is the water surface elevation (m) and z is the probe measuring point elevation (m). We measured vertical groundwater head gradients (I_z) from the floodplain surface to 30 cm BGS, surface to 100 cm BGS, and 30 cm BGS to 100 cm BGS.

$$I_{xij} = \frac{h_j - h_i}{Z_j - Z_i} \quad (7)$$

We also calculated horizontal head gradients (I_x) between piezometers of equivalent depth (i.e. XS1-Center-30 cm to XS2-Center-30 cm, XS1-Center-100 cm to XS2-Center-100 cm, etc.) using Equation 8 where h is water surface elevation (m) and x is the horizontal distance between measuring points (m). We manually measured horizontal distances between cross sections at the flood site.

$$I_{zij} = \frac{h_j - h_i}{X_j - X_i} \quad (8)$$

2.3 Results

2.3.1 Site Characteristics

2.3.1.1 Lithology

A clay lens was prevalent at the site (Figure 2). Gravel mixed with sand and finer sediment exists beneath the clay, and may be an abandoned streambed or paleochannel.

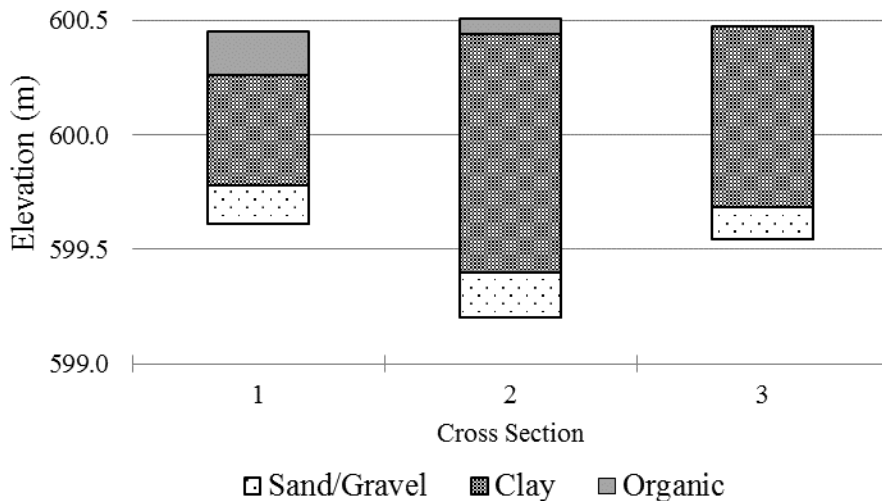


Figure 2: Soil cores extracted along site centerline

2.3.1.2 Hydraulic Conductivity

Overall, the hydraulic conductivity of soils was low. Soils near XS1 generally had the highest hydraulic conductivity while soils near XS3 generally had the lowest (Table 2). Piezometers 100 cm BGS along the centerline show higher hydraulic conductivity than those at 30 cm BGS. This is consistent with the piezometers 100 cm BGS being screened in a layer with more gravel and the piezometers 30 cm BGS being screened in a clay layer (Figure 2). The only exception is XS1-Center-30 cm, which also showed high hydraulic conductivity relative to other piezometers. This is likely due to the presence of a preferential flow path (see water level and conductivity data in Sections 2.3.3.2 and 2.3.3.6). A more pronounced difference in hydraulic conductivity between piezometers 30 cm BGS and 100 cm BGS may have been observed if the gravel layer was cleaner and not filled with fine sediments.

Table 2: Hydraulic conductivity (K) results using the Hvorslev method in each of the piezometers located throughout the study site.

Location	K (m s ⁻¹)	
	Test 1	Test 2
XS1-Left-30 cm	3.8E-07	ND
XS1-Center-30 cm	3.2E-06	5.42E-06
XS1-Center-100 cm	2.3E-06	8.36E-06
XS1-Right-30 cm	1.2E-07	1.86E-06
XS2-Left-30 cm	3.4E-08	1.54E-05
XS2-Center-30 cm	5.0E-08	1.04E-05
XS2-Center-100 cm	2.5E-07	3.34E-07
XS2-Right-30 cm	3.4E-08	1.02E-07
XS3-Center-30 cm	6.6E-10	NS
XS3-Center-100 cm	1.0E-09	NS
Upgradient	1.1E-09	NS
Downgradient	1.0E-09	NS

ND- No data collected due to equipment malfunction

NS- Not sampled during specified series of tests

The data collected for the first set of rising head tests for XS3-Center-30 cm and XS3-Center-100 cm were affected by the overbank storm event in on July 3, 2013 due to the long recovery time of water levels in the piezometers. The storm likely overtopped both piezometers even though the 15-minute logging interval does not allow certainty on this point. The piezometers, while capped, are vented to the atmosphere through a small hole in the cap, so overtopping would result in direct connection between the flood water on the floodplain surface and groundwater at the piezometer screen. This was the only overtopping of any piezometers at the site during the yearlong study. Water levels in XS3-Center-30 cm and XS3-Center-100 cm did not return to pre-storm elevations until two to three months following the overbank storm event (See Section 2.3.2.1), confirming low hydraulic conductivity at this location. Although the rising head tests were interrupted by the overbank storm event, hydraulic conductivity at these two locations was estimated by interpolating water level data obtained prior to the storm.

2.3.2 Background Data Collected Throughout the Year

2.3.2.1 Surface and Groundwater Levels

Water elevations measured at the floodplain surface, piezometer 30 cm BGS, and piezometer 100 BGS at the XS1 centerline were closely related throughout the entire time frame (Figure 3). Water levels generally decreased between June and November. Decreases in groundwater elevation appeared to be correlated with a decrease in rainfall frequency at the site.

There was a reduction in head gradient between the hillslope (Upgradient) and riparian groundwater (Downgradient) during dry periods. The piezometer located at XS1-Center-100 cm appeared to be impacted to a greater degree by the surface water conditions rather than the larger scale head gradients driven by seasonal variations. Water elevations at XS2-Center-100 cm were often either greater or less than both the Upgradient and Downgradient piezometers rather than

being at an elevation between the two as would be expected if water elevations were dictated by upgradient groundwater contributions.

Seasonal variations in groundwater elevation were interrupted by the artificial floods conducted over the course of the year, with the greatest change taking place during the Late Summer and Fall floods. However, the groundwater elevation tend to continue with their seasonal trends following the end of each artificial flood (i.e. Late Summer).

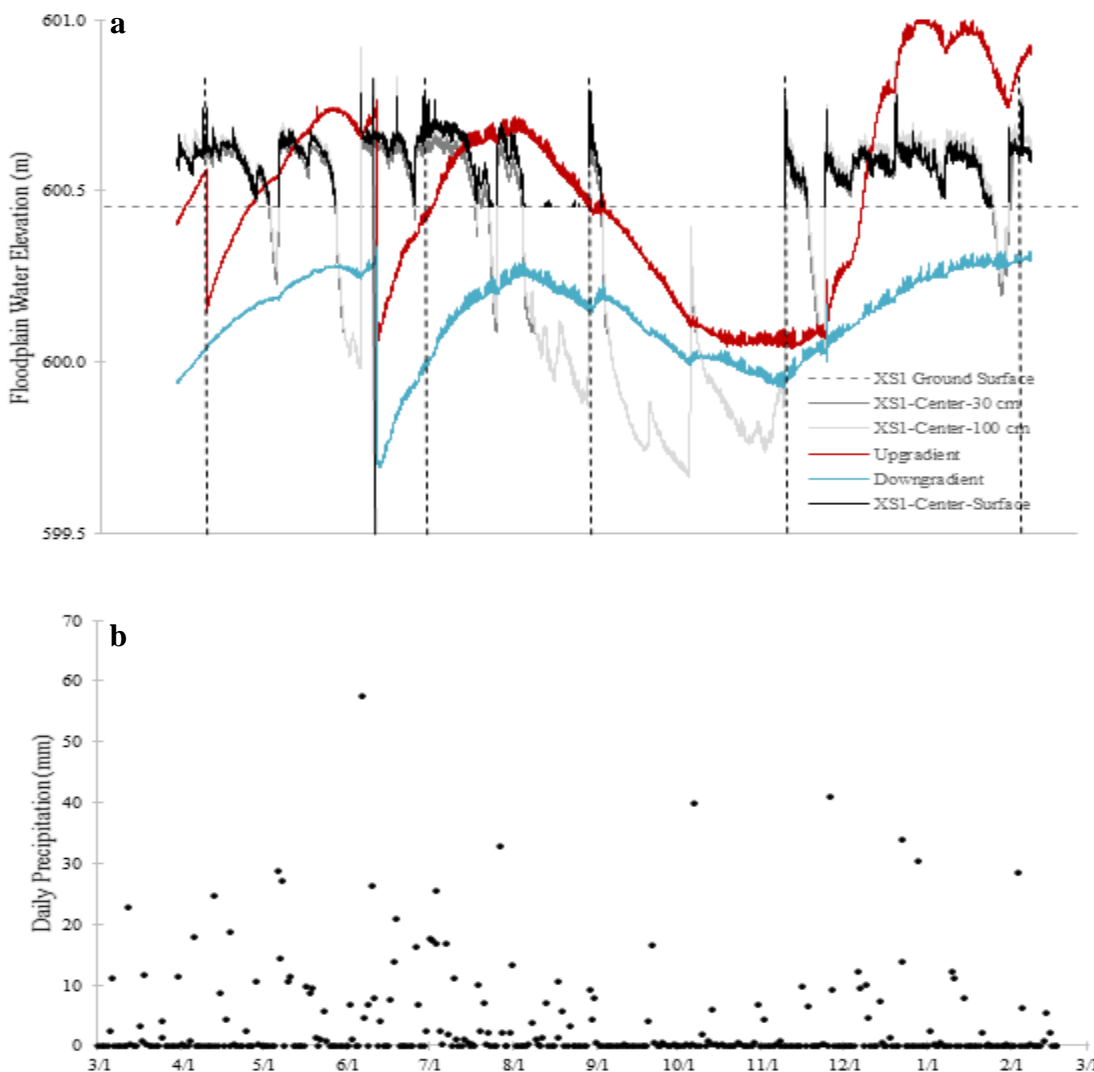


Figure 3: (a) Background surface water and groundwater levels measured at upgradient and downgradient piezometers (100 cm BGS), XS1-Center-Surface, XS1-Center-30 cm (piezometer 30 cm BGS) and XS1-Center-100 cm (piezometer 100 cm BGS) and (b) precipitation at study site from March 2013 through March 2014. Vertical dashed lines signify flood artificial flood events and the vertical solid line signifies the time when rising head tests were performed.

2.3.2.2 Soil Moisture Content

Moisture content decreased throughout the floodplain between March and November (Figure 4). The magnitude of decrease is lower along the floodplain centerline than the transverse locations, and is also lower at XS1 than at XS2 because those locations are topographically lower and were therefore inundated for longer periods. Moisture content increased quickly after each rainfall event (Figure 3).

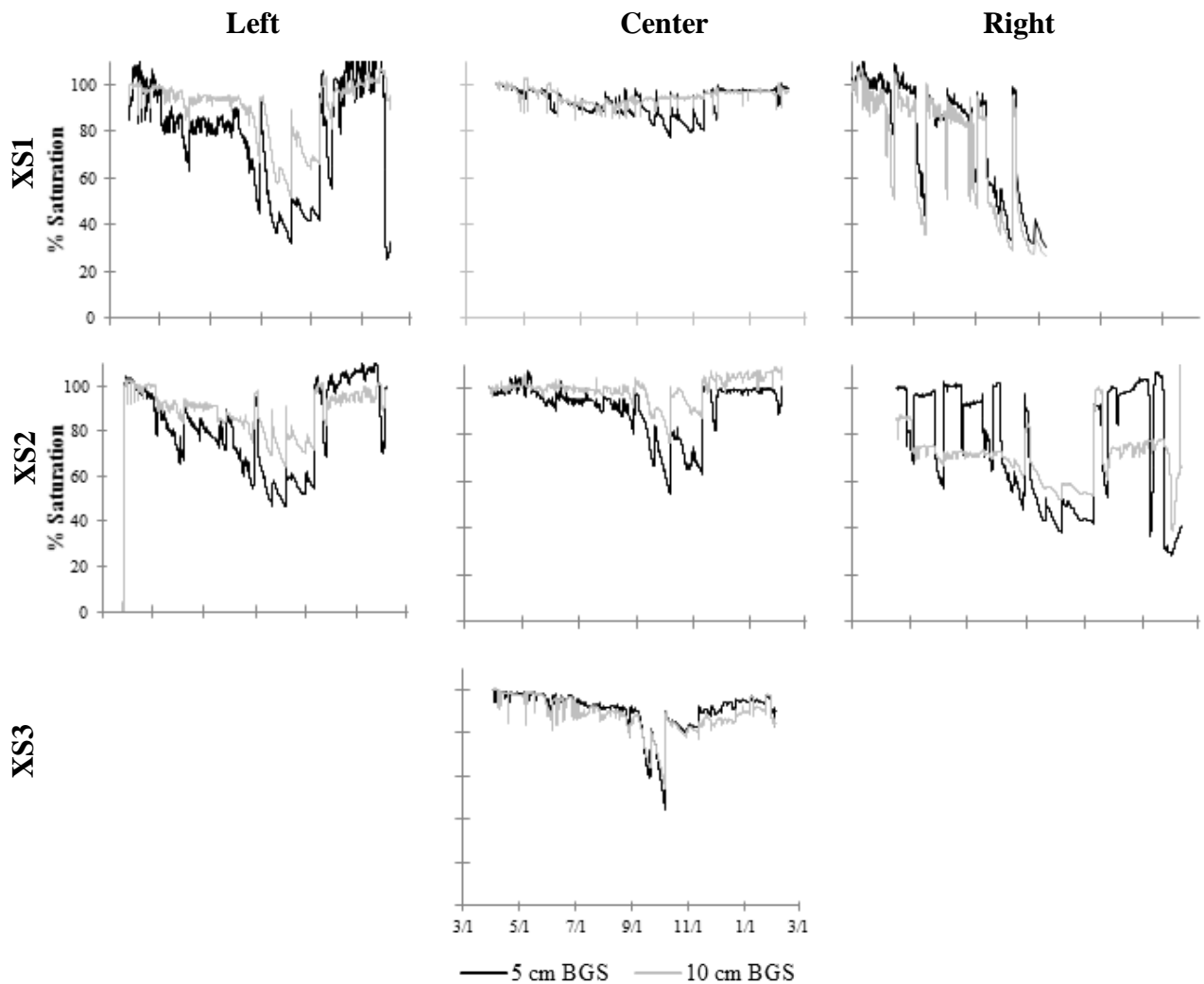


Figure 4: Background moisture content throughout floodplain. Data were not collected from XS1-R for the second half of the year due to malfunction of the data logger being used.

2.3.3 Data Collected During Experimental Floods

2.3.3.1 Site Water Balance

Flow rates of surface water entering and leaving the flood site were measured by the pump flow meter and parshall flume, respectively. In all cases the inflow was approximately equal to the peak outflow at steady state (Figure 5). For this reason, water losses due to leakage of flood water around the flume were likely minor relative to surface flow through the site. The greatest discrepancy ($\sim 1.8 \text{ L s}^{-1}$) between inflow and steady state outflow occurred during the second day of the Fall flood. This difference may be due to inaccuracy of the pump flow meter or unaccounted surface water leaving the site.

Flood wave arrival times were generally earlier during the second day flood than the first due to greater volume of pre-existing water on the floodplain surface (Figure 6c). The one exception is the Spring flood, when floodplain conditions had been saturated for an entire month before the experiment and floodplain inundation prior to flooding was more extensive. This led to identical moisture conditions on each day of flooding and similar volumes of pre-existing water on the floodplain surface during both days. Similarly, earlier flood wave arrival times were observed during the first day flood during Spring, Early Summer, and Winter relative to those in Late Summer and Fall, again due to pre-event standing water and the need for water to fill in topographic depressions during dry floods before outflow is observed. The total storage of flood water (i.e. the water pumped onto the site) was greatest during the Late Summer and Fall flood when antecedent soil moisture and water levels were lowest (Figure 6e).

The volume of drained flood water (normalized to the total water pumped) increased steadily between the Spring and Fall experimental floods (Figure 6a). Assuming the floodplain topography does not change significantly throughout the study duration the drained volume can be used as a surrogate for total surface water storage because the storage occurring due to floodplain topography is likely constant. As the floodplain vegetation density increases from Spring to Summer (Figure 7), the average floodplain roughness increases and may result in slower average water velocities across the surface, assuming constant inflow rate. Therefore, the total surface water volume stored on the floodplain at steady state increases as is reflected in the total drained volume. Although the flume and pump flow rates varied among seasons, a constant flume flow rate indicates steady state being reached at the site.

When determining the relative impact of surface water storage versus groundwater storage, we estimated the storage capacity for each using the assumptions listed in Section 2.2.3.1. The

total subsurface water storage was estimated as being 16.3 m³ during floods with low antecedent soil moisture and water levels while the surface storage was estimated as being 16.1 m³.

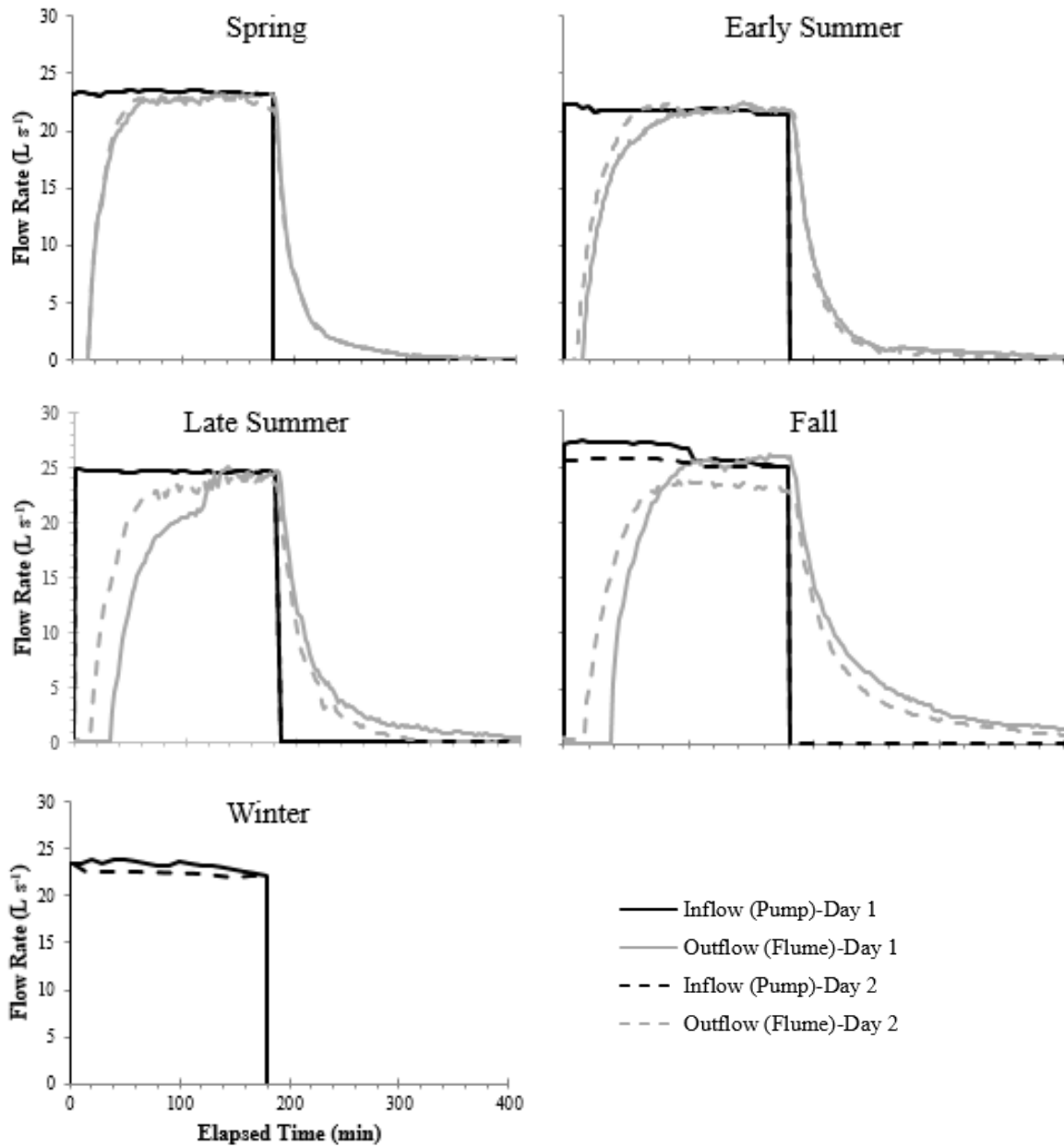


Figure 5: Inflow and outflow of surface water at flood site. Flow rates are shown for both days of each flood, although in some cases similar values make the lines overlap. Flume data were not recorded during the Winter flood due to a malfunction in the HOBO at that location.

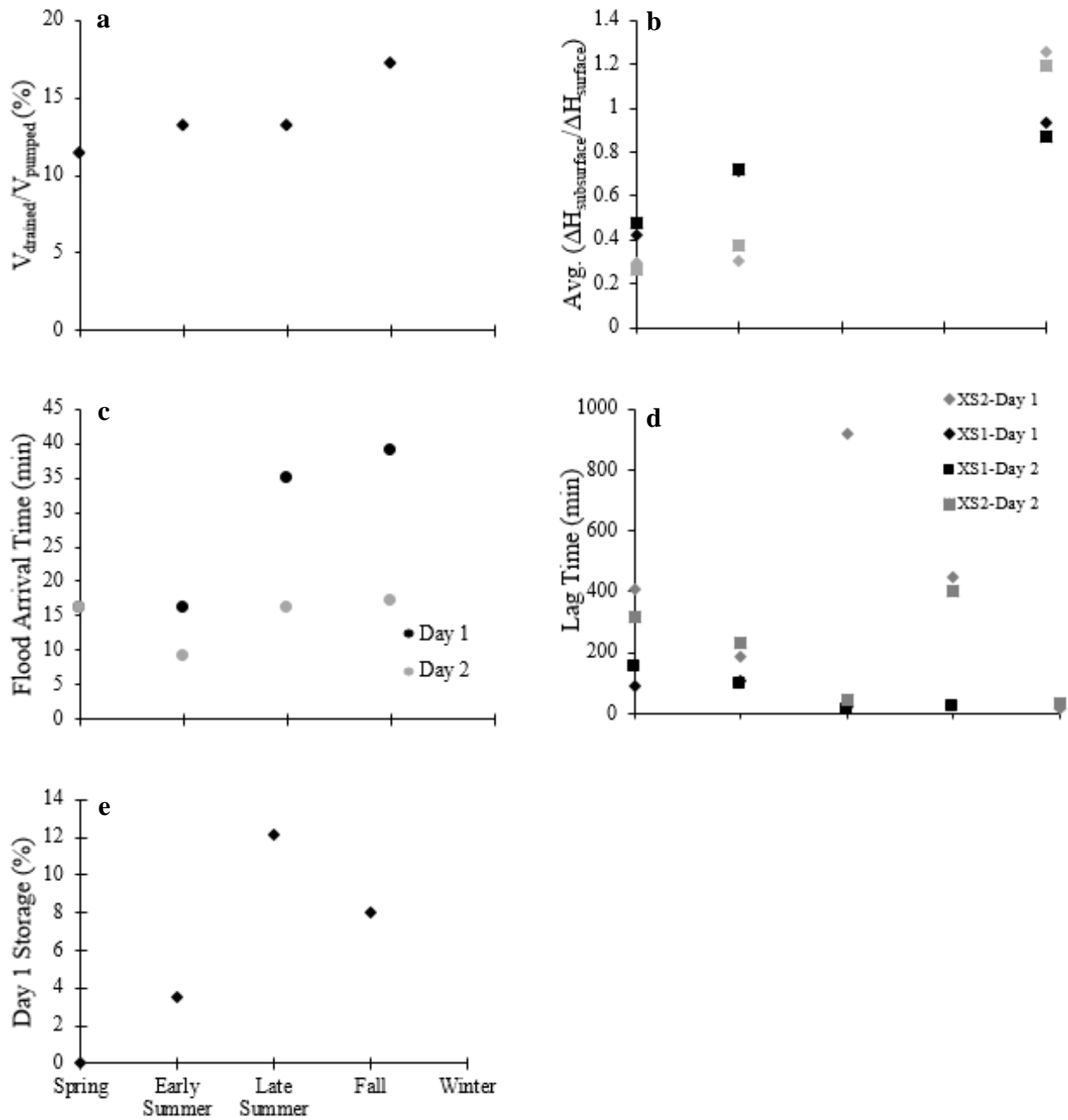


Figure 6: (a) Percent of total water applied to site which drained out of site following the end of each flood, (b) change in groundwater elevation normalized to change in surface water elevation at XS1 and XS2, (c) arrival time of flood pulse at parshall flume following the beginning of each flood, (d) the average lag time between surface water peak elevation and groundwater peak elevation being observed, and (e) total storage as a percent of flood water pumped onto the site during the first day of flooding.



Figure 7: Seasonal variation in floodplain vegetation.

2.3.3.2 Surface Water and Groundwater Levels

Water level data for surface probes showed trends that would be expected, with clear increases and subsequent decreases during each flood event (Figure 8). Three types of pressure response were observed in the subsurface during the floods. In some cases, an immediate response was observed in the subsurface (Figure 8a). However, in other locations a delayed and muted pressure response was recorded (Figure 8b). In contrast, a complete lack of pressure response was observed at XS3 (Figure 8c).

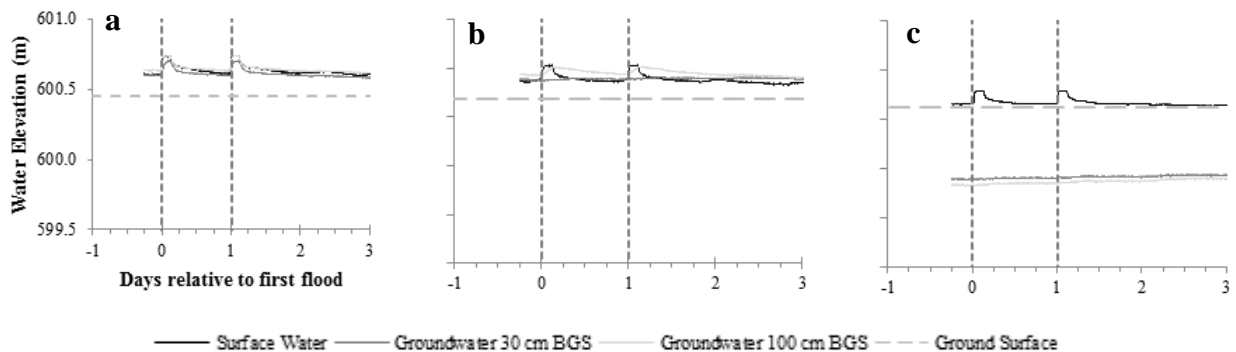


Figure 8: Types of observed pressure responses resulting from the artificial flood events. These data showing the three types of pressure responses were recorded during the Spring flood with floods occurring on April 8, 2013 and April 9, 2013.

2.3.3.3 Vertical Connectivity Between Surface Water and Groundwater

The relationship between groundwater elevation change and surface water elevation change during floods showed a general increase in vertical connectivity over the course of the year (Figure 6b). Similarly, the lag time between observed surface water and groundwater peaks decreases over the course of the year (Figure 6d). These data indicate that an increase in vertical connection may have occurred at the site over the course of the year resulting in groundwater levels increasing quicker and in greater magnitude in response to the application of surface water.

2.3.3.4 Vertical Head Gradients in Surface Water and Groundwater

Vertical gradients at XS1-Center quickly approached neutral conditions during each of the five floods regardless of pre-flood groundwater levels (not shown). By contrast, XS2-Center often showed more pronounced losing conditions at the beginning of the floods, particularly during the first of the two floods in both Late Summer and Fall where antecedent moisture conditions were dryer. Gradients approach neutral during the Winter flood in both XS1 and XS2. Due to minimal vertical connectivity at XS3, vertical head gradients show strong losing conditions. Gradients at XS3-Center become more losing upon the start of pumping due to increases in water level on the floodplain surface with no corresponding changes in water levels in the subsurface.

Arrival times of surface water to each centerline piezometer were calculated using Darcy's Law (Table 3). These arrival times show that if Darcy's law governed surface water-groundwater exchange at the site the required time for surface water to reach each monitoring point would be substantial and range from five hours to multiple years.

Table 3: Darcy travel times between surface and centerline piezometers. The average hydraulic conductivity was used from the two rising head tests performed at the site. The theoretical arrival times were compared to the actual arrival times calculated using the pressure data obtained from the first day of flooding during the Winter flood.

Piezometer	Darcy Arrival Time (hrs)	Actual Arrival Time (min)
XS1-Center-30 cm	5	7
XS1-Center-100 cm	12	3
XS2-Center-30 cm	4	0
XS2-Center-100 cm	566	30
XS3-Center-30 cm	42088	N/A
XS3-Center-100 cm	69288	N/A

2.3.3.5 Soil Moisture Content

Prior to the Spring, Early Summer, and Winter floods, shallow soil moisture content was the same (saturated) throughout the site. By contrast, soil moisture was lowest during the Late Summer and Fall floods. Soil probes located at 5 cm BGS generally experienced the greatest fluctuation in moisture conditions indicated by a greater reduction in moisture content between Early Summer (saturated) and the beginning of the Late Summer flood compared to soil probes located at 10 cm BGS (Figure 9). Due to the flow centerline being topographically lower than the transverse monitoring locations, moisture fluctuations are less pronounced in these three locations.

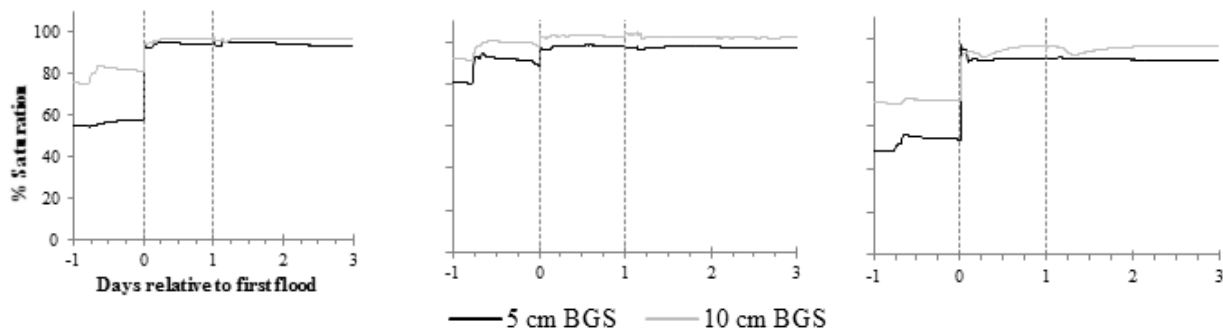


Figure 9: Percent saturation in shallow subsurface during Late Summer flood event. Soil moisture content at XS2 is representative to other soil moisture data collected during the Late Summer. These floods were completed on August 30, 2013 and August 31, 2013.

The arrival of the moisture front following the start of flood events with low antecedent moisture conditions (i.e. Late Summer and Fall) showed increases in moisture content at both depths occurring simultaneously with surface inundation (Figure 10). An increase in soil moisture content 5 cm BGS would be observed before an increase 10 cm BGS if vertical infiltration were occurring. The moisture front may therefore be moving laterally across the clay layer as the flood begins. Without higher temporal resolution data distinguishing between quick vertical infiltration and horizontal flow may not be possible. However, particularly during Late Summer, the soil moisture 10 cm BGS appears to have increased prior to 5 cm BGS, which is consistent with horizontal flow across the top of the clay layer.

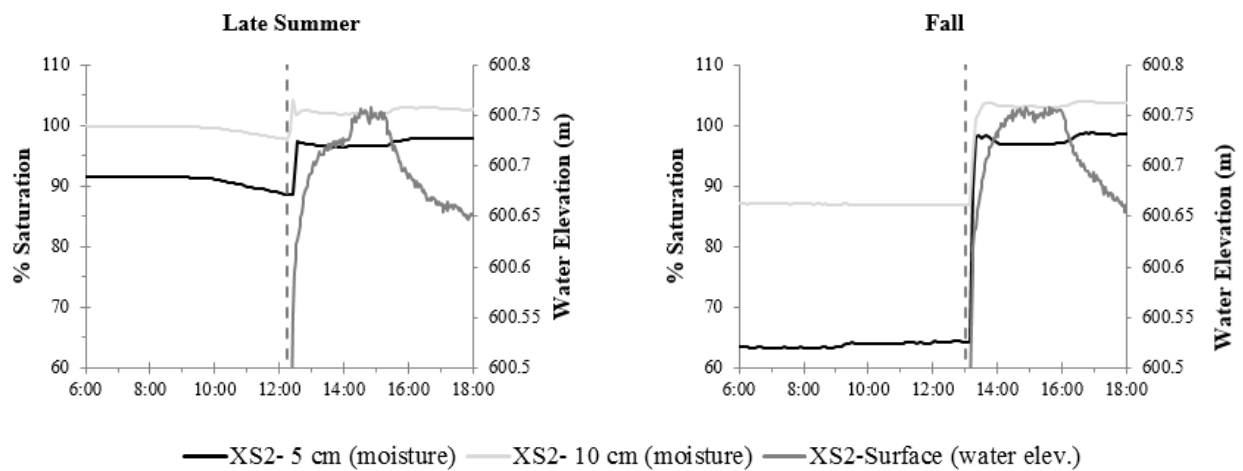


Figure 10: Moisture front at XS2 centerline during Late Summer and Fall floods

2.3.3.6 Electrical Conductivity in Surface Water and Groundwater

The specific conductance (SC) trends were fairly complex, so we focus here on two main types of responses during the experimental floods. The first is due to the salt injection pulse that occurred 120 minutes after start of each flood. A clear spike is often observed in surface water. Some surface water measurements showed a step increase and/or no response to the pulse injection during the Early Summer and Fall events while XS2-Center-Surface showed no pulse signal in any flood (not shown). This variation in surface SC signal was likely a result of surface water flow paths changing with vegetation density and/or changes in water velocity affecting exchange between the water column and the stilling well interior.

The second type of response is due to the pumping of stream water onto the floodplain. The SC of water on the floodplain surface approached the SC recorded in Stroubles Creek during each flood event. Three types of groundwater SC responses were observed from the application of surface water. The first response was a step increase in groundwater SC with no decrease following the end of pumping (Figure 11b). This type of response was most common during floods when antecedent moisture conditions were low (i.e. Late Summer and Fall). The second type of response was a pulse increase (Figure 11a). This rise and fall of groundwater SC coincides with the pump being turned on and off during each experiment. Not shown are data from the Fall flood in which SC recorded at XS2-Center-30 cm increased at the start of flooding and decreased approximately three hours following the pump being turned off. The third type of response is no SC response at all (Figure 11c). Although variability exists in SC response in groundwater throughout the first four floods, no change in groundwater SC occurred during the Winter flood throughout the entire site.

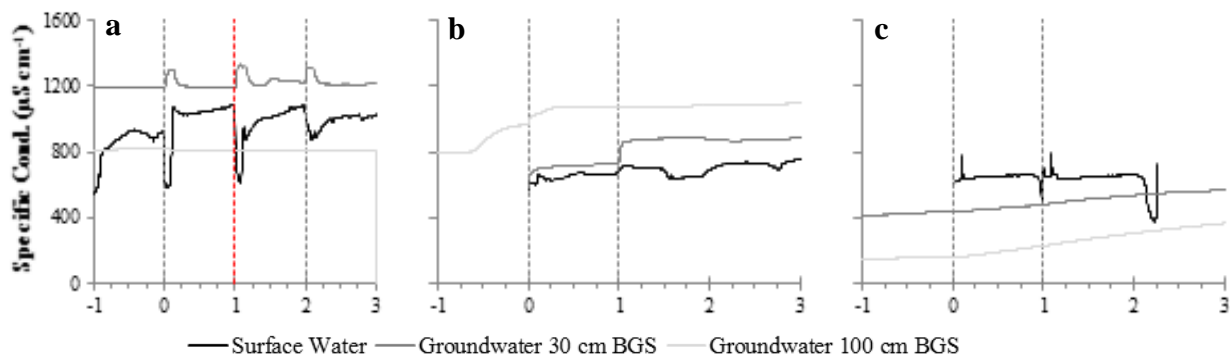


Figure 11: Observed responses in surface water and groundwater electrical conductivity during artificial flood events. Response type (a) was recorded during the Early Summer flood (June 29, 2013) and response types (b) and (c) were observed during the Late Summer flood where flooding began on August 30, 2013. Red vertical line signifies a flood event where a malfunction occurred and repeating the flood was necessary

2.3.3.7 Temperature in Surface Water, Groundwater, and Soil

Diel temperature fluctuations were greatest in surface water and decreased with depth BGS (not shown). Surface temperature fluctuations were greatest during the Spring and Fall floods due to greater diel air temperature variability during those seasons. Subsurface temperature fluctuations were greatest during the Late Summer and Fall floods due to decreased moisture content in soils. The presence of ice on the floodplain during the Winter flood reduced subsurface temperature variation. A reversal in temperature gradients at the site takes place between the Late Summer and Fall floods due to a drop in air temperatures.

Flood events had little to no effect on subsurface temperatures but had a direct impact on surface temperatures. Due to stream water being warmer than the pre-existing water on the floodplain surface during the Winter flood, clear increases in surface water temperatures were observed for this event.

2.4 Discussion

2.4.1 Background Hydraulics

Groundwater elevations monitored throughout the site show seasonal water level variations. Head gradients between the Upgradient piezometer and the Downgradient piezometer are continually in the direction of the stream channel. During dry periods this gradient reduces in magnitude as expected, but a reversal in gradient never occurs. A comparison of water elevations at the floodplain surface and elevations recorded in the Upgradient and Downgradient piezometers shows evidence that locations in the inundated area are predominantly influenced by vertical infiltration rather than lateral inflow. This is based on groundwater elevations in the flooded area often exceeding or dropping lower than both the Upgradient and Downgradient groundwater elevations. The paleochannel that XS1-Center-100 cm is screened in is likely allowing quick transport of groundwater compared to the transport rates through the clay layer above causing a draining effect throughout the floodplain. Although the output of the PFP created by the gravel layer cannot be determined based on the soils data we collected, heterogeneity of floodplain sediments may be leading to heterogeneity in exchange mechanisms.

2.4.2 Spatial and Temporal Variation in Types of Vertical Connectivity

Exchange between surface water and floodplain groundwater is a key mechanism behind water quality transformations during overbank flooding. Although the overall magnitude of exchange of water between surface water and groundwater within the swale during the experiment was negligible from the perspective of surface water balance (see Section 2.2.3.1), evidence of exchange is present in the subsurface. We evaluated such vertical connectivity using the surface/subsurface monitoring network described in the Methods which measured SC, pressure, and temperature data throughout the flood area. These different kinds of data in combination allow us to surmise the different exchange mechanisms that are dominant in different parts of the floodplain and during different flood events. We found evidence of preferential flow and immediate propagation of hydrostatic pressure (i.e. pressure wave) in the data (Table 4). Knowing that Darcy flow, described as laminar flow through porous media driven by hydraulic head gradients where viscous forces dominate [*Darcy*, 1856], must be occurring to some degree we then also see a combination of Darcy flow and preferential flow. We observed varying response times in groundwater, yet these were too quick to be described by the Darcy arrival times (Table 3). Without more detailed soils data, distinguishing between slow PFPs and Darcy flow becomes difficult. In our experiments, we refer to Darcy groundwater flow where preferential flow is absent

as Darcy flow through bulk sediments or bulk Darcy flow. Non-Darcy flow is flow at higher Reynolds numbers where inertial forces start to become important. Preferential flow is either Darcy or non-Darcy flow that occurs through either higher K areas of the soil or through void spaces formed by animal burrows or root channels [Aubertin, 1971; Beasley, 1976; Beven and Germann, 1982]. The mechanisms for hydrostatic pressure propagation into the subsurface (pressure wave) are not well understood but appear to be heterogeneous within small spatial scales [Käser *et al.*, 2009; Vidon, 2012]. In some cases none of these mechanisms applied and no groundwater response was observed during floods.

Table 4: SW-GW Vertical Connectivity Classifications

Type of Vertical Connectivity	Observed subsurface signal in response to application of surface water and tracer
Hydrostatic Pressure Propagation	Pressure responds immediately and in parallel with changes in surface water elevation. No change in temperature or EC.
Preferential Flow	Pressure increases immediately following the application of surface water, but peak is delayed relative to hydrostatic propagation. Yet peak occurs too early to be explained by Darcy flow. EC and/or temperature also shift toward those of surface water.
Darcy Flow through Bulk Sediments (Bulk Darcy Flow)	Pressure increases following the application of surface water, but increase is delayed relative to preferential flow or hydrostatic propagation. EC and/or temperature also shift toward those of surface water.
Lack of Connectivity	No change in pressure, temperature, or EC.

Subsurface pressure and SC signals during each flood event at the XS1-Center-100 cm piezometer were consistent with hydrostatic pressure propagation into the subsurface. By contrast, subsurface signals at the XS2-Center-100 cm piezometer were consistent with a mix of bulk Darcy flow and preferential flow. Based on the hydraulic conductivity at XS2-Center-100 cm and the depth to measuring point, the peak in water elevation occurs too quickly to be explained by Darcy flow alone. It is therefore likely that the dominant flow mechanism is either a combination of preferential flow and bulk Darcy flow, or rather a slower preferential flow path. Preferential flow influencing XS2-Center-100 cm is particularly apparent based on the lack of signal in XS2-Center-30 cm. Distinguishing between these two processes may only be possible with greater spatial resolution of floodplain soil structure allowing for a clearer picture of where soil strata and PFPs

such as soil pipes are located. The tracer concentration in XS2-Center-100 cm has the greatest change in SC during the Late Summer and Fall floods, both of which had dry antecedent moisture conditions. For each of these events the SC measured at XS2-Center-100 cm approaches the surface SC. When high antecedent moisture conditions were present (i.e. Spring, Early Summer, and Winter) the SC measured in the subsurface did not change during the flood. Mixing of infiltrating surface water with pre-existing groundwater may have resulted in this lack of SC signal.

Preferential flow is likely occurring in XS1-Center-30 cm. The pressure signal recorded at this location mirrors the changes in pressure on the floodplain surface. Unlike cases where bulk Darcy flow would be the governing flow mechanism, the increases and subsequent decreases in pressure are not delayed. The pressure signal is not merely an increase in hydrostatic pressure because SC also starts to increase and peaks at the same times (Figure 12).

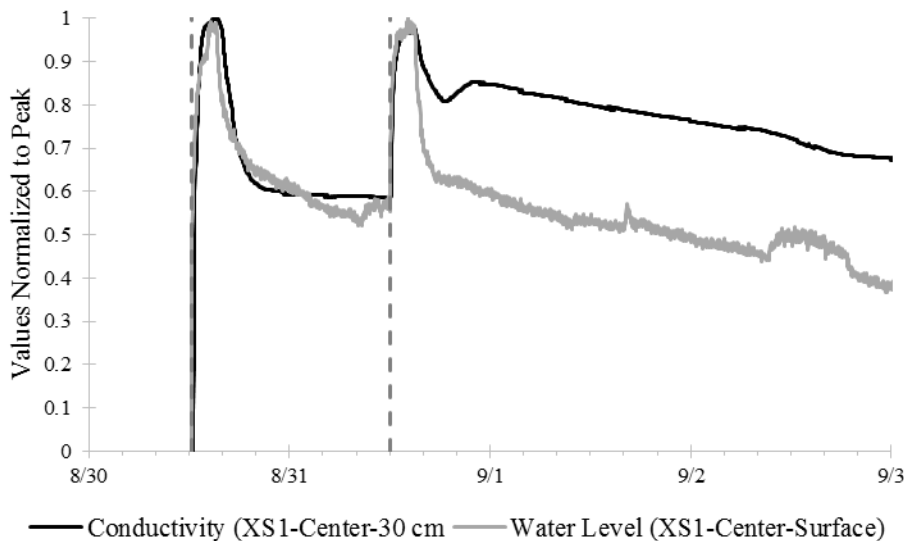


Figure 12: Water level and SC normalized to peak values during Late Summer.

While many piezometers in the groundwater monitoring network exhibited varying degrees of vertical connection, XS3-Center-30 cm and XS3-Center-100 cm consistently show a lack of vertical connectivity with no changes in SC, temperature, or pressure during and immediately following flood events. This lack of connection is observed despite high moisture conditions at XS3 during the Spring, Early Summer and Winter floods. Higher moisture content can increase the hydraulic conductivity of soil and therefore increase vertical connectivity [Pirastru and Niedda, 2013].

With the exception of XS3, groundwater levels during floods indicate an increase in vertical connectivity over the course of the year (Figures 6c and 6d). This increase in vertical connectivity was largely a result of the expansion of pressure propagation with only a few piezometers

indicating transport of water occurring. Increases in pressure propagation and preferential flow paths may have been a result of soil piping. This can occur at the interface of two soils with considerably different hydraulic conductivities [Jones, 1971], which appears to be the case at our site. The water levels applied to the site during floods exceeded those present during natural storm events over the course of the experiment duration. This increase in head resulting from a greater surface water depth may have accelerated the formation of PFPs through increases in erosion. Furthermore, the more frequent inundation and application of nutrients in the surface water may have led to greater vegetation root structure and/or floodplain habitat and further increased preferential flow between the floodplain surface and subsurface.

The hydraulic conductivity measured throughout the inundated area of the floodplain at the beginning of the experiment duration and the end varied between one and three orders of magnitude. However, the vertical connectivity between the surface and subsurface increased from no propagation of signal to showing an immediate propagation of pressure signal. Therefore, the PFPs are likely beyond the extent of the bulk soil measured by the rising head tests and therefore the increase in abundance of PFPs may not be directly observed through performing rising head tests.

While pressure and SC signals are heterogeneous throughout the subsurface, temperature data do not show the same variability. Little to no deviation from the background daily temperature fluctuation is observed in the subsurface.

2.4.3 Seasonal Effects

Changing seasons strongly affected vegetation density in the experimental flood area (Figure 7). Due to unseasonably wet conditions during the first half of the summer, the Spring and Early Summer floods had essentially identical antecedent moisture conditions (i.e. saturated soils), which allowed us to control for moisture and attribute observed changes to effects of vegetation density and/or evapotranspiration. The increase in vegetation density between these two events increased the floodplain roughness leading to an increase in the drained volume of surface water (Figure 6a). Surface water storage due to floodplain topography is likely relatively constant over the course of the year and the volume of drained water can therefore be used as a surrogate for the total surface water storage. With equivalent inflow discharge onto the site greater surface water storage volume will result in an increased residence time and therefore slower average surface water velocities. The increase in total surface water storage, as is evident by the corresponding

increase in drained surface water volume, can influence surface water elevations. This change has the potential to then impact the vertical head gradients which drive SW-GW exchange.

The total drained volume continually increased between the Spring and Fall floods despite the greatest vegetation growth occurring during the Summer. The dieback and consequent collapse of floodplain vegetation prior to the Fall flood appears to concentrate more biomass in the water column than when the vegetation is upright during the summer floods. This creates a correspondingly greater impact on floodplain hydraulic roughness and hence results in greater total surface water storage during the Fall compared to the Summer. In other words, rather than the vegetation height or growth status, the most important factor appears to be the amount of vegetation that directly impedes surface flow [Luhar and Nepf, 2013]. This information can be used in future restoration designs by incorporating shorter vegetation (e.g. shrubs and tall grasses) rather than large trees due to the greater impact short and dense land cover has on overbank flow

2.4.4 Antecedent Moisture Effects

Surface water levels, groundwater levels, and soil moisture content prior to the first day of flooding influenced surface water and groundwater hydraulics during the floods. When antecedent soil moisture and water levels were low and there was no standing water prior to the first flood (i.e. Late Summer and Fall) the arrival of surface water at the outlet was much later (relative to the start of pumping) than during floods where the floodplain was saturated and had standing water (i.e. Spring, Early Summer and Winter) (Figure 6c). Vegetation conditions were nearly identical during the Early and Late Summer floods, which allowed us to attribute observed differences to changes in antecedent soil moisture and water levels. While the total volume drained from the site following the pump being turned off was almost identical between these two floods (Figure 6a) the storage of applied flood water was greatest during the Late Summer (Figure 6e). Therefore, while the vegetation density impacts the total surface water storage (i.e. pre-event water and applied surface water), antecedent moisture conditions directly affect the storage of applied surface water (i.e. not considering pre-existing water). In addition to antecedent soil moisture and water levels, the floodplain topography is also a driving factor for how much flood water (i.e. applied water) will be stored during flood events. The increase at this site can be largely attributed to the topographic depression located near XS1 and XS2 at this site and the ability for the floodplain to naturally retain water at the surface.

The storage volume of applied surface water (Equation 1, Equation 2, and Figure 6e) was much higher during floods with low antecedent moisture conditions and is likely dictated by the

floodplain topography along with sediment porosity and hydraulic conductivity. The estimated surface water storage due to floodplain topography (16.1 m^3) is assumed to be constant throughout each flood regardless of antecedent conditions because the floodplain topography is the parameter that controls this storage volume. The subsurface storage during floods with low antecedent soil moisture and water levels (16.3 m^3) is likely a severe overestimate based on data that show lack of water transport to many piezometers. Furthermore, the hydraulic conductivity is quite low throughout the floodplain and rather than uniform infiltration throughout, the infiltration is likely localized near PFPs leading to a much smaller volume of water stored in the subsurface than estimated here. Assuming the actual subsurface storage volume is actually much lower than what was calculated, we see that surface water storage has the greatest effect on the flood water balance.

Antecedent moisture conditions did not appear to affect the type of flow mechanism present at each monitoring location as is seen by the consistent increase in pressure signal propagation between the Spring and Winter floods. However, lower antecedent moisture conditions and water levels resulted in a greater increase in groundwater levels compared to floods which had higher water levels prior to flooding. Increases in SC signal in the subsurface were also observed during floods with low antecedent moisture conditions likely due to reduced mixing between the surface water and pre-existing groundwater. Therefore, antecedent moisture has the greatest impact on the magnitude of water elevation and SC change in the subsurface but the methods in which these signals reach the monitoring locations are not directly affected.

Antecedent soil moisture and water levels had the greatest effect on the hydraulic response to the application of surface water. For example, the arrival time of the flood pulse and subsurface storage volumes were directly affected. While the change in seasons affected the total storage volume, the increase in vegetation density may have also influenced preferential flow at the site due to increased root structure. The effects associated with each parameter were similar in magnitude and appeared to alter the hydraulic response to flooding independently from each other.

2.4.5 Implications of Heterogeneous Flow Mechanisms

Floodplains act as a potential hotspot for biogeochemical reactions due to steep redox gradients and contact between stream water and floodplain sediments. The effectiveness of floodplains for removing pollutants is directly dependent on the hydraulics during overbank storm events [Helton *et al.*, 2012]. Although the overall magnitude of exchange of water between surface water and groundwater during the experiment appeared to be minor, evidence of exchange nevertheless is present in the groundwater levels (Figure 8). Our data indicate that multiple flow

mechanisms are likely occurring within a small area of floodplain. It is therefore unreasonable to assume that the subsurface of floodplains and riparian areas are generally homogeneous [Bates *et al.*, 2000; Krause *et al.*, 2007]. This makes field assessment and also numerical modeling of floodplain groundwater flow and surface water-groundwater interactions in floodplains more difficult. In such a setting, traditional point measurement methods like those using piezometers may be less useful than more recently developed distributed methods like electrical resistivity imaging or distributed temperature sensing [Menichino *et al.*, 2014; Selker *et al.*, 2006].

Nevertheless, multiple flow mechanisms through the floodplain subsurface may offer benefits. Darcy flow allows for the greatest contact time and therefore results in the greatest potential for reactions. Preferential flow has the ability to enhance transport of flood water into the subsurface depending on the nature of the PFP outlet (e.g. enclosed in clay vs open outlet into adjacent stream) [Nieber, 2000]. Although the quick transport of flood water through PFPs back to the surface or channel reduces the contact between the water column and floodplain sediments, PFPs are beneficial when they allow for the quick conveyance of flood water to bypass restrictive (low K) layers to depths where high K sediments are prevalent. This may allow for greater contact with roots and redox conditions conducive for biogeochemical reactions [Fuchs *et al.*, 2009; Heeren *et al.*, 2010]. This is of particular interest in areas where the restrictive layer is extensive and infiltration rates governed by Darcian flow are drastically reduced.

Increases in floodplain vegetation density indicated a greater storage volume of flood water and therefore the average residence time of flood water was likely increased. This allows for increased sediment deposition [Kronvang *et al.*, 2007] and contact with terrestrial plants that can increase nutrient removal via plant uptake [Lewandowski and Nützmann, 2010]. Antecedent moisture affected the total fraction of flood water stored on the floodplain, with low antecedent moisture allowing for greater storage of applied flood water.

2.4.6 Limitations of Study

Vegetation was most dense along the flow centerline due to the highest frequency of inundation in that area. When visually comparing vegetation density at the time of instrument installation (March, 2013) to the density at the end of the experimental year (March, 2014) it is clear that the flood events themselves significantly altered the natural vegetation growth and decay patterns. Nutrients were added during each flood to quantify surface water quality and biogeochemical parameters as part of a separate study [Jones *et al.*, In Preparation]. This seasonal application of nutrients likely accelerated vegetation growth within the flooded area.

Our experiment improves understanding regarding how repeated inundation affects floodplain hydraulics and transport across the floodplain surface, yet these floods do not fully replicate conditions during natural overbank events. In our experiment, the application of surface water on the floodplain surface was decoupled from an increase in stream stage. Variations in groundwater elevation as a result of changing stream stage have been well documented [*Burt et al.*, 2002; *Jung et al.*, 2004; *Sawyer et al.*, 2009] and by not having an increase in stream stage in our experimental setup we must assume that during natural events the groundwater levels near the stream would have increased as stream stage approached overbank elevation. Changes in background water elevation and groundwater flow rates into our site were also not affected as they may have been during a natural rainfall event [*Burt et al.*, 2002]. Additionally, surface water runoff from the adjacent hillslope and direct precipitation onto our site were not factors due to the localized nature of our experiments. The presence of hillslope runoff can directly affect the surface water hydraulics and impact mixing and storage of flood water [*Mertes*, 1997].

2.5 Conclusions

Exchange mechanisms were variable throughout the year and highly heterogeneous in space, coexisting in small areas. The dominant exchange mechanism(s) do not appear to be dependent on season or moisture variations as was evident by the consistent increase in vertical connectivity experienced over the course of one year. The presence of a paleochannel beneath the flooded area added to the heterogeneity, increasing the range of hydraulic conductivity of floodplain sediments to five orders of magnitude. A key conclusion is that the act of flooding itself appears to increase surface water-groundwater exchange across the floodplain surface. Our artificial increase in flooding at our field had this effect.

Changes in season led to noticeable changes in vegetation density at the floodplain surface. These changes directly influenced the floodplain roughness and resulted in greater surface water storage during periods where vegetation was most dense. Although vegetation growth was greatest during the summer floods, the matting down of this vegetation during the Fall resulted in the greatest surface water storage. By increasing total storage the average surface water residence time likely increased as well, which has the potential to decrease nutrient loads through contact with vegetation and/or sediment deposition. Fully understanding the effect of these hydraulic parameters on nutrient cycling is important when determining the potential benefits stemming from floodplain reconnection [*Jones et al.*, In Preparation]. The hydraulic complexity seen in this

study suggests that a more accurate quantification of floodplain hydraulics may be obtained through the use of distributed methods that give a more holistic picture of groundwater movement.

Antecedent soil moisture and water levels altered the magnitude of elevation change seen in groundwater levels during floods. Greater increase was observed when antecedent moisture conditions were low compared to periods where antecedent moisture conditions were high. There was stronger evidence of solute migration into the subsurface with low antecedent moisture conditions due to a decrease in pre-existing groundwater volume. Of potentially more importance is the increasing fraction of applied flood water stored on the floodplain as antecedent moisture conditions decreased. This is important because as the stream stage recedes following the flood event, stored surface water will remain present on the floodplain. This water then has the ability to infiltrate into the groundwater and the potential for nutrient removal is much greater. Results from this study can be used to engineer more effective sites for stream restoration. Greater topographic complexity and vegetation density will allow for increased flood water retention and therefore increase the potential for nutrient removal.

2.6 Acknowledgements

The authors thank the National Science Foundation (ENG-CBET-1066817) for support. Opinions expressed here are those of the authors and not necessarily those of the NSF. The authors thank Cully Hession and Laura Lehmann for access to the VT BSE StREAM Lab and the many volunteers for their field assistance.

2.7 References

- Amoros, C., and G. Bornette (2002), Connectivity and biocomplexity in waterbodies of riverine floodplains, *Freshw. Biol.*, 47(4), 761-776.
- Andersen, H. E. (2004), Hydrology and nitrogen balance of a seasonally inundated Danish floodplain wetland, *Hydrological Processes*, 18(3), 415-434.
- Aubertin, G. M. (1971), *Nature and extent of macropores in forest soils and their influence on subsurface water movement*, Northeastern Forest Experiment Station.
- Bates, P. D., M. D. Stewart, A. Desitter, M. G. Anderson, J. P. Renaud, and J. A. Smith (2000), Numerical simulation of floodplain hydrology, *Water Resources Research*, 36(9), 2517-2529.
- Bear, J. (2012), *Hydraulics of groundwater*, Courier Dover Publications.
- Beasley, R. S. (1976), Contribution of subsurface flow from the upper slopes of forested watersheds to channel flow, *Soil Science Society of America Journal*, 40(6), 955-957.

- Berg, J., J. Burch, D. Cappuccitti, S. Filoso, L. Fraley-McNeal, D. Goerman, N. Hardman, S. Kaushal, D. Medina, and M. Meyers (2014), Recommendations of the Expert Panel to Define Removal Rates for Individual Stream Restoration Projects *Rep.*
- Bernhardt, E. S., et al. (2005), Ecology - Synthesizing US river restoration efforts, *Science*, 308(5722), 636-637.
- Beven, K., and P. Germann (1982), Macropores and water flow in soils, *Water resources research*, 18(5), 1311-1325.
- Boon, P. J. (1998), River restoration in five dimensions, *Aquatic Conservation: Marine and Freshwater Ecosystems*, 8(1), 257-264.
- Booth, D. B. (1990), Stream-channel incision following drainage-basin urbanization, *JAWRA Journal of the American Water Resources Association*, 26(3), 407-417.
- Bramley, H., J. Hutson, and S. D. Tyerman (2003), Floodwater infiltration through root channels on a sodic clay floodplain and the influence on a local tree species *Eucalyptus largiflorens*, *Plant and Soil*, 253(1), 275-286.
- Bukaveckas, P. A. (2007), Effects of channel restoration on water velocity, transient storage, and nutrient uptake in a channelized stream, *Environmental Science & Technology*, 41(5), 1570-1576.
- Burt, T. P., P. D. Bates, M. D. Stewart, A. J. Claxton, M. G. Anderson, and D. A. Price (2002), Water table fluctuations within the floodplain of the River Severn, England, *Journal of Hydrology*, 262(1), 1-20.
- Craig, L. S., et al. (2008), Stream restoration strategies for reducing river nitrogen loads, *Frontiers in Ecology and the Environment*, 6(10), 529-538.
- Dahan, O., B. Tatarsky, Y. Enzel, C. Kull, M. Seely, and G. Benito (2008), Dynamics of flood water infiltration and ground water recharge in hyperarid desert, *Ground Water*, 46(3), 450-461.
- Darcy, H. (1856), *Les fontaines publiques de la ville de Dijon*.
- Doble, R. C., R. S. Crosbie, and B. D. Smerdon (2011a), Aquifer recharge from overbank floods, *IAHS-AISH publication*, 169-174.
- Doble, R. C., R. S. Crosbie, B. D. Smerdon, L. Peeters, and F. J. Cook (2012), Groundwater recharge from overbank floods, *Water Resources Research*, 48, 14.
- Doble, R. C., R. S. Crosbie, B. D. Smerdon, L. Peeters, F. Chan, D. Marinova, and R. S. Andersson (2011b), Examining the controls on overbank flood recharge for improved estimates of national water accounting.
- Doll, B. A., D. E. Wise-Frederick, C. M. Buckner, S. D. Wilkerson, W. A. Harman, R. E. Smith, and J. Spooner (2002), Hydraulic geometry relationships for urban streams throughout the piedmont of north carolina1, *JAWRA Journal of the American Water Resources Association*, 38(3), 641-651.

- Dunne, T. (1978), *Water in environmental planning*, Macmillan.
- Fuchs, J. W., G. A. Fox, D. E. Storm, C. J. Penn, and G. O. Brown (2009), Subsurface transport of phosphorus in riparian floodplains: Influence of preferential flow paths, *Journal of environmental quality*, 38(2), 473-484.
- Graf, W. L. (1975), The impact of suburbanization on fluvial geomorphology, *Water Resources Research*, 11(5), 690-692.
- Harrison, M. D., P. M. Groffman, P. M. Mayer, S. S. Kaushal, and T. A. Newcomer (2011), Denitrification in alluvial wetlands in an urban landscape, *Journal of environmental quality*, 40(2), 634-646.
- Haycock, N. E., and T. P. Burt (1993), Role of floodplain sediments in reducing the nitrate concentration of subsurface run-off: A case study in the Cotswolds, UK, *Hydrological Processes*, 7(3), 287-295.
- Heeren, D. M., R. B. Miller, G. A. Fox, D. E. Storm, T. Halihan, and C. J. Penn (2010), Preferential flow effects on subsurface contaminant transport in alluvial floodplains.
- Helton, A. M., G. C. Poole, R. A. Payn, C. Izurieta, and J. A. Stanford (2012), Scaling flow path processes to fluvial landscapes: An integrated field and model assessment of temperature and dissolved oxygen dynamics in a river-floodplain-aquifer system, *Journal of Geophysical Research-Biogeosciences*, 117, 13.
- Helton, A. M., G. C. Poole, R. A. Payn, C. Izurieta, and J. A. Stanford (2014), Relative influences of the river channel, floodplain surface, and alluvial aquifer on simulated hydrologic residence time in a montane river floodplain, *Geomorphology*, 205, 17-26.
- Hester, E. T., and M. W. Doyle (2008), In-stream geomorphic structures as drivers of hyporheic exchange, *Water Resources Research*, 44(3).
- Hester, E. T., and M. N. Gooseff (2010), Moving Beyond the Banks: Hyporheic Restoration Is Fundamental to Restoring Ecological Services and Functions of Streams, *Environmental Science & Technology*, 44(5), 1521-1525.
- Hofmeister, K., T. Weiglan, C. N. Jones, D. T. Scott, and E. T. Hester (2012), Experimental Flooding of a Restored Floodplain within an Urbanized Watershed.
- Hvorslev, M. J. (1951), Time lag and soil permeability in ground-water observations, *U.S. Army Corps of Engineers Waterways Experiment Station, Bulletin 36. Vicksburg, MS.*
- Jolly, I. D., G. R. Walker, and K. A. Narayan (1994), Floodwater recharge processes in the Chowilla anabranch system, South Australia, *Soil Research*, 32(3), 417-435.
- Jones, D. T. Scott, E. T. Hester, and C. R. Guth (In Preparation), Seasonal Variation in Biogeochemical Processing of a Restored, Headwater Floodplain in Central Appalachia.
- Jung, M., T. P. Burt, and P. D. Bates (2004), Toward a conceptual model of floodplain water table response, *Water Resources Research*, 40(12), 13.

- Junk, W. J., P. B. Bayley, and R. E. Sparks (1989), The flood pulse concept in river-floodplain systems, *Canadian special publication of fisheries and aquatic sciences*, 106(1), 110-127.
- Käser, D. H., A. Binley, A. L. Heathwaite, and S. Krause (2009), Spatio-temporal variations of hyporheic flow in a riffle-step-pool sequence, *Hydrological Processes*, 23(15), 2138-2149.
- Kaushal, S. S., P. M. Groffman, P. M. Mayer, E. Striz, and A. J. Gold (2008), Effects of stream restoration on denitrification in an urbanizing watershed, *Ecological Applications*, 18(3), 789-804.
- Klocker, C. A., S. S. Kaushal, P. M. Groffman, P. M. Mayer, and R. P. Morgan (2009), Nitrogen uptake and denitrification in restored and unrestored streams in urban Maryland, USA, *Aquatic Sciences*, 71(4), 411-424.
- Knispel, S., M. Sartori, and J. E. Brittain (2006), Egg development in the mayflies of a Swiss glacial floodplain, *Journal Information*, 25(2).
- Krause, S., and A. Bronstert (2007), The impact of groundwater–surface water interactions on the water balance of a mesoscale lowland river catchment in northeastern Germany, *Hydrological Processes*, 21(2), 169-184.
- Krause, S., A. Bronstert, and E. Zehe (2007), Groundwater–surface water interactions in a North German lowland floodplain–Implications for the river discharge dynamics and riparian water balance, *Journal of hydrology*, 347(3), 404-417.
- Kronvang, B., I. K. Andersen, C. C. Hoffmann, M. L. Pedersen, N. B. Ovesen, and H. E. Andersen (2007), Water exchange and deposition of sediment and phosphorus during inundation of natural and restored lowland floodplains, *Water Air and Soil Pollution*, 181(1-4), 115-121.
- Landers, J. (2010), Entering the Mainstream, *Civil Engineering*, 80(8), 58-+.
- Landon, M. K., D. L. Rus, and F. E. Harvey (2001), Comparison of instream methods for measuring hydraulic conductivity in sandy streambeds, *Ground water*, 39(6), 870-885.
- Lane, E. W. (1955), Design of stable channels, *Transactions of the American Society of Civil Engineers*, 120(1), 1234-1260.
- Langhans, S. D., and K. Tockner (2006), The role of timing, duration, and frequency of inundation in controlling leaf litter decomposition in a river-floodplain ecosystem (Tagliamento, northeastern Italy), *Oecologia*, 147(3), 501-509.
- Leopold, L. B. (1968), Hydrology for urban land planning: A guidebook on the hydrologic effects of urban land use.
- Lerner, D. N. (2002), Identifying and quantifying urban recharge: a review, *Hydrogeology Journal*, 10(1), 143-152.
- Lewandowski, J., and G. Nützmann (2010), Nutrient retention and release in a floodplain's aquifer and in the hyporheic zone of a lowland river, *Ecological Engineering*, 36(9), 1156-1166.

- Luhar, M., and H. M. Nepf (2013), From the blade scale to the reach scale: A characterization of aquatic vegetative drag, *Advances in Water Resources*, 51, 305-316.
- Mayer, P. M., S. K. Reynolds, M. D. McCutchen, and T. J. Canfield (2007), Meta-analysis of nitrogen removal in riparian buffers, *Journal of Environmental Quality*, 36(4), 1172-1180.
- Menichino, G. T., A. S. Ward, and E. T. Hester (2014), Macropores as preferential flow paths in meander bends, *Hydrological Processes*, 28(3), 482-495.
- Mertes, L. A. K. (1997), Documentation and significance of the perirheic zone on inundated floodplains, *Water Resources Research*, 33(7), 1749-1762.
- Moser, D. P., J. K. Fredrickson, D. R. Geist, E. V. Arntzen, A. D. Peacock, S. M. W. Li, T. Spadoni, and J. P. McKinley (2003), Biogeochemical processes and microbial characteristics across groundwater-surface water boundaries of the Hanford Reach of the Columbia River, *Environmental Science & Technology*, 37(22), 5127-5134.
- Mostaghimi, S., B. Benham, K. Brannan, T. A. Dillaha, R. Wagner, and J. Wynn (2003), Benthic TMDL for Stroubles Creek in Montgomery County, Virginia, *Prepared for VADEQ, Virginia Department of Environmental Quality. Richmond, Virginia.*
- Nieber, J. L. (2000), The relation of preferential flow to water quality, and its theoretical and experimental quantification, *Preferential Flow: Water Movement and Chemical Transport in the Environment*, 1-10.
- Noe, G. B., and C. R. Hupp (2007), Seasonal variation in nutrient retention during inundation of a short-hydroperiod floodplain, *River Research and Applications*, 23(10), 1088-1101.
- O'Driscoll, M., S. Clinton, A. Jefferson, A. Manda, and S. McMillan (2010), Urbanization effects on watershed hydrology and in-stream processes in the southern United States, *Water*, 2(3), 605-648.
- Orr, C. H., E. H. Stanley, K. A. Wilson, and J. C. Finlay (2007), Effects of restoration and reflooding on soil denitrification in a leveed Midwestern floodplain, *Ecological Applications*, 17(8), 2365-2376.
- Osborne, L. L., and D. A. Kovacic (1993), Riparian vegetated buffer strips in water-quality restoration and stream management, *Freshw. Biol.*, 29(2), 243-258.
- Peter, S., R. Rechsteiner, M. F. Lehmann, R. Brankatschk, T. Vogt, S. Diem, B. Wehrli, K. Tockner, and E. Durisch-Kaiser (2012), Nitrate removal in a restored riparian groundwater system: functioning and importance of individual riparian zones, *Biogeosciences*, 9(11), 4295-4307.
- Pirastru, M., and M. Niedda (2013), Evaluation of the soil water balance in an alluvial flood plain with a shallow groundwater table, *Hydrological Sciences Journal-Journal Des Sciences Hydrologiques*, 58(4), 898-911.
- Poff, N. L., J. D. Allan, M. B. Bain, J. R. Karr, K. L. Prestegard, B. D. Richter, R. E. Sparks, and J. C. Stromberg (1997), The Natural Flow Regime, *Bioscience*, 47(11), 12.

- Poole, G. C., J. A. Stanford, C. A. Frissell, and S. W. Running (2002), Three-dimensional mapping of geomorphic controls on flood-plain hydrology and connectivity from aerial photos, *Geomorphology*, 48(4), 329-347.
- Pringle, C. (2003), What is hydrologic connectivity and why is it ecologically important?, *Hydrological Processes*, 17(13), 2685-2689.
- Prosser, I. P., A. O. Hughes, and I. D. Rutherford (2000), Bank erosion of an incised upland channel by subaerial processes: Tasmania, Australia, *Earth Surface Processes and Landforms*, 25(10), 1085-1101.
- Roley, S. S., J. L. Tank, and M. A. Williams (2012), Hydrologic connectivity increases denitrification in the hyporheic zone and restored floodplains of an agricultural stream, *Journal of Geophysical Research-Biogeosciences*, 117, 16.
- Rood, S. B., G. M. Samuelson, J. H. Braatne, C. R. Gourley, F. M. R. Hughes, and J. M. Mahoney (2005), Managing river flows to restore floodplain forests, *Frontiers in Ecology and the Environment*, 3(4), 193-201.
- Sawyer, A. H., M. B. Cardenas, A. Bomar, and M. Mackey (2009), Impact of dam operations on hyporheic exchange in the riparian zone of a regulated river, *Hydrological processes*, 23(15), 2129-2137.
- Selker, J. S., L. Thevenaz, H. Huwald, A. Mallet, W. Luxemburg, N. Van De Giesen, M. Stejskal, J. Zeman, M. Westhoff, and M. B. Parlange (2006), Distributed fiber-optic temperature sensing for hydrologic systems, *Water Resources Research*, 42(12).
- Sholtes, J. S., and M. W. Doyle (2010), Effect of channel restoration on flood wave attenuation, *Journal of Hydraulic Engineering*, 137(2), 196-208.
- Simon, A., S. J. Bennett, and J. M. Castro (Eds.) (2011), *Stream Restoration in Dynamic Fluvial Systems: Scientific Approaches, Analyses, and Tools*, 1 ed., Wiley, John & Sons, Incorporated.
- Singh, V. P. (2002), Is hydrology kinematic?, *Hydrological processes*, 16(3), 667-716.
- Thien, S. J. (1979), A flow diagram for teaching texture-by-feel analysis, *Journal of Agronomic Education*, 8, 54-55.
- Thompson, T. W., W. C. Hession, and D. Scott (2012), The StREAM Lab at Virginia Tech, *Resource Magazine*, 8-9.
- Tockner, K., F. Malard, and J. V. Ward (2000), An extension of the flood pulse concept, *Hydrological processes*, 14(16-17), 2861-2883.
- USEPA (2010), Chesapeake Bay Total Maximum Daily Load for Nitrogen, Phosphorus and Sediment.
- Valett, H. M., M. A. Baker, J. A. Morrice, C. S. Crawford, M. C. Molles Jr, C. N. Dahm, D. L. Moyer, J. R. Thibault, and L. M. Ellis (2005), Biogeochemical and metabolic responses to the flood pulse in a semiarid floodplain, *Ecology*, 86(1), 220-234.

- Vidon, P. (2012), Towards a better understanding of riparian zone water table response to precipitation: surface water infiltration, hillslope contribution or pressure wave processes?, *Hydrological Processes*, 26(21), 3207-3215.
- Vitousek, P. M., J. D. Aber, R. W. Howarth, G. E. Likens, P. A. Matson, D. W. Schindler, W. H. Schlesinger, and D. Tilman (1997), Human alteration of the global nitrogen cycle: Sources and consequences, *Ecological Applications*, 7(3), 737-750.
- Walter, R. C., and D. J. Merritts (2008), Natural streams and the legacy of water-powered mills, *Science*, 319(5861), 299-304.
- Ward, J. V. (1997), An expansive perspective of riverine landscapes: pattern and process across scales, *GAIA-Ecological Perspectives for Science and Society*, 6(1), 52-60.
- Welti, N., E. Bondar-Kunze, G. Singer, M. Tritthart, S. Zechmeister-Boltenstern, T. Hein, and G. Pinay (2012), Large-scale controls on potential respiration and denitrification in riverine floodplains, *Ecological Engineering*, 42, 73-84.
- Wohl, E., P. L. Angermeier, B. Bledsoe, G. M. Kondolf, L. MacDonnell, D. M. Merritt, M. A. Palmer, N. L. Poff, and D. Tarboton (2005), River restoration, *Water Resources Research*, 41(10).
- Wondzell, S. M., and F. J. Swanson (1999), Floods, channel change, and the hyporheic zone, *Water Resources Research*, 35(2), 555-567.
- Yagow, G., B. Benham, T. Wynn, and T. Younos (2006), Upper Stroubles Creek watershed TMDL implementation plan, Montgomery County, Virginia. VDEQ. 81 pp, edited.
- Zarnetske, J. P., R. Haggerty, S. M. Wondzell, and M. A. Baker (2011), Dynamics of nitrate production and removal as a function of residence time in the hyporheic zone, *Journal of Geophysical Research-Biogeosciences*, 116, 12.
- Zarnetske, J. P., R. Haggerty, S. M. Wondzell, V. A. Bokil, and R. Gonzalez-Pinzon (2012), Coupled transport and reaction kinetics control the nitrate source-sink function of hyporheic zones, *Water Resources Research*, 48, 15.

3 Engineering Applications

The relationship between restoring hydrologic connectivity in stream systems and water quality is not well understood. The effects of reconnecting a degraded stream to its floodplain show this connection as being either a nutrient source, having no significant effect on water quality, or acting as a nutrient sink. Since the biogeochemical processes that influence nutrient removal rates are dependent on the hydraulic properties of surface water, groundwater, and the exchange between the two, we observed these properties at a high spatial and temporal scale in a controlled environment. While replicating conditions that would typically occur during an overbank event we artificially inundated a natural floodplain reach over the course of one year in an effort to quantify the effects that variations in season and antecedent moisture conditions have on floodplain hydraulics. Through increased control of flood timing and direct measurement of surface water inputs and outputs we were able to observe how moisture content and season independently affect the hydraulics.

Nutrient removal can occur during overbank storm events through a variety of mechanisms. Examples include uptake by terrestrial plants, sediment deposition, and/or removal via biogeochemical reactions. Of particular interest here is the potential for biogeochemical reactions because processes such as denitrification can reduce nitrate into unreactive dinitrogen gas resulting in permanent removal from the system. In order for these reactions to take place there must be sufficient time, contact with bio-available carbon acting as the electron source, and the absence of oxygen, therefore allowing nitrate to become the terminal electron acceptor in the redox reaction. Since different flow mechanisms result in varying conditions which are pertinent to biogeochemical processing, by better understanding the hydraulics we may be able to gain a better understanding of what to expect in terms of nutrient removal at proposed restoration sites.

Floodplain topography and antecedent moisture conditions had a significant impact on the storage of applied flood water. As antecedent soil moisture and water levels decreased, the percentage of applied flood water stored on the floodplain increased. Although we did not test it in our study, as floodplain topographic complexity increases the surface water storage volume will also increase, particularly if that complexity includes basins that do not drain quickly. These factors will benefit water quality but also attenuate the flood pulse to help alleviate downstream flooding. This may be important in urban environments where there is an emphasis placed on protecting downstream infrastructure. On the water quality side, stored water will eventually infiltrate into the subsurface resulting in greater contact with sediment conducive to reactions such as denitrification.

Changes in floodplain vegetation density induced by seasonal variation affected the total surface water storage (pre-existing surface water and applied surface water) during overbank floods. Increases in vegetation density lead to greater roughness on the floodplain surface and assuming a constant inflow rate, the surface water storage volume is increased. This increase in volume therefore results in a reduction of average surface water velocities. This effect was greatest during the Fall flood when vegetation dieback was taking place. During this time we observed the vegetation becoming matted down near the ground surface. Since the water depths were relatively shallow, the matting of vegetation within the flooded area resulted in a greater influence within the water column. This information can be used in future restoration designs by incorporating shorter vegetation (i.e. shrubs and tall grasses) rather than large trees due to the greater impact short and dense land cover has on overbank flow. Not only will this potentially result in increased SW-GW exchange by increasing vertical head gradients, but greater nutrient reduction through plant uptake and sediment deposition may also occur and lead to greater water quality benefits.

When reducing nutrient loads is a main concern during stream restoration design it is important to restore a reach of stream that will have the greatest net benefit. While Darcy flow allows for the greatest exposure time between dissolved constituents and conditions needed for biogeochemical reaction to occur, preferential flow can increase infiltration rates and help contaminated water bypass shallow sediments with low hydraulic conductivity. It may therefore be important to have both of these processes since each have their respective benefits. Stream restoration designers should consider the overall benefits associated with heterogeneity within floodplain systems (i.e. topographic, hydraulic, and vegetative heterogeneity) and incorporate these attributes into restoration designs which restore floodplain connectivity. This heterogeneity may also develop naturally after restoration construction is finished.

When restoring hydrologic connectivity between a stream and its floodplain during stream restoration one of the main engineering decisions involves setting an appropriate floodplain height. The height of the floodplain directly relates to the frequency that overbank flood events happen. Lowering the floodplain would allow for increased inundation and may therefore have the greatest effect on water quality as well as attenuate flood pulses more often. However, having a lower floodplain may result in a system that is not in quasi-equilibrium and result in increased sediment deposition and a floodplain elevation that slowly increases. If it is known that the floodplain acts as a sink of nutrients then we recommend implementing a lower floodplain elevation. However, if it is uncertain as to whether or not the floodplain is a nutrient source or sink, we recommend that

the floodplain elevation be set at the stage corresponding to the estimated bankfull discharge in order to restore stream bank stability.

Restoring floodplain connectivity is often necessary due to changes in watershed characteristics which then lead to changes in the natural flow regime. While flashy streams typically have a greater frequency of overbank events (and therefore greater potential for benefits stemming from floodplain connectivity), this increased flashiness in stream discharge can often result in increased bank degradation. Higher stream discharge is then required to reach floodplain height and these benefits are then reduced. On the other hand, extensive implementation of stormwater best management practices (BMPs) such as retention ponds and pervious pavement can reduce flashiness in an urban environment. While the frequency of overbank events decreases in this case, the channel will not degrade and the floodplain will remain hydrologically connected to the stream. Having a lower floodplain elevation will alleviate some of the pitfalls of the decrease in discharge flashiness by allowing for more frequent overbank flood events.

Appendix A: Experiment Site Setup and Maintenance

A.1 Site Configuration

An outlet structure was created in an effort to replicate conditions typical of overbank flood events. A combination of cinder blocks and sandbags were used to disperse flow and reduce surface water velocities (Figure A-1a). The monitoring network was into three main transects. These were installed along the visually estimated flow centerline across the floodplain. In order to minimize the effect that walking on the site may have over the course of one year, we installed walkways in order to prevent any unnatural changes to the landscape (Figure A-1b). The 3” parshall flume at the floodplain outlet was installed in order to measure outflow discharge and was reinforced with sandbags, aluminum sheeting, and plywood (Figure A-1c).

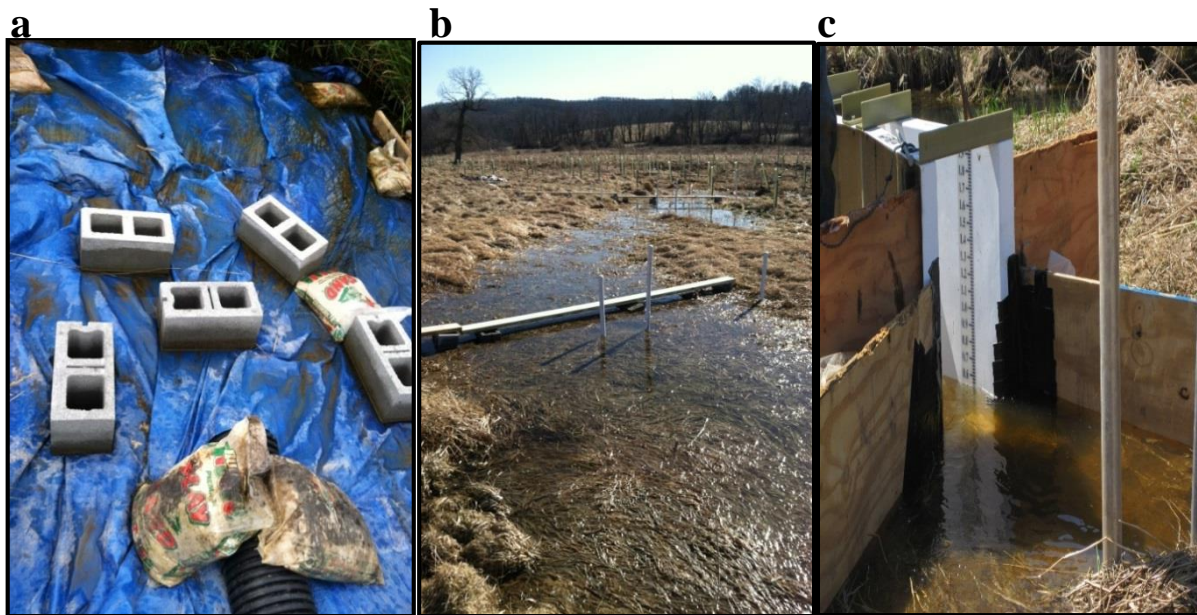


Figure A-1: (a) Pump outlet structure used to disperse flow, (b) typical cross section construction method used throughout the site, and (c) site outflow point through 3” parshall flume

A.2 Piezometer Installation

Each piezometer used throughout the site was constructed in the same way (Figure A-2). Due to the number of piezometers used in such close proximity, we installed the piezometers using boreholes of equal diameter to the piping used for the piezometers. This was done in order to minimize the impact of site setup on the natural hydraulic conductivity and site characteristics.



Figure A-2: Piezometer construction method used for all piezometers throughout the site. The screen length was kept constant at 10 cm with the screened interval being between 4 and 14 cm from the piezometer base for each piezometer constructed.

During the installation of the deep piezometers along the floodplain centerline we classified soils by placing the extracted soil core on a clear surface for visual classification to go along with the textural analysis we conducted by feel when removing the soil from the auger bit (Figure A-3). We recommend using a split spoon sampler when soil cores want to be analyzed following extraction. Using a hand auger with a closed in bit resulted in difficulty maintaining the integrity of the soil core distances because only small portions of the soil could be extracted at a time. This was particularly problematic at this site due to the extensive clay present. Soils that are not as compact are easier to extract and therefore the problem of keeping the core intact may be less of an issue.



Figure A-3: Example of the method used to visually classify soils during the installation of piezometers 100 cm BGS.

A.3 Instrumentation

A.3.1 Soil Moisture Probes

Soil moisture probes were used at each of the seven monitoring locations throughout the flooded area. Decagon TM3 soil moisture probes (Figure A-4a) were used at 5 cm and 10 cm BGS in the transverse piezometer locations while Decagon GS3 soil moisture probes (Figure A-4b) were used at 5 cm and 10 cm BGS at each of the three centerline locations.

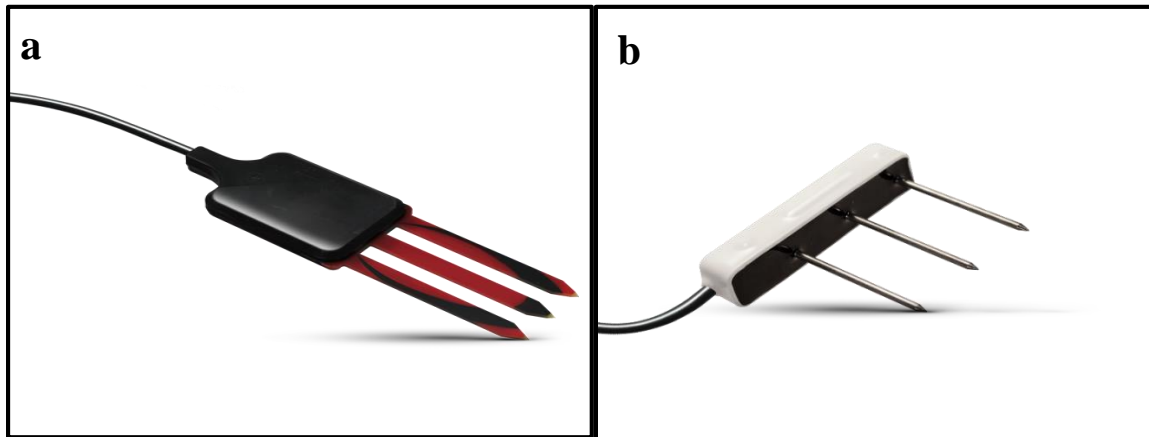


Figure A-4: (a) Decagon Devices 5TM soil moisture probes and (b) Decagon Devices GS3 soil moisture probes (www.decagon.com, used under fair use, 2014)

Each pair of soil moisture probes were connected to Campbell Scientific CR200 data loggers with a solar panel drip charge applied to extend battery life (Figure A-5). The CR200 data logger was programmed to take measurements every ten seconds and output the average recording over the specified logging frequency.



Figure A-5: Campbell Scientific CR200 data logger used for each pair of soil moisture probes (left, www.campbellsci.com, used under fair use, 2014). The method for housing the data loggers at the site for the entire experiment duration while charging with solar panels (right).

A.3.2 Onset HOBO U20 Pressure Transducers

For areas where knowing the hydraulics was deemed of lesser importance (such as in the parshall flume), Onset HOBO U20 Pressure Transducers were installed (Figure A-6). Upon receiving these pressure transducers, verification of accuracy was completed by performing a “bucket test”. This test is completed by placing submerging all pressure transducers in a known depth of water ensuring that all readings are within the accepted error provided by the manufacturer.



Figure A-6: Onset HOBO pressure transducer (www.onsetcomp.com, used under fair use, 2014).

A.3.3 Solinst LTC Levellogger Junior

Solinst LTC Levellogger Junior probes (Figure A-7) were placed throughout the floodplain to measure electrical conductivity, pressure, and temperature in surface water and groundwater.



Figure A-7: 3001 Solinst LTC Levellogger used throughout the floodplain (www.solinst.com, used under fair use, 2014).

A.3.3.1 LTC Three Point Calibration

Prior to deploying this set of probes the Solinst calibration in the software provided was used. A three point calibration was completed using the three conductivity calibration solution standards provided by Solinst with specific conductivity values of $1,413 \mu\text{S cm}^{-1}$, $5,000 \mu\text{S cm}^{-1}$, and $12,880 \mu\text{S cm}^{-1}$. Each probe was rinsed with deionized water when switching from one calibration solution to the next. Due to the amount of probes being used in this study (11) gradual dilution of the calibration solutions began to occur and changed the electrical conductivity out of the acceptable range. When this happened, the LTCs could no longer be calibrated and new solution had to be used. For this reason we recommend using a small amount of solution during calibration in case something of this nature happens. The calibration of the LTCs was checked once during the experiment duration by placing them all in the same solution and ensuring that each recorded a specific conductivity $\pm 5\%$ of the actual value since this is the error that the instrument has in electrical conductivity readings according to the manufacturer user manual. If the LTCs measure outside of this threshold it is recommended that the Solinst calibration solution be used for an additional calibration or the K calibration method described below be used.

A.3.3.2 LTC K Calibration

In the absence conductivity solution, LTCs may also be calibrated using the K calibration technique. In order to run the K calibration a secondary solution of known salt concentration must be created (100 mL of solution is sufficient). Initially use the LTCs to measure the conductivity of stream water with no salt added. Once that that measurement has plateaued add 1 mL of the secondary solution and mix with the LTCs being calibrated until the electrical conductivity readings reach a steady value. Repeat this process by adding 5 mL, 10 mL, 10 mL, and 20 mL of secondary solution. Employing this method will allow the user to relate each of the LTC output measurements by converting all specific conductivity outputs to relative conductivity. This allows for direct comparison between probes and accounts for offsets and drift for each probe independently. The downside to this technique is that the actual electrical conductivity is not measured and therefore if the precise values for electrical conductivity are desired the three point calibration through using the Solinst calibration solution should be used instead.

A.3.4 Instrument Configuration Along Flood Centerline

Each of the three centerline locations consisted of an LTC measuring surface water properties, soil moisture probes 5 cm and 10 cm BGS measuring pore water properties, and LTCs at 30 cm and 100 cm BGS measuring groundwater properties (Figure A-8).

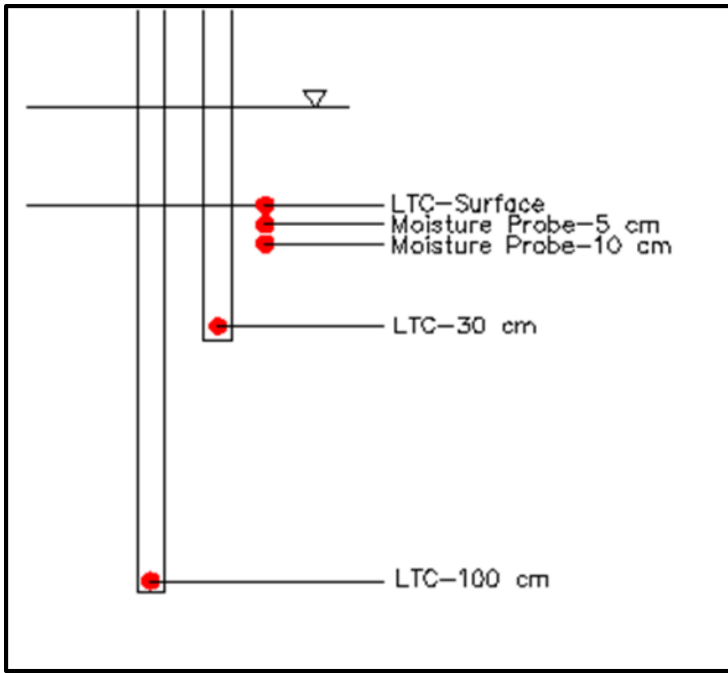


Figure A-8: Instrumentation located at flood centerline locations.

Appendix B: Additional (Complete) Data Not Included In Journal Article

B.1 Background Data Collected Throughout the Year

This section includes data collected by the surface water and groundwater monitoring network used throughout the duration of the study. Using water elevations and inflow/ outflow rates we were able to calculate new datasets, which give additional description as to what is occurring hydraulically at the study site.

B.1.1 Surface Water and Groundwater Elevation

Water elevations at each measuring point are closely related throughout the year at XS1 and there it is clear that standing water was present at XS1 for the majority of the experiment duration (Figure B-1). The groundwater measured 30 cm BGS (XS2-Center-30 cm) at XS2 shows a delayed response in pressure during quick increases and decreases in water initially. Towards the end of the experiment year, this delay no longer existed and is consistent with the increase in vertical connectivity experienced throughout the site. The piezometers 100 cm BGS along the centerline of XS1 and XS2 are closely related throughout the study duration. Water elevation recorded at XS3 show that the surface at this location was inundated less frequently than the other two cross sections. Furthermore, precipitation appears to have little to no effect on groundwater elevations as it does in XS1 and XS2. Rather than responding to rainfall events, groundwater elevations at XS3 are likely depend on seasonal variations due to the lower hydraulic conductivity in the soil surrounding these piezometer locations.

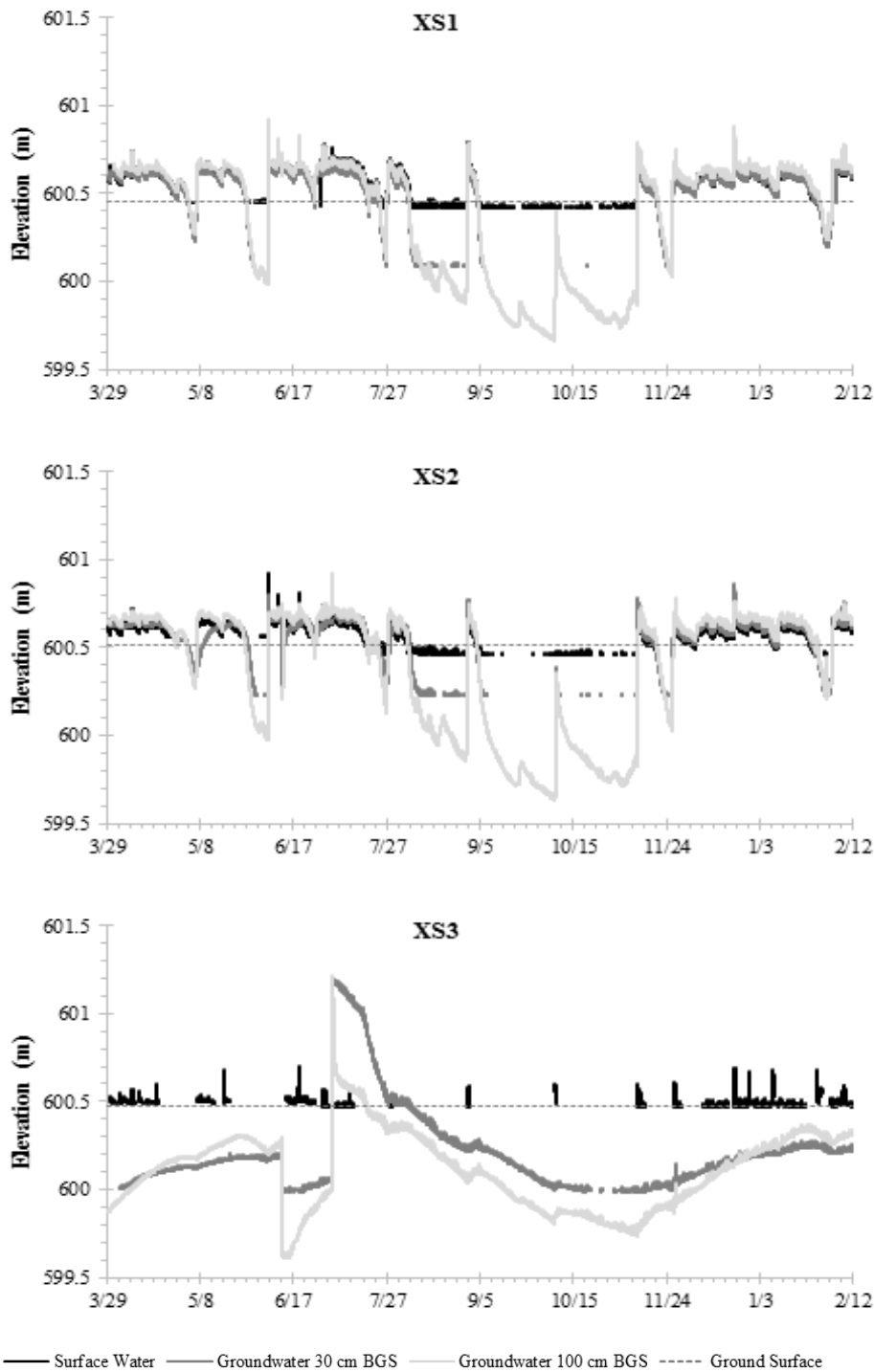
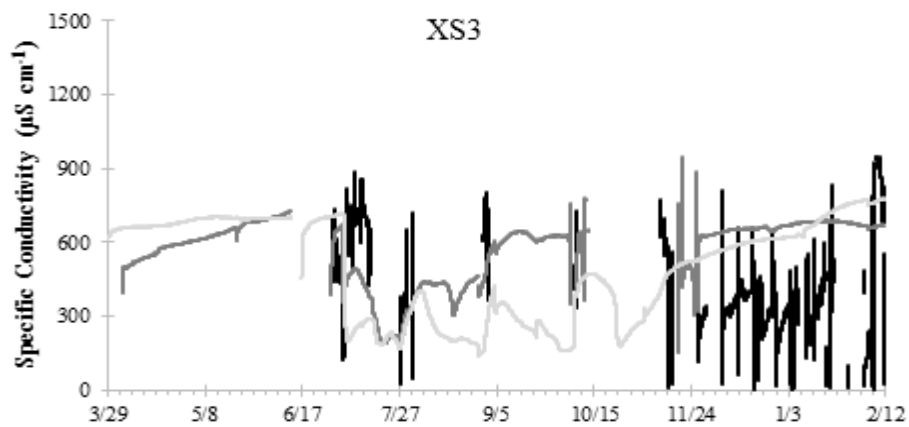
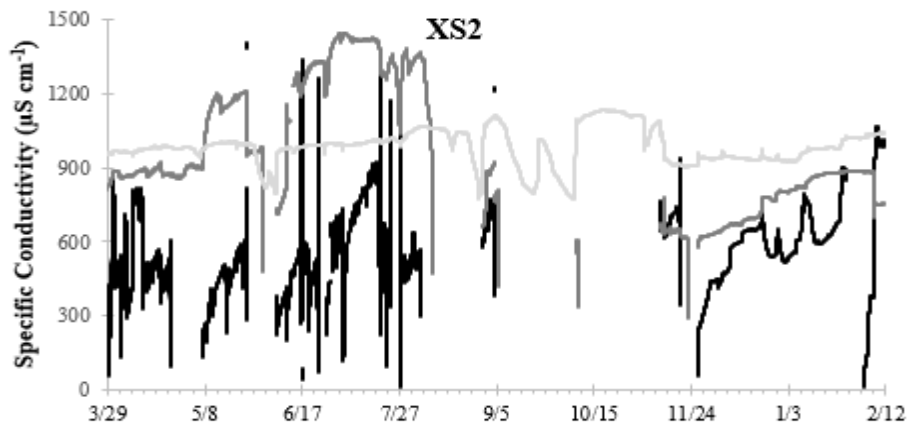
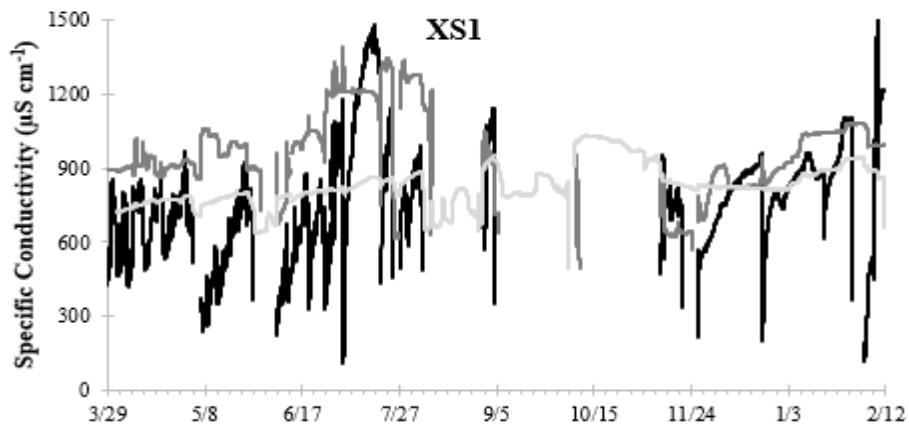


Figure B-1: Background water elevations along centerline. Data recorded during times when measuring point on device was not submerged were omitted. Decreases in groundwater levels experienced on June 12, 2013 were a result of rising head tests being conducted. The sharp increases in groundwater levels in XS3-Center-30 cm and XS3-Center-100 cm that occur on July 3, 2013 are a result of an overbank storm event in which surface water levels increased to a stage that exceeded the TOC elevation.

B.1.2 Electrical Conductivity in Surface Water and Groundwater

Electrical conductivity was recorded in surface water, groundwater 30 cm BGS, and groundwater 100 cm BGS throughout the year (Figure B-2). The electrical conductivity outputs were then converted to specific conductivity to account for changes in temperature. Surface water SC is much more variable due to the direct influence natural rainfall events have on the floodplain surface. Increases in SC occur during dry periods and very steep decreases occur during storm events due to the low SC present in rainwater. Piezometers XS1-Center-30 cm and XS1-Center-100 cm have SC data that are roughly correlated over the course of the year. Despite the time between March and June being a wet period, groundwater at 30 cm and 100 cm BGS at XS3 shows a consistent increase in SC during this time. This is additional evidence pointing towards a strong disconnect between conditions on the floodplain surface and groundwater properties.

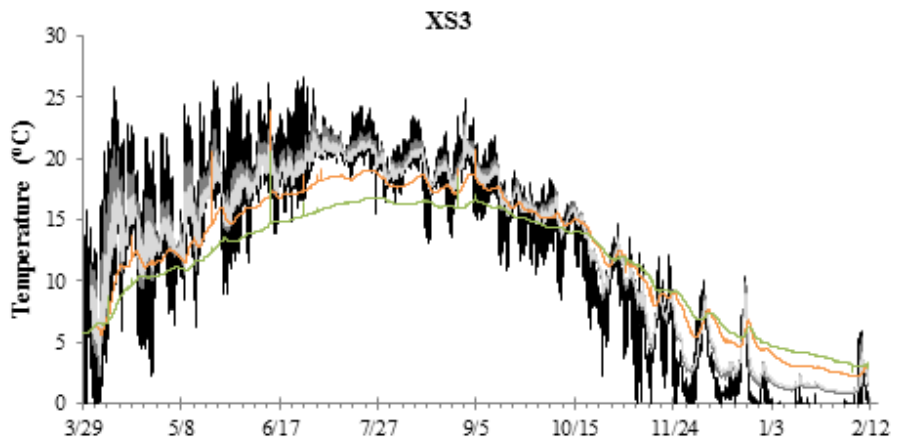
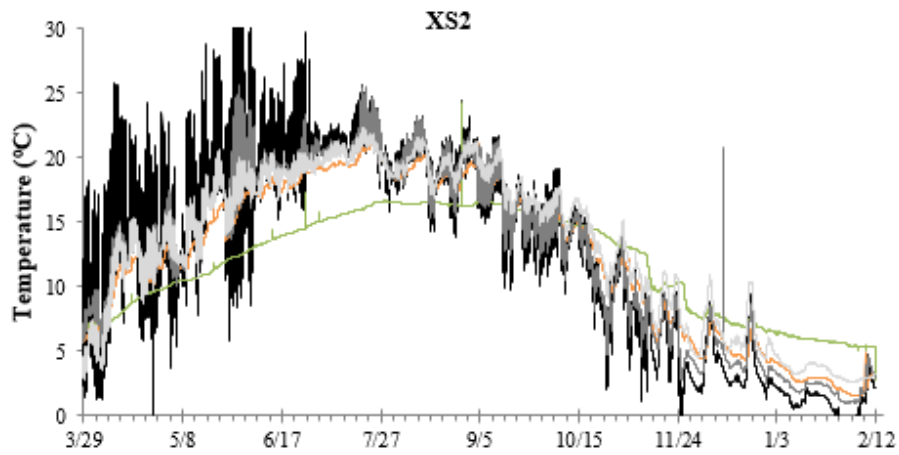
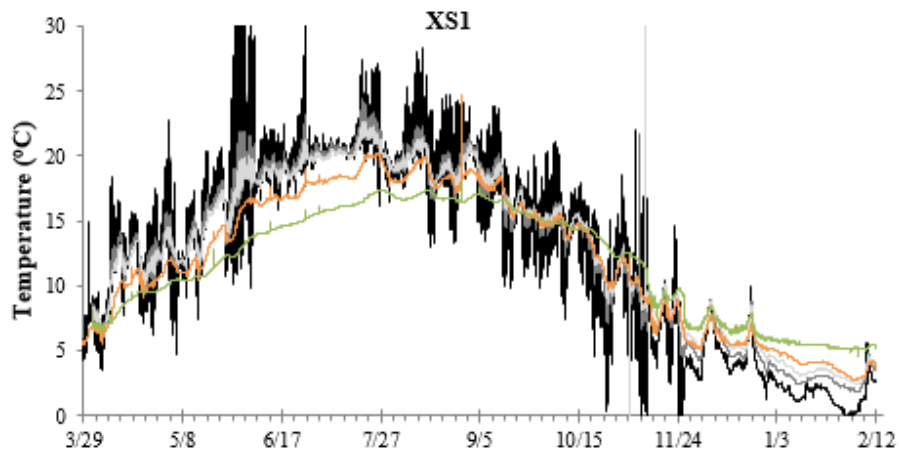


— Surface Water — Groundwater 30 cm BGS — Groundwater 100 cm BGS

Figure B-2: Background electrical conductivity along centerline. Conditions in which the monitoring devices were not fully submerged in water were present occasionally over the deployment year for all probes. In these instances readings were altered resulting in either values of zero or values far greater than what would be expected and for this reason these outliers were removed.

B.1.3 Temperature in Surface Water, Groundwater, and Soil

Temperature was recorded throughout the year in surface water, shallow sediments (5 cm and 10 cm BGS), groundwater 30 cm BGS, and groundwater 100 BGS (Figure B-3). When looking at the entire year of data we observed the seasonal temperature variations clearly happening at each locations. Monitoring points closer to the floodplain surface (i.e. surface water and shallow sediments) appear to be influenced to a much greater degree by daily temperature fluctuations than deeper measuring points, which show no observable changes in some cases. Temperature gradients reverse near the beginning of September at both XS1 and XS2 with the average daily surface temperature decreasing below the average daily temperature experienced in the deep subsurface. Daily temperature fluctuations generally decrease as time progresses from March to November. The range of temperature fluctuation throughout the year varies significantly. One cause of this lack of consistency in the temperature fluctuation is the fact that the floodplain was not inundated at all times and there is less of a temperature buffering effect by standing water during these dry periods.



— Surface Water — Soil 5 cm BGS — Soil 10 cm BGS — Groundwater 30 cm BGS — Groundwater 100 cm BGS

Figure B-3: Temperature recorded in surface water, soil 5 cm BGS, soil 10 cm BGS, groundwater 30 cm BGS, and groundwater 100 cm BGS at each cross section centerline location.

B.1.4 Soil Moisture Content

Soil moisture content throughout the floodplain was high (saturated) between the time of instrument installation and the Early Summer flood (Figure B-4). Total rainfall depth during the Early Summer in 2013 was much greater than average for Blacksburg, VA.

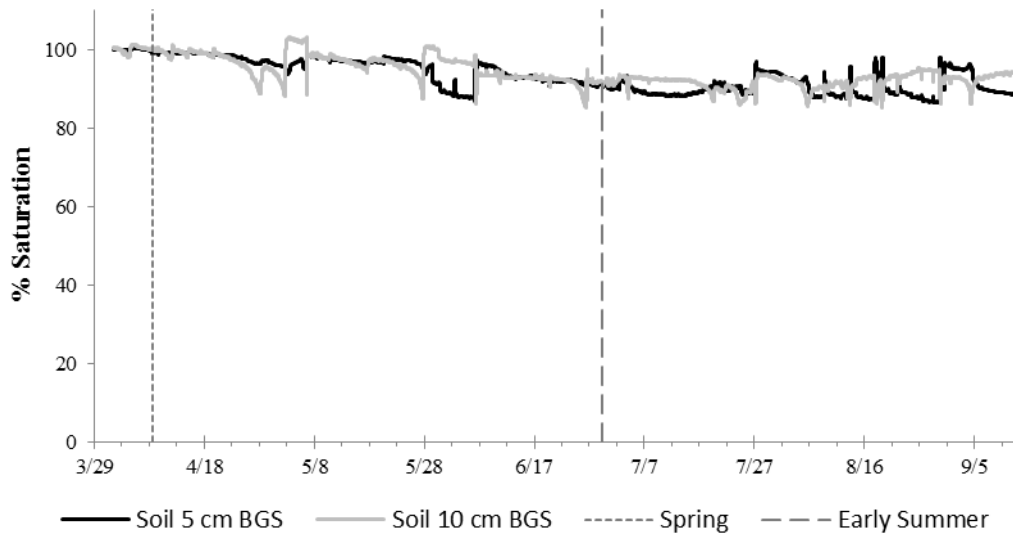
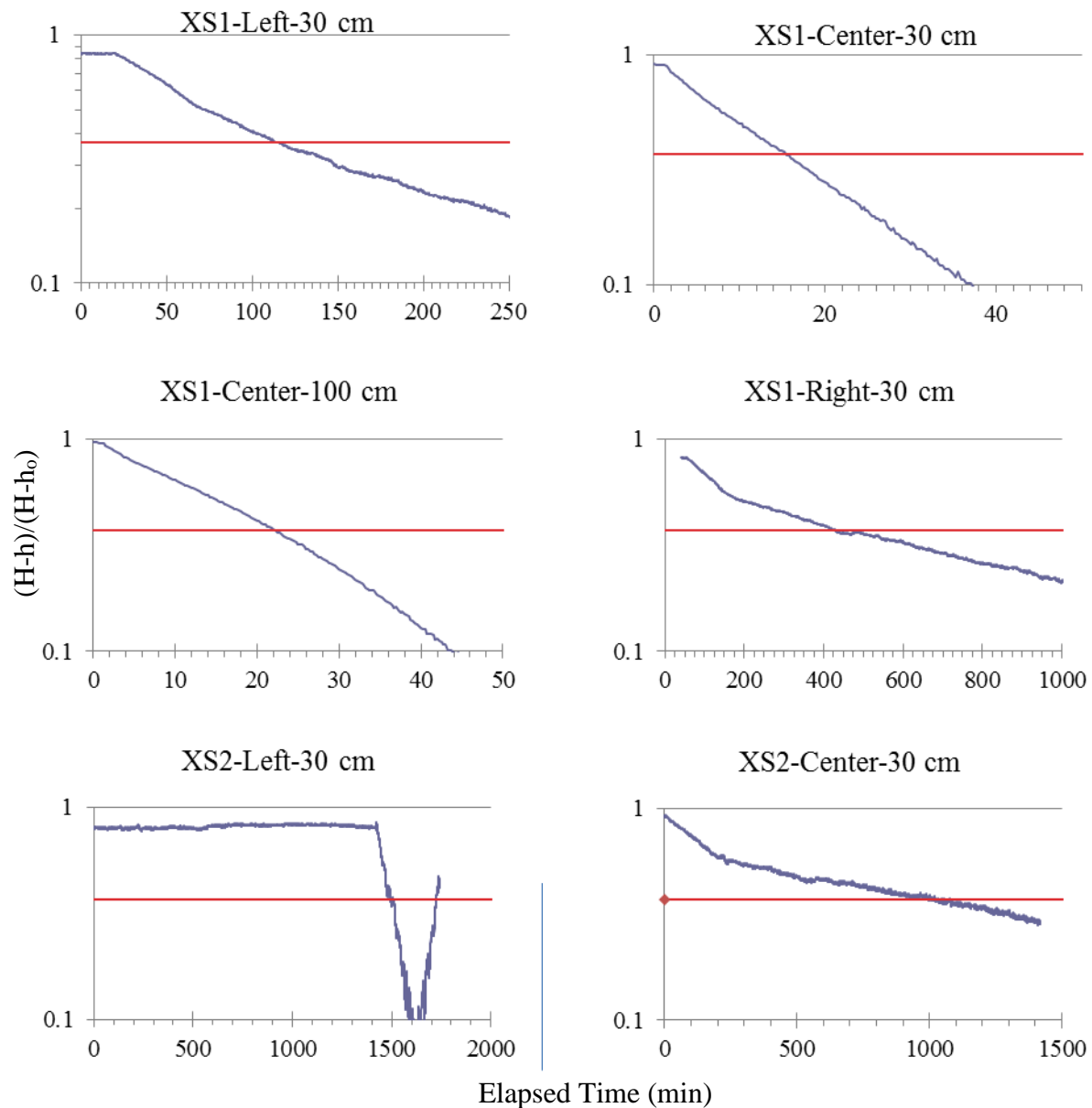


Figure B-4: Percent saturation in shallow sediments for Spring and Early Summer floods. Variability in moisture probe measurements caused values exceeding 100% saturation to be calculated at some points when converting the probe output (volumetric moisture content) to percent saturation.

B.1.5. Rising Head Tests

B.1.5.1 June 12, 2013 Rising Head Tests

Rising head tests were completed in each of the piezometers throughout the site towards the beginning of the experiment duration (Figure B-5). During each test, the logging interval for each probe was decreased and initial water column depth within each piezometer was recorded. Once this initial water depth was measured, water was extracted from each piezometer using a Geotech Geopump. The logging interval was then set back to the standard 15 minute interval following the point in which the water elevation returned to pre-test elevation or returned to 63% of the initial depth in accordance with the Hvorslev method employed for this test.



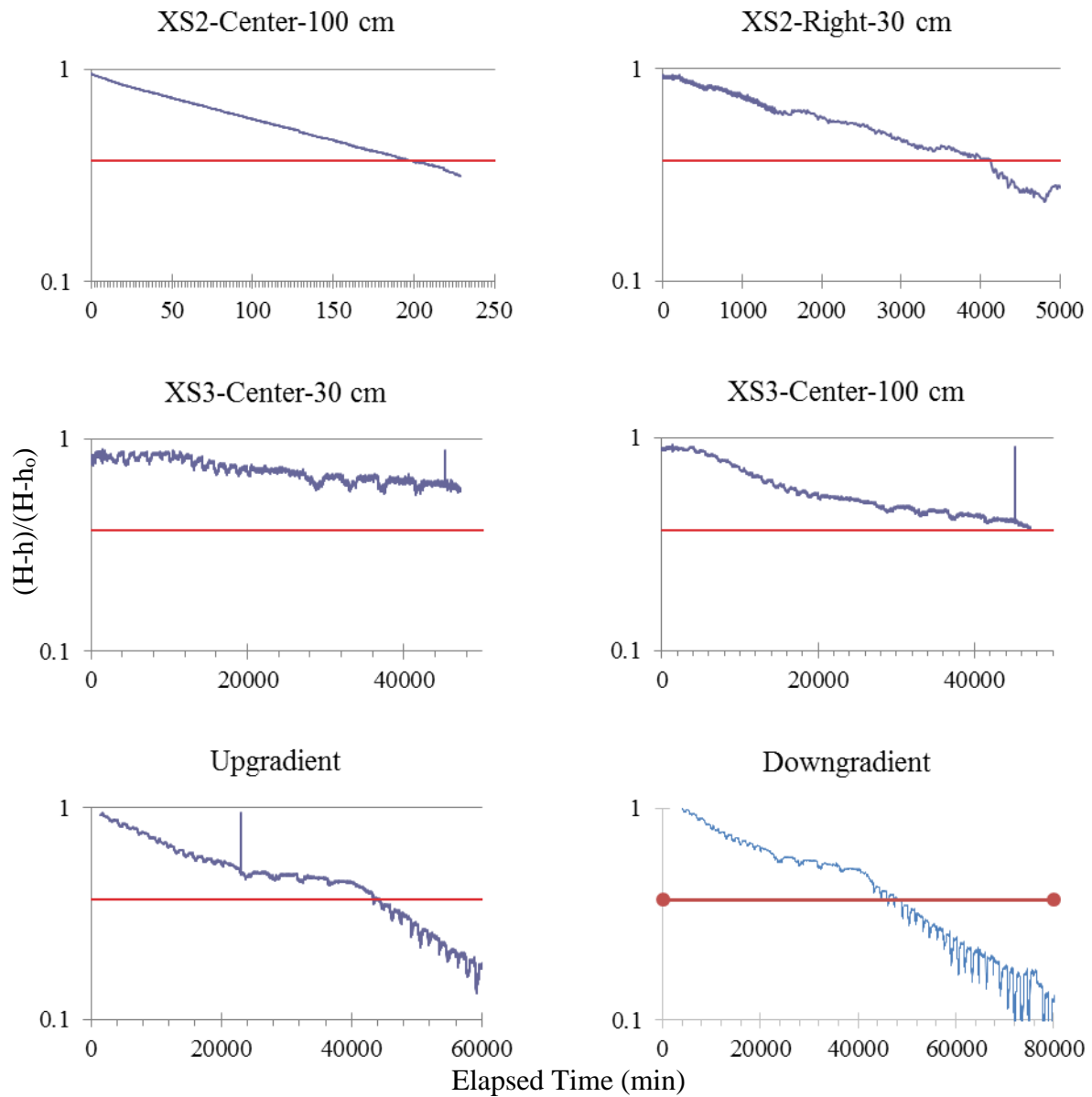
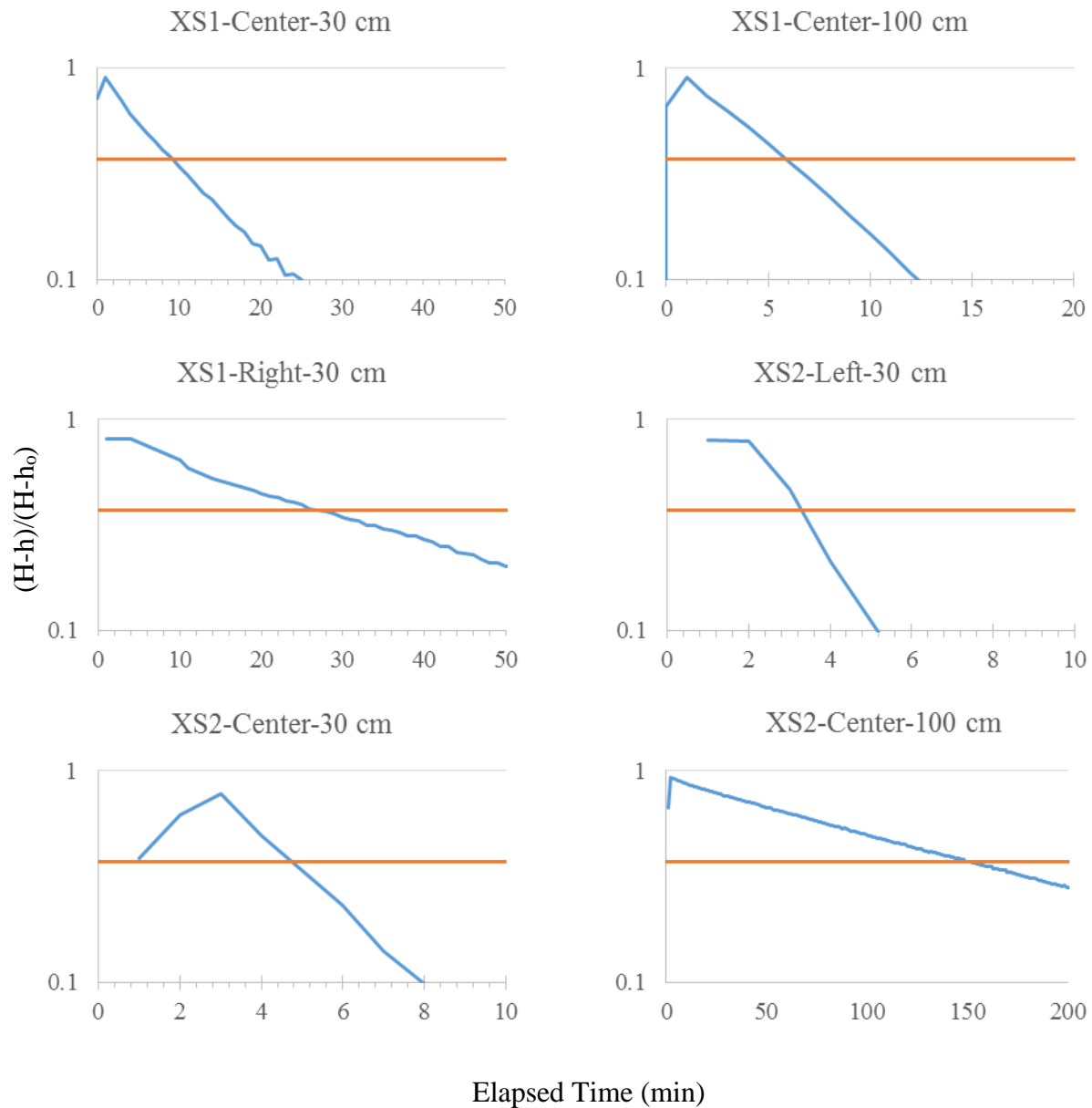


Figure B-5: Results obtained from the initial rising head tests performed throughout the site using the Hvorslev method. Tests were started on June 12, 2013.

B.1.5.2 March 8, 2014 Rising Head Tests

The process of measuring the hydraulic conductivity through the use of rising head tests was repeated at the end of the experiment duration to check for any changes that may have occurred throughout the inundated area (Figure B-6). We observed increases in hydraulic conductivity throughout the site between the first and the second set of rising head tests completed at the site.



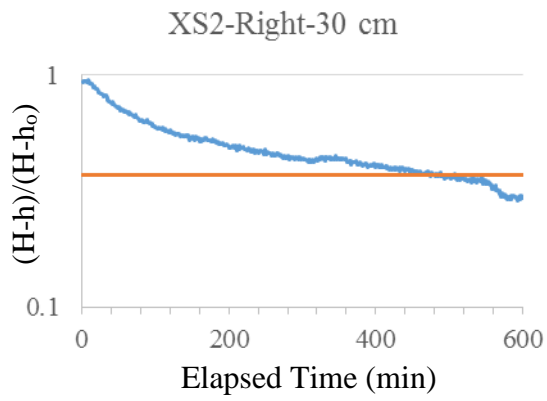


Figure B-6: Results obtained from the second set of rising head tests performed throughout the inundated using the Hvorslev method. Tests were started on March 8, 2014.

B.2 Data Collected During Flood Experiments

B.2.1 Surface Water and Groundwater Levels Along Centerline

Surface water and groundwater elevations were recorded along the flow centerline during each flood event (Figure B-7). The vertical read line during the Early Summer flood represents the time at which a malfunction occurred causing the second day of flooding to be repeated.

B.2.2 Groundwater Levels in Transverse Piezometers

Vertical connectivity tends to increase in the transverse piezometers throughout the year (Figure B-8). No significant response in groundwater levels to the increase in surface water levels is observed in the transverse wells during the Fall flood despite being fully inundated during each flood. Data recorded during the Early Summer flood show small responses in each of the four wells, with XS1 showing a greater increase in pressure relative to XS2. The increased vertical connection continues through the Winter flood where all piezometers show an significant increase in groundwater elevation in response to the application of surface water. Water levels recorded in XS2-L elevate above the floodplain surface during the Late Summer, Fall, and Winter floods. This increase may be a result of this location acting similar to an artesian well. These significant increases can likely not be attributed to probe inaccuracy since the initial groundwater elevation at XS2-L during the Late Summer and Fall floods is roughly equivalent to the other transverse well locations.

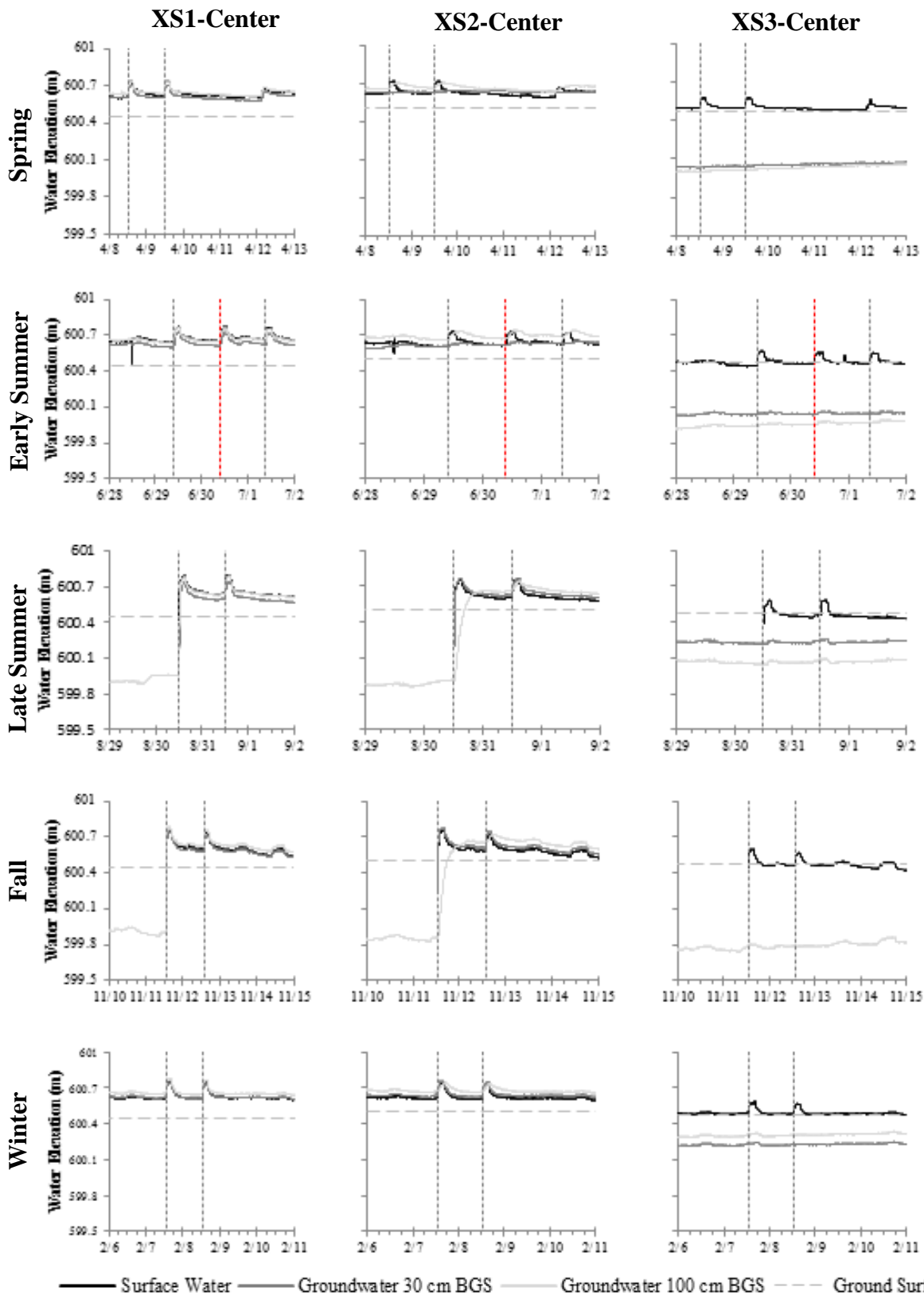


Figure B-7: Surface water and groundwater elevations recorded along the flow centerline during each flood

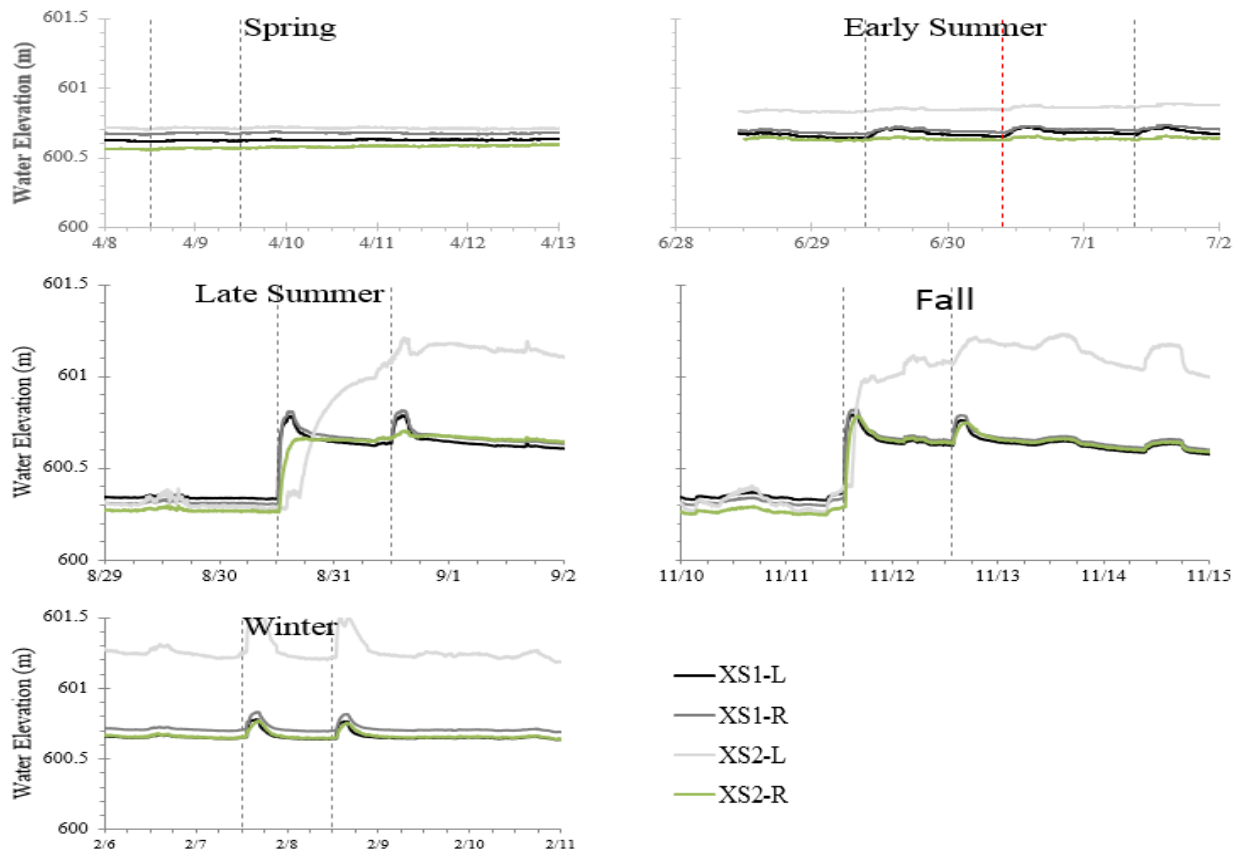


Figure B-8: Flood event water levels in groundwater 30 cm BGS at the transverse piezometers.

B.2.3 Vertical Head Gradients

In order to determine the vertical flow direction throughout the floodplain we calculated vertical head gradients at each of the three flood centerline locations during each flood (Figure B-9). Overall trends in vertical head gradients remain constant throughout each flood. The losing conditions present prior to the first day of flooding during both the Late Summer and Fall floods are a result of a lower table prior to each event. The water elevation in XS3-Center-100 cm exceeded the water elevation in XS3-Center-30 cm during the Winter flood causing a reversal in vertical gradient and gaining conditions between those two locations.

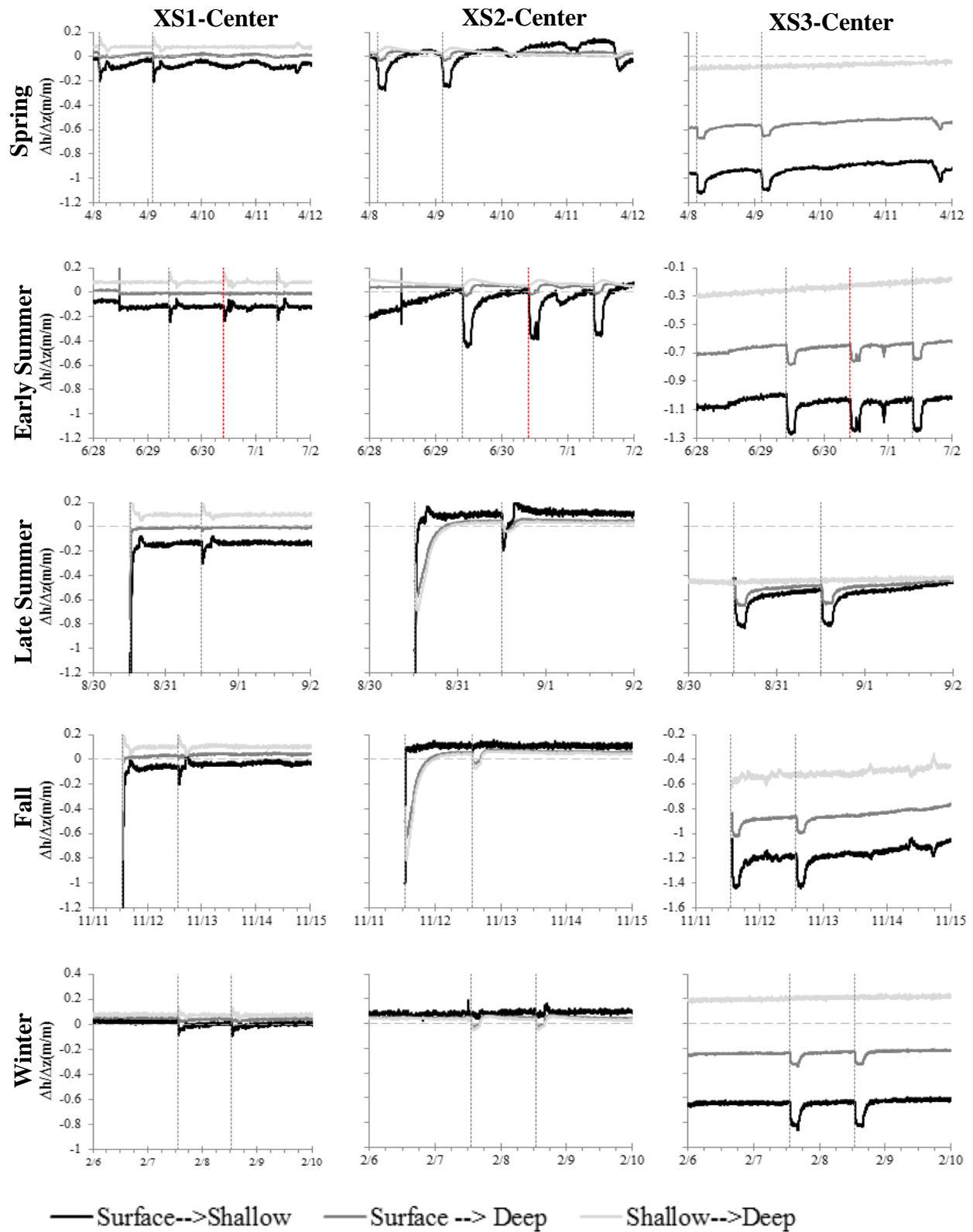


Figure B-9: Vertical head gradients calculated along the floodplain centerline during each flood. Water elevations from the floodplain surface, 30 cm BGS (shallow), and 100 cm BGS (deep) were used in the calculation

B.2.4 Horizontal Head Gradients

Horizontal head gradients between piezometers of equivalent depth (i.e. surface, 30 cm BGS, and 100 cm BGS) were calculated along the floodplain centerline between each of the three cross sections (Figure B-10). Due to XS1 and XS2 being in the same topographic depression on the flood site, horizontal head gradients between them are near zero during each flood event. Gradients calculated between surface water at the first two cross sections and surface water at XS3 show head losses toward XS3, mainly due to steeper floodplain slope and therefore shallower surface water levels where the monitoring equipment is placed at XS3. Groundwater horizontal gradients calculated between these location continue to show head losses. The drop in head calculated between XS1 and XS3 compared to XS2 and XS3 is less due to a greater horizontal distance between these two locations. Groundwater levels prior to the Late Summer and Fall floods were low and in many cases dropped to an elevation lower than the measuring point. Data were omitted when this was the case.

Piezometric surfaces were calculated using the groundwater depths for piezometers 30 cm BGS throughout the site (Figure B-11). These surfaces were made using pre-event groundwater elevations and elevations two hours into pumping. It is important to note that the groundwater response was often delayed and therefore the magnitude of spatial variation is magnified in these instances. The surface domain is restricted by the locations of the XS3 monitoring location and the XS1-L monitoring location.

The results consistently show that the water levels decrease in the direction of XS3. The centerline of XS1 shows a response form the application of surface water for each flood, with the greatest magnitude of water level increase occurring during the Late Summer and Fall floods. The piezometric surfaces illustrate the lack of exchange at XS3 during each event. We see that between Early Summer and Late Summer, XS2-Center-30 cm goes from having little to no response to the increase in surface water to having a significant response. The subsurface response to the application of flood water varies dramatically between flood events and a high degree of spatial variation in vertical connectivity is apparent.

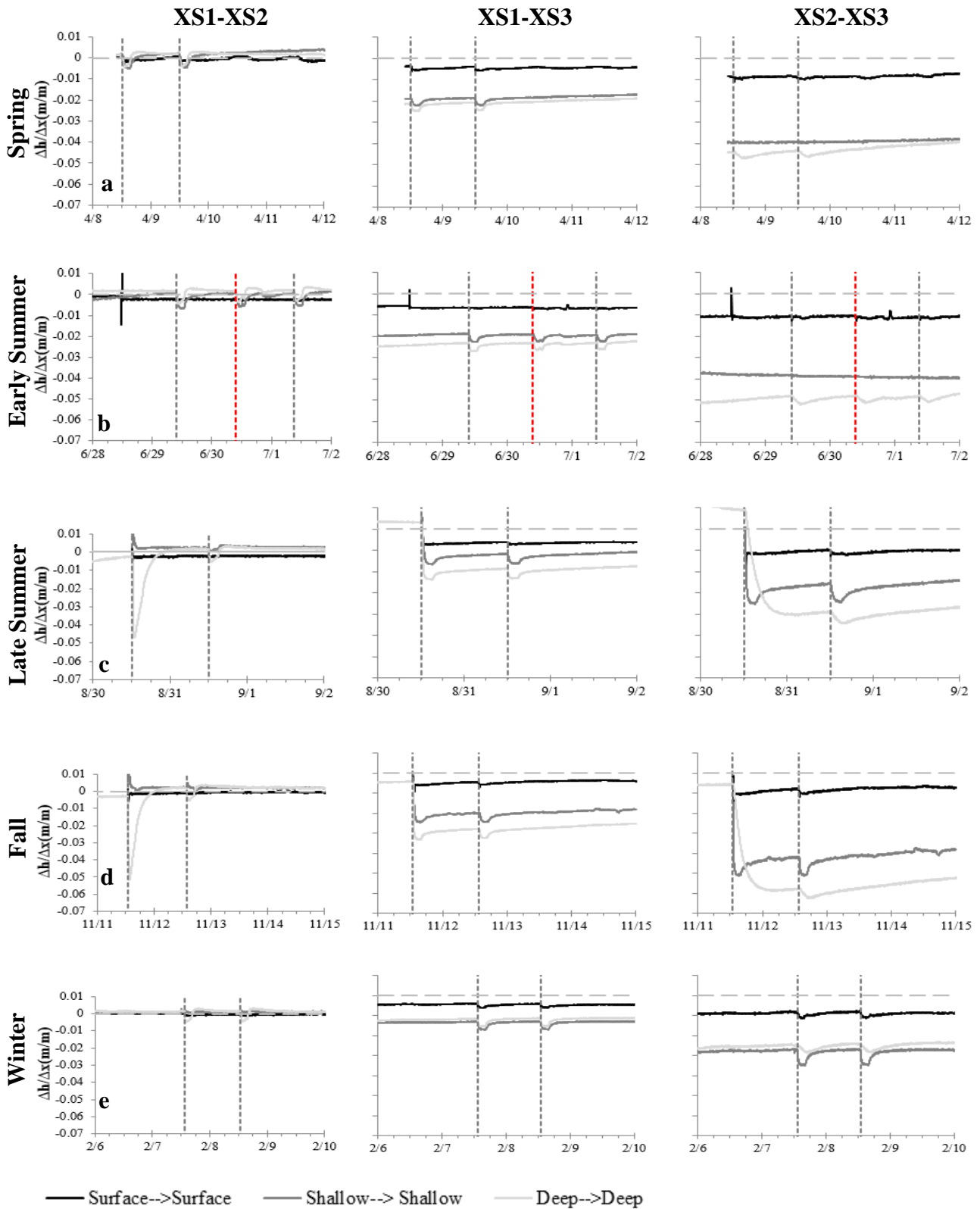


Figure B-10: Horizontal head gradients calculated between piezometers of equivalent depth BGS between centerline locations.

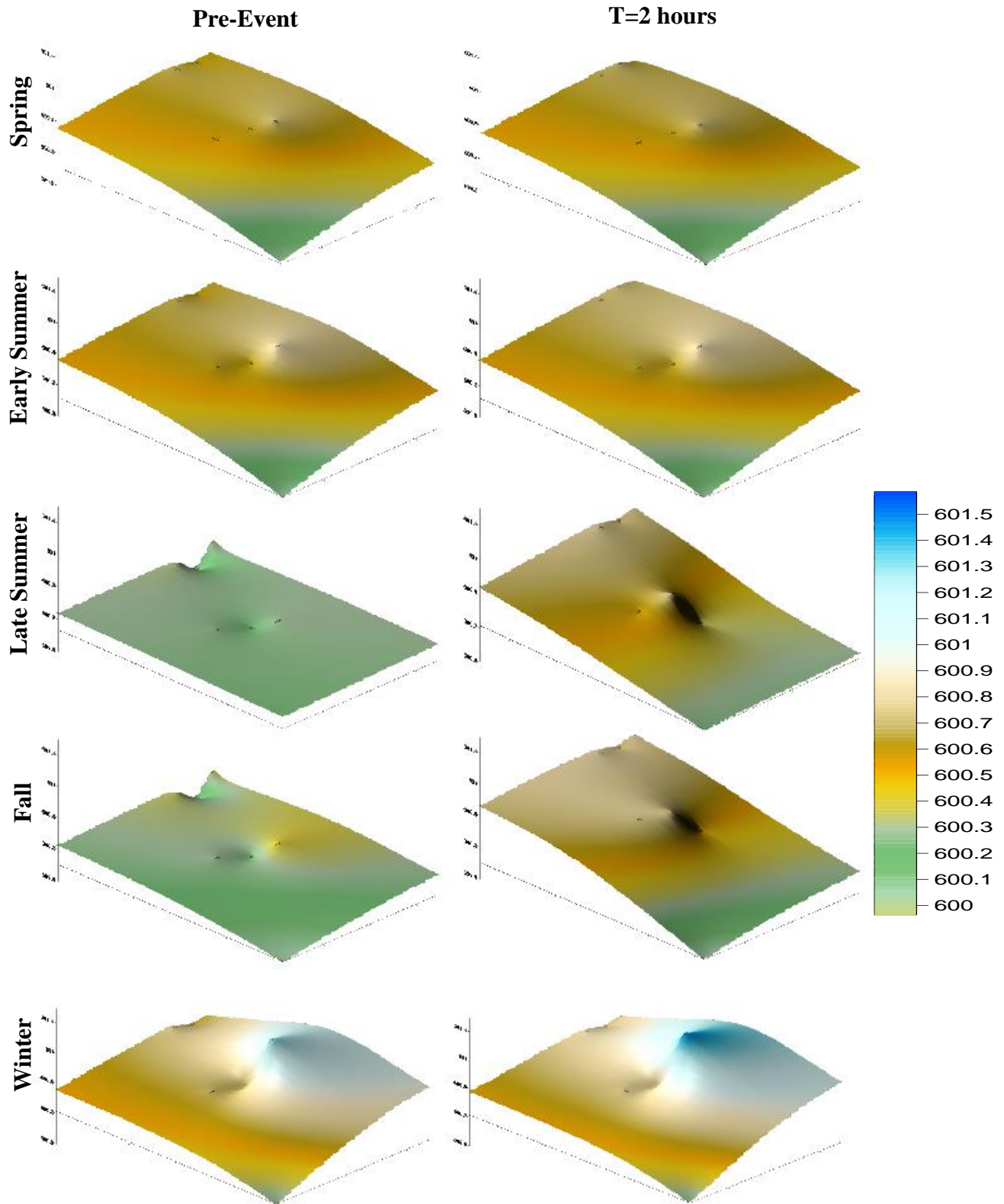


Figure B-11: Floodplain piezometric surfaces created using pre-event water levels and water levels two hours after the flood began. The piezometric surface domain is bounded by XS3 (bottom) and XS1-L (top).

B.2.5 Soil Moisture Content

Soil moisture content decreased prior the Late Summer (Figure B-12) and Fall floods (Figure B-13). Soil moisture content along the site centerline continually remained greater than the transverse locations likely due to the slight difference in centerline elevation compared to the transverse monitoring locations. The extensive clay layer further added to the consistently high soil moisture content by preventing quick infiltration of floodplain surface water.

While the center of the flooded region remains saturated for an extended time after the Late Summer flood, a decrease in moisture content is observed in the transverse locations more quickly. Evapotranspiration rates should generally be highest during the summer months allowing for quicker removal of water throughout the site, which would explain the quicker recession in soil moisture content following the Late Summer flood compared to the Fall flood

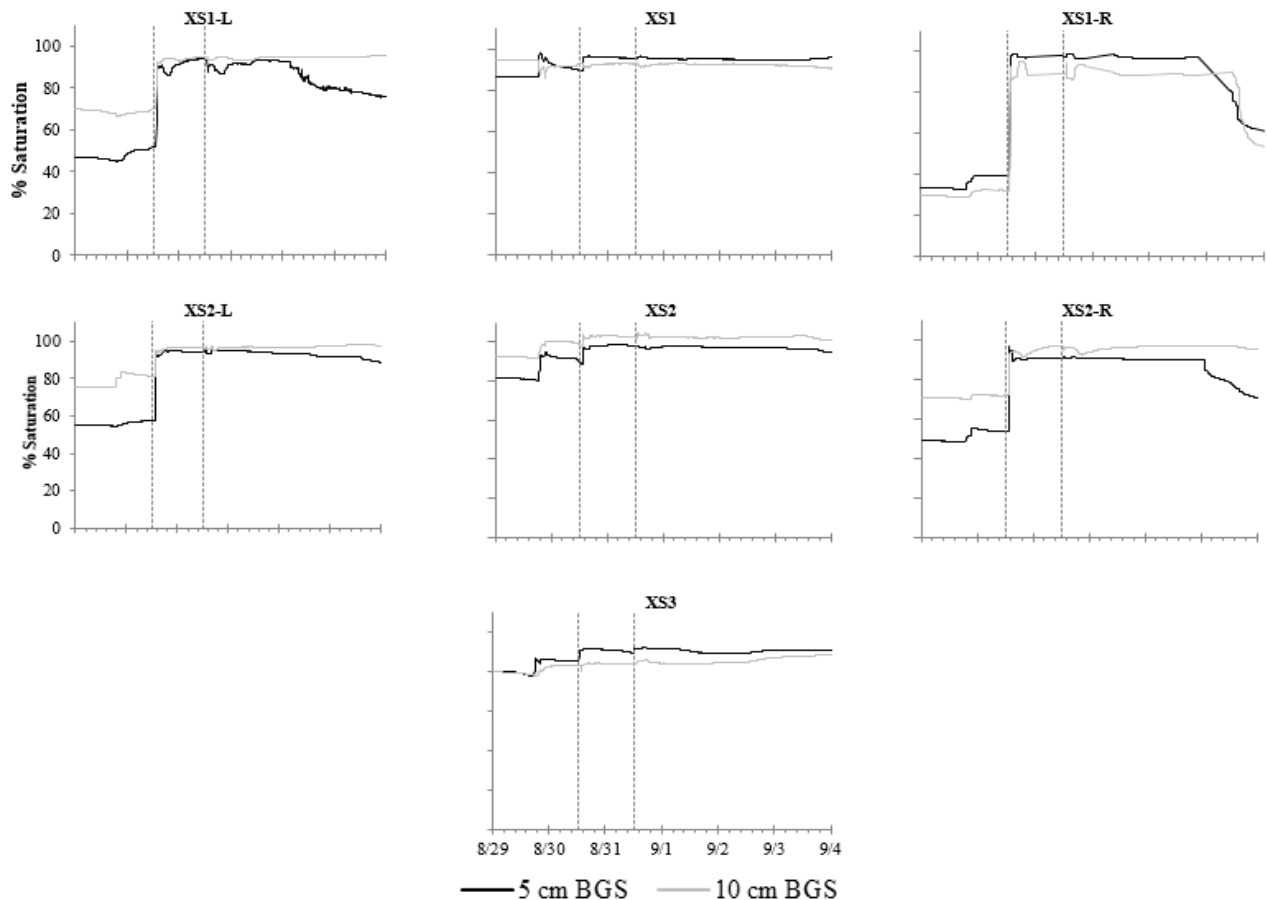


Figure B-12: Percent saturation in shallow subsurface during Late Summer flood event.

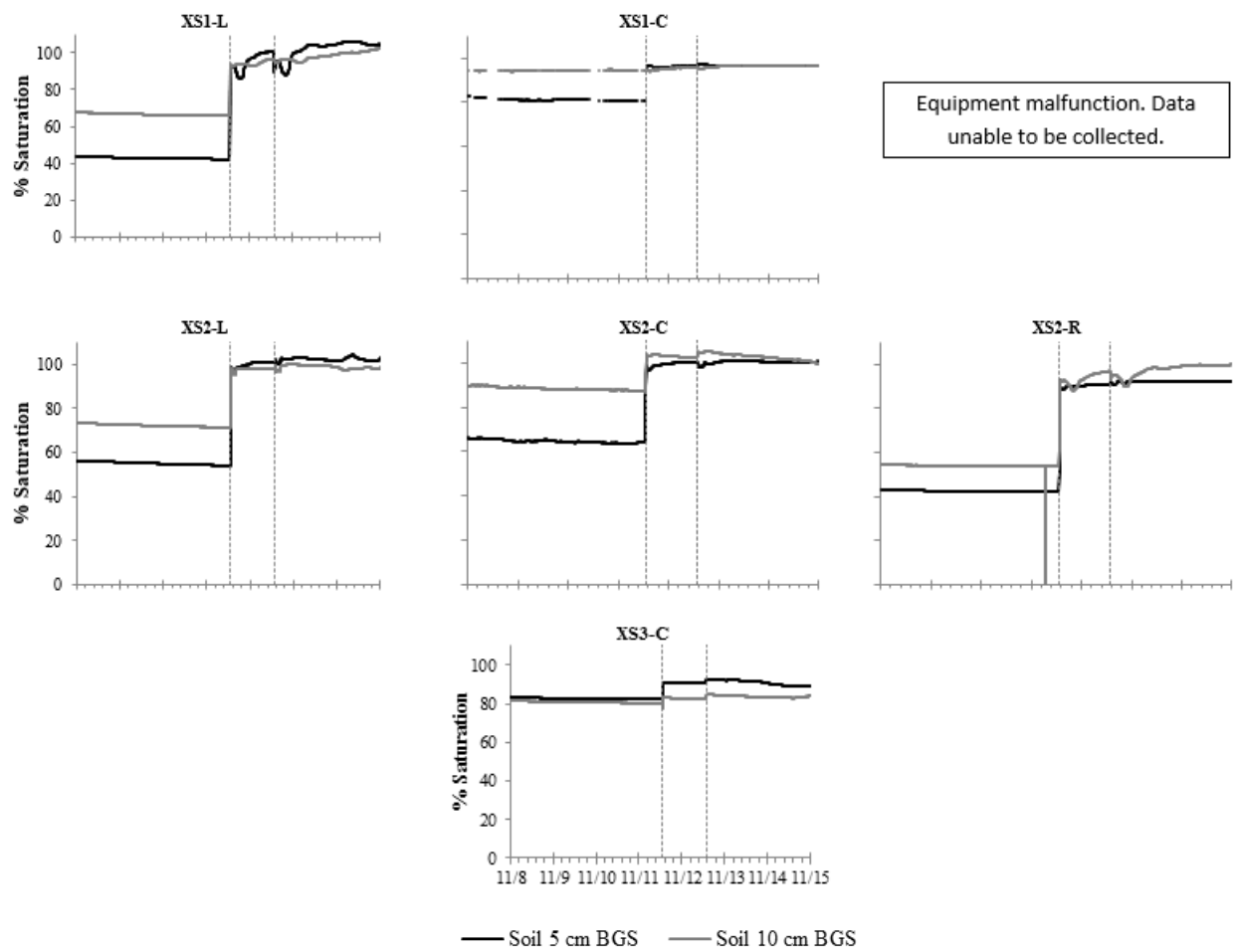


Figure B-13: Percent saturation in shallow subsurface during Fall flood event.

B.2.6 Electrical Conductivity in Surface Water and Groundwater

Electrical conductivity was measured and converted to specific conductivity in the surface water, groundwater 30 cm BGS, and groundwater 100 cm BGS along the flow centerline for each flood (Figure B-14). Results show varying SC signals in response to the application of surface water. These responses include step increases (e.g. 30 cm BGS at XS2 during Late Summer), spikes the mirror the spikes in water elevation observed at the surface (e.g. 30 cm BGS at XS1 during Spring), and no observed change (e.g. 30 cm and 100 cm BGS at XS3 during each flood).

In addition to measuring electrical conductivity in the surface water and groundwater monitoring network, additional probes which measure electrical conductivity were placed in the bypass region (Figure B-15) and along the flood centerline (Figure B-16). Particularly during the two Summer floods, a significant difference in electrical conductivity is measured in the bypass region on the second day compared to the first. When a reduction in SC is observed in the bypass region on the second day it may be a result of vegetation along the centerline being matted down.

There were noticeable differences in vegetation over the course of each flood. Vegetation was typically most dense along the centerline and less dense throughout the bypass area. The variability in SC recorded in surface water indicates that surface water flow paths were heavily influenced by vegetation conditions and not only changed seasonally but also over the course of individual floods.

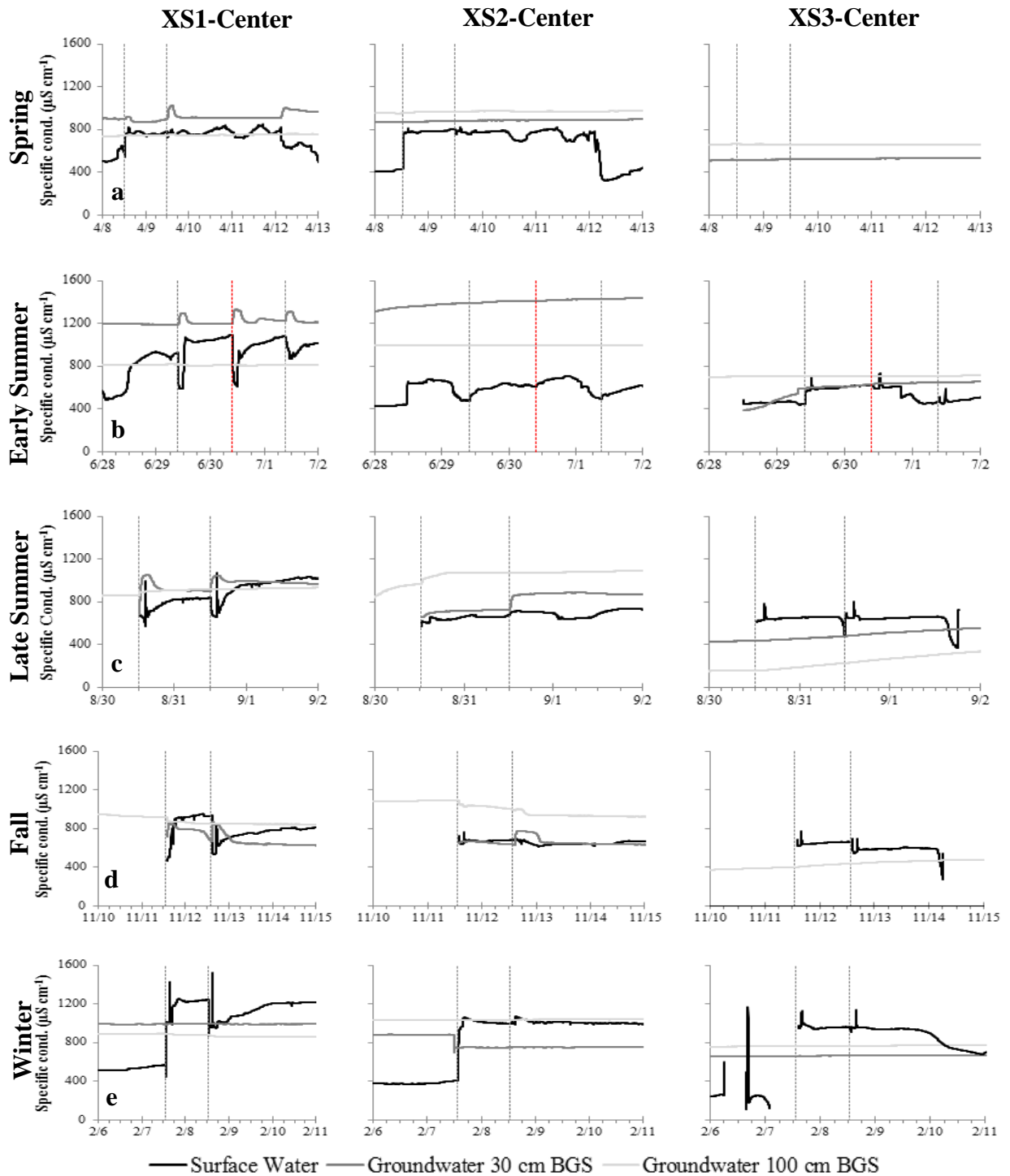


Figure B-14: Flood event electrical conductivity. The decrease in SC measured at XS2-Center-30 cm immediately preceding the first day of the Winter flood was due to changing logging intervals for the probe at that location. Lower water table elevations during the Fall flood prevented the measurement of SC in the shallow piezometer at XS3.

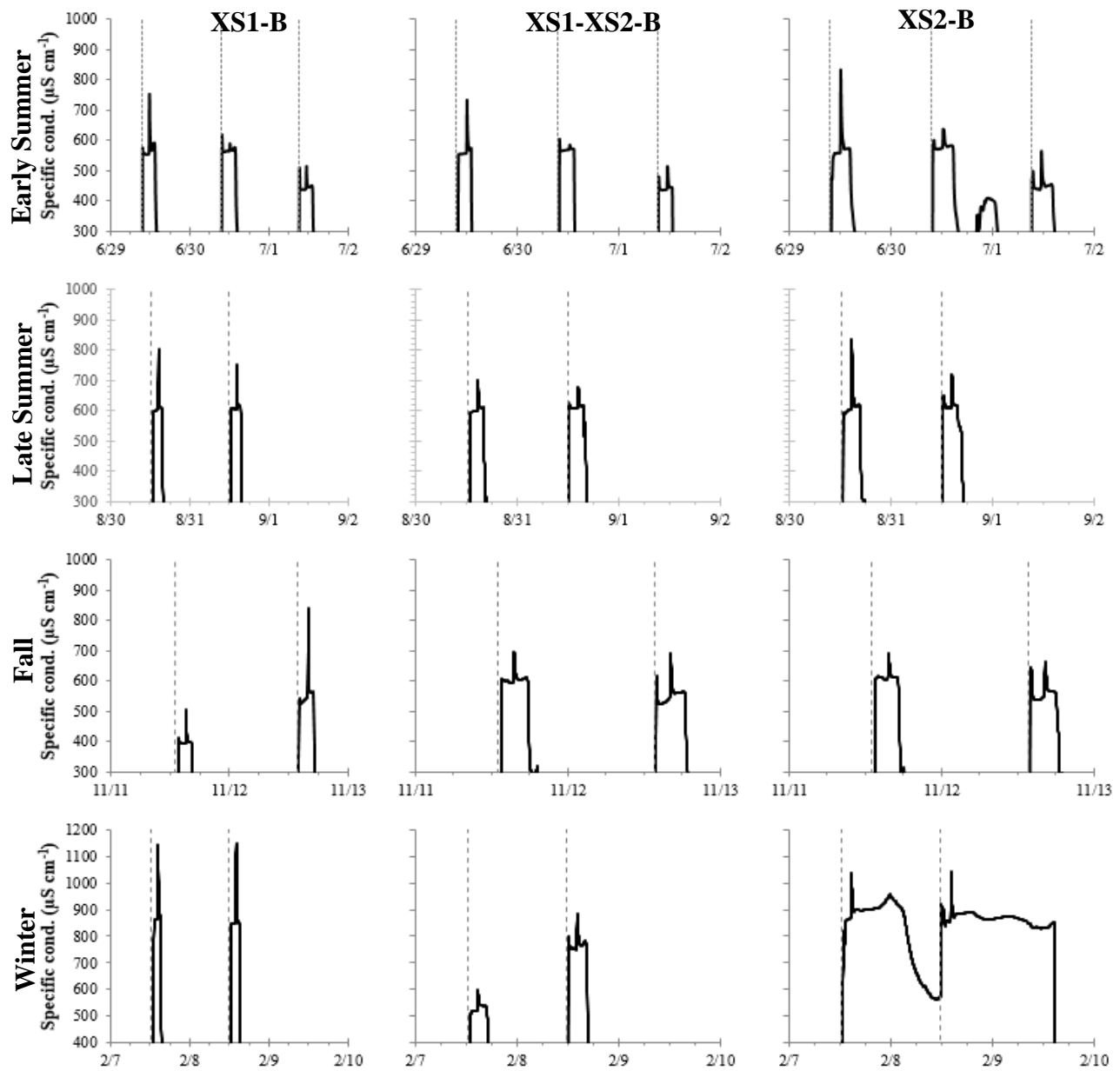


Figure B-15: Electrical conductivity measured in the bypass region.

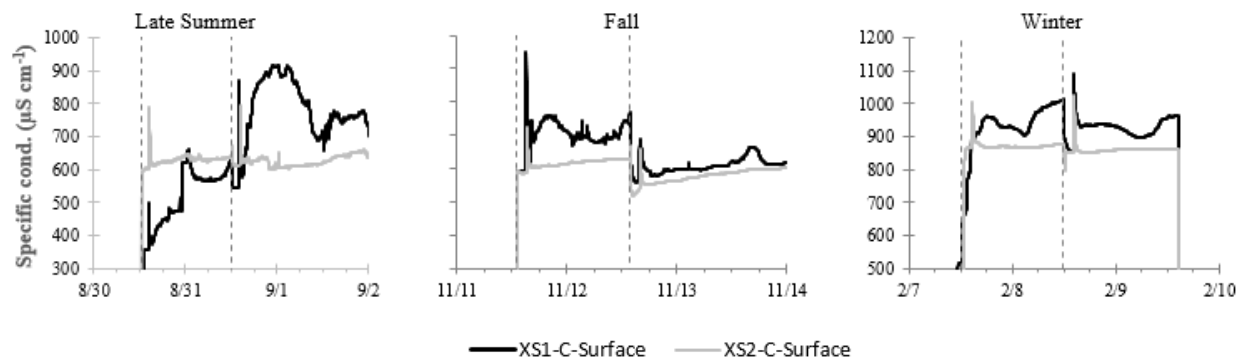


Figure B-16: Centerline Aquatroll Data.

Evidence of potential variation in surface water flow paths is present when examining surface water residence times at steady state using the time to peak electrical conductivity in surface water at XS3 following the injection of salt during each flood (Figure B-17). If flow was uniform throughout the site and consistent between floods an inverse relationship between pump flow rate and residence time would be expected. However, during the Late Summer flood pump flow rate was measured as being much greater than during the other four floods. However, rather than a decrease in residence time due to increased flow rate, the residence time is much longer. This observed difference could either be a result of the flow meter giving highly inaccurate results or a change in surface water flow paths. Distinguishing between these two potential sources of error is not feasible without verifying the pump flow rate in some way.

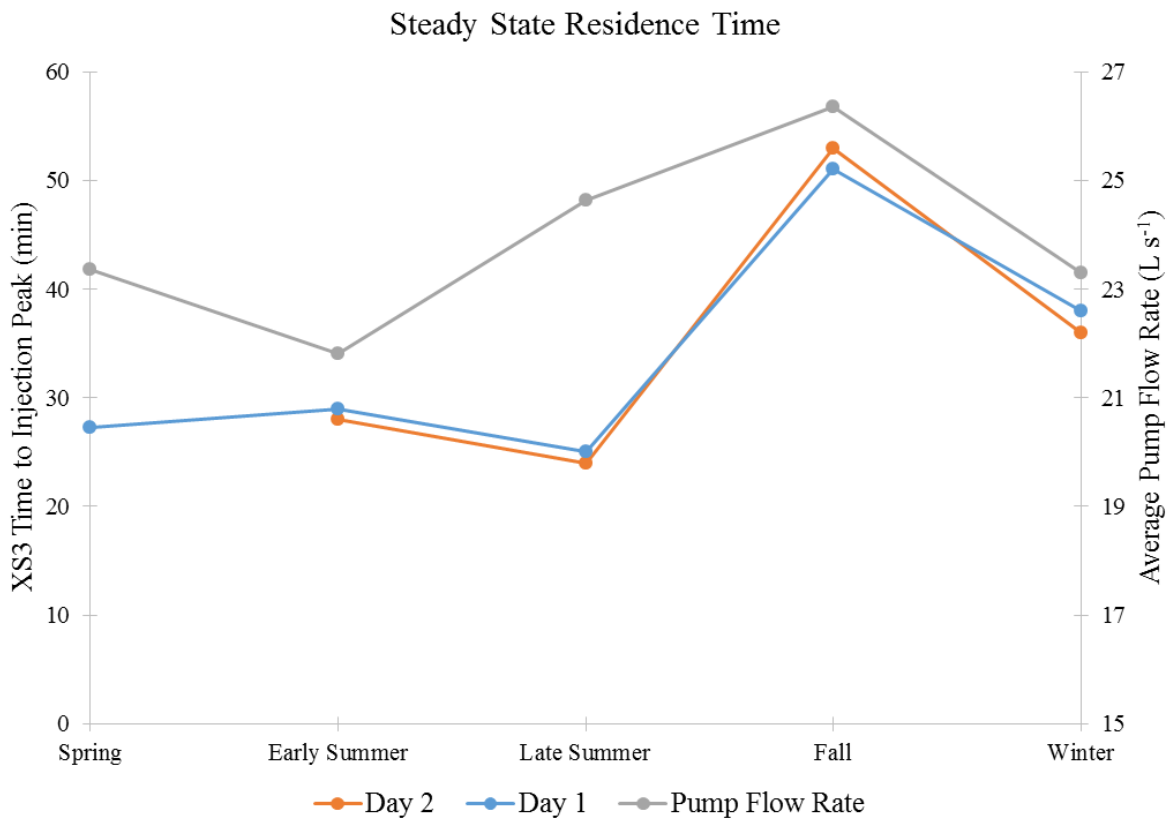


Figure B-17: Steady state residence time calculated by measuring the time required to observe the peak in electrical conductivity in surface water at XS3 following the pulse injection. Pump flow rates measured at the inlet are also included for comparison.

B.2.7 Water Temperature During Floods

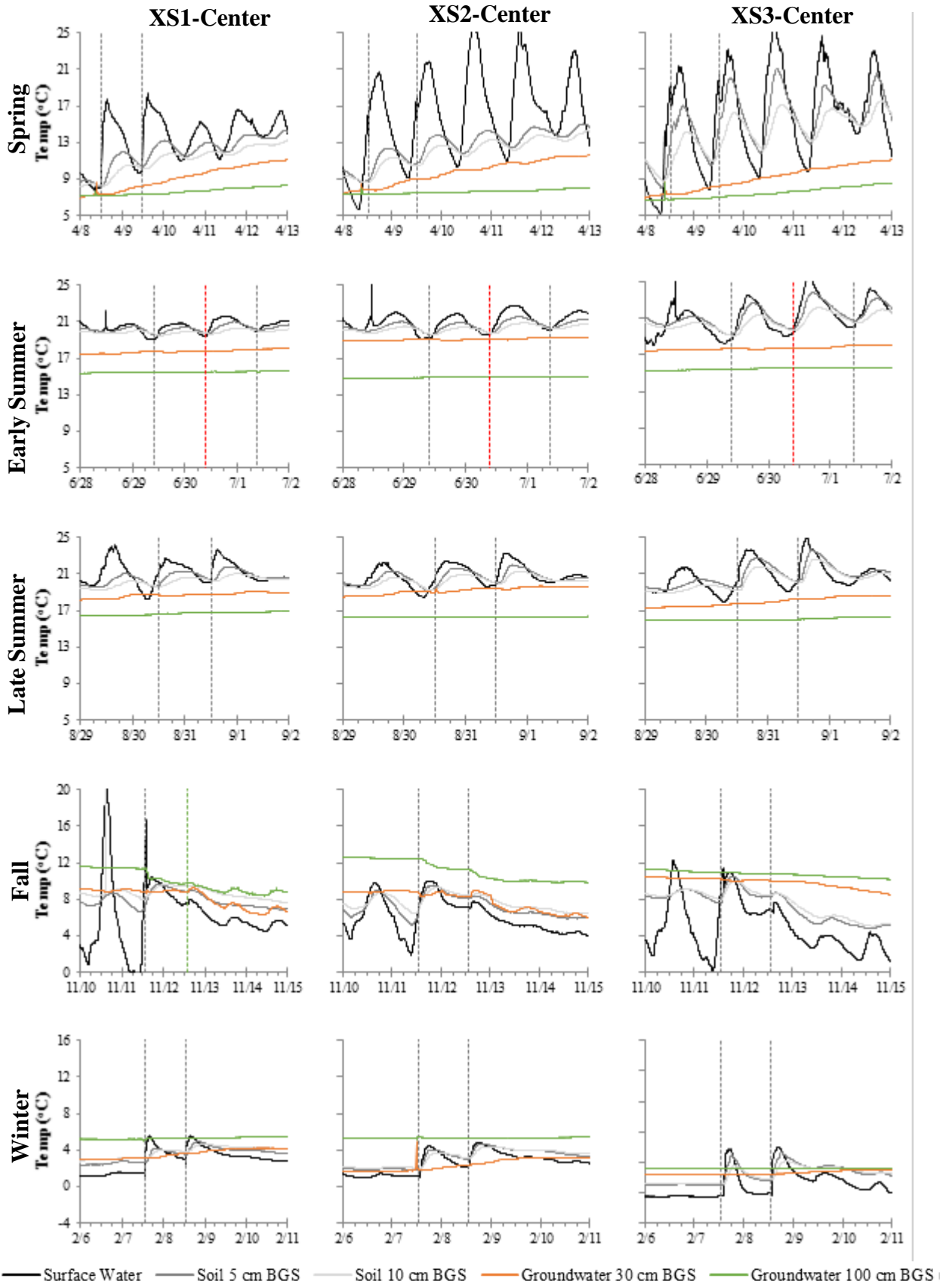


Figure B- 18: Water temperature recorded during flood events

B.2.8 Air Temperature During Floods

Comparisons in air temperature recorded at the StREAM Lab weather station show the magnitude of diurnal variation in temperature varied between seasons (Figure B-19). The air temperature explains why noticeable differences were observed in surface water during different floods.

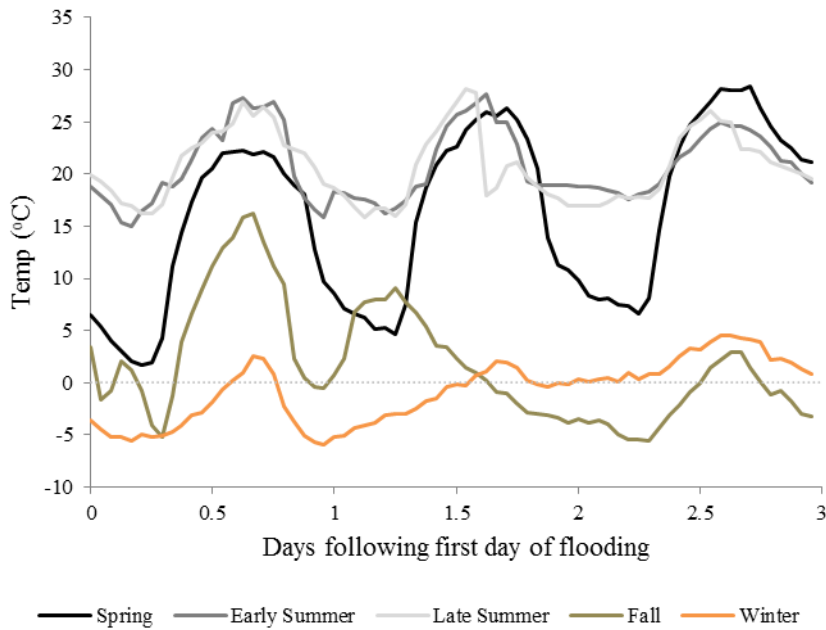


Figure B-19: Air temperature recorded at the StREAM Lab weather station during floods.

B.3 Data From Rising Head Tests

The second set of rising head tests were completed for each of the piezometers located in the swale to ensure that the increase in vertical connectivity observed over the course of the year was a result of natural processes rather than artificial connection resulting from an insufficient seal between the piezometer and ground surface. Hydraulic conductivity for each set of tests is provided above (Table 2). During the second set of tests the temperature and SC of the surface water was recorded and compared to the temperature and SC the groundwater approached during the test (Table B-1). There appears to be no clear indication of measurements of temperature and SC recorded in groundwater approaching values similar to those recorded in surface water.

Table B-1: Temperature and SC that the groundwater approached during rising head tests compared to the surface water temperature and SC.

Location	Temperature (°C)	Specific Conductivity ($\mu\text{S cm}^{-1}$)
Surface Water	3.9	621
XS1-Center-30 cm	4.4	573
XS1-Center-100 cm	5.5	684
XS1-Right-30 cm	3.4	
XS2-Left-30 cm	2.9	
XS2-Center-30 cm	3.5	695
XS2-Center-100 cm	5.5	1025
XS2-Right-30 cm	3.0	880

Appendix C: Supplemental Analyses Not Included in Journal Article

C.1 Site Characteristics

XS1 and XS2 are located in a natural topographic depression that retains water while XS3 is at a location that sheds water (Figure C-1). This topography resulted in many of the observed soil moisture and water level properties throughout the experiment duration. The percentage of time each centerline was inundated was compared between each of the three cross sections and reinforces the idea that the large storage area located near XS1 and XS2 consistently caused the presence of surface water at these locations (Figure C-2).

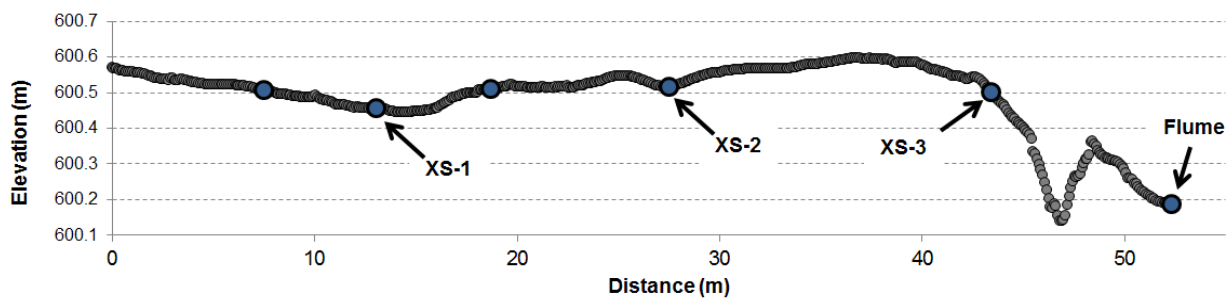


Figure C-1: Floodplain elevation along the flow centerline.

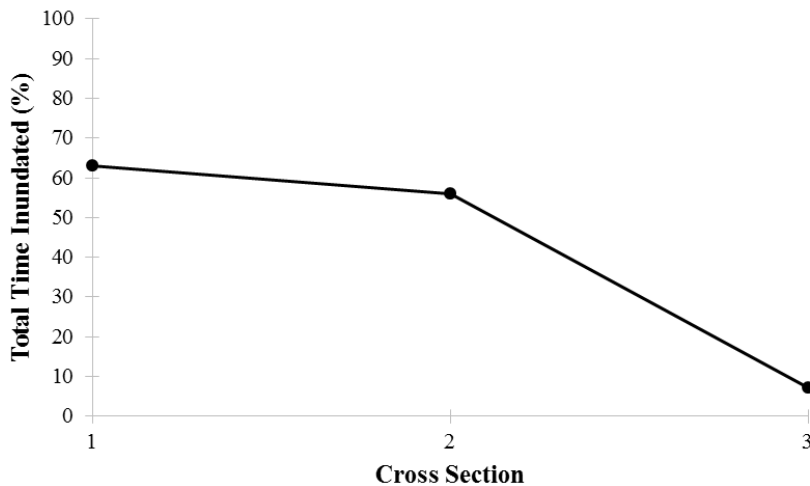


Figure C-2: Percent of the time that each cross section centerline location was inundated over the course of the year.

The topographic depression located at the site coupled with the gravel layer observed approximately 100 cm BGS provide evidence of a paleochannel beneath the flooded area. Aerial photos further show that the flood area appears to be an old meander bend of Stroubles Creek (Figure C-3) based on changes in vegetation and the shape of the swale.



Figure C-3: Aerial photo of the flood site showing changes in vegetation throughout our study site and showing that our site is likely an old meander bend of Stroubles Creek.

C.2 Storage of Flood Water

Using the flow through the parshall flume following the second day of flooding during each season we were able to calculate the recession constant for each flood (Figure C-4). Antecedent moisture conditions were assumed as constant for the second day of flooding each season. Therefore the only differences can be attributed to vegetation. In order to ensure that differences in total storage volume were not a result of slight changes in inflow discharge rate, the relationship between inflow and recession constant were compared. Recession constants were calculated by plotting the log of the water depth through the flume versus the elapsed time following the pump being turned off (i.e. $t=0$ is equivalent to three hours after the flood began). The slope of this now linearized line is taken as the recession constant.

There appears to be no significant correlation between pump flow rate and recession constant. Therefore, rather than attributing increases in total storage to pump flow rate we can claim that the pump flow rate had minimal impact and since moisture conditions were taken as being identical, the change in recession rates and total storage are assumed to be a direct result of vegetation density on the floodplain surface.

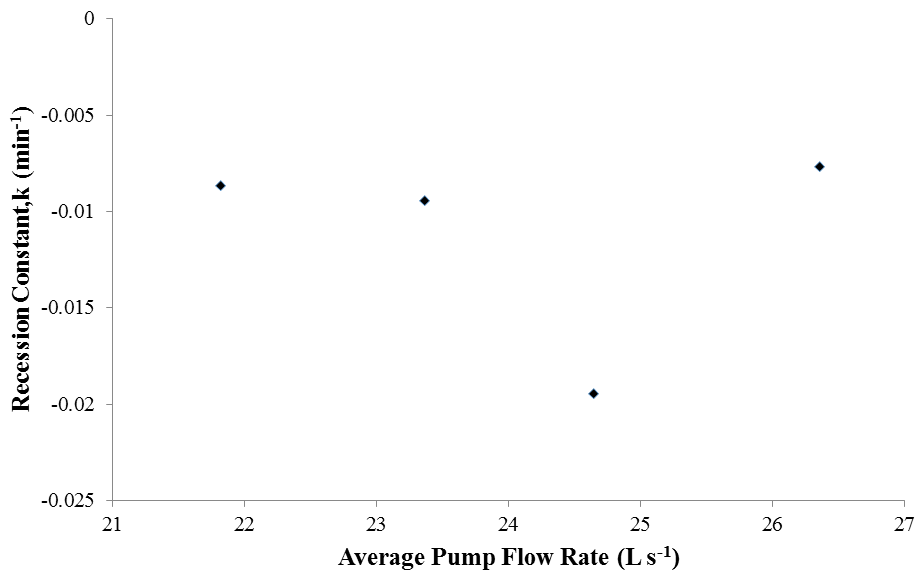


Figure C-4: Comparison of the recession constant calculated using the flow through flume following the second day of each flood (not including the Winter flood due to equipment malfunction) to the corresponding average pump flow rate.

The analysis of recession constants following the second day of flooding directly compared vegetative conditions. We also compared the total volume of stored water on the first day to the volume stored on the second (Equations 1 and 2). Season is assumed to be constant since measurements were taken on consecutive days and therefore observed difference were attributed to changes in antecedent moisture conditions. The Spring flood, which had been saturated for the months prior to the flood showed minimal change in total storage volume between the first and second day of flooding (Figure C-5). However, during the Late Summer flood when antecedent moisture conditions were low the volume of stored water was much greater on the first day compared to the second. Similar to the steady state residence times (Figure B-17), there appears to be discrepancy in the Fall flood. This again may be due to discharge measurements provided by the flow meter being inaccurate during this flood.

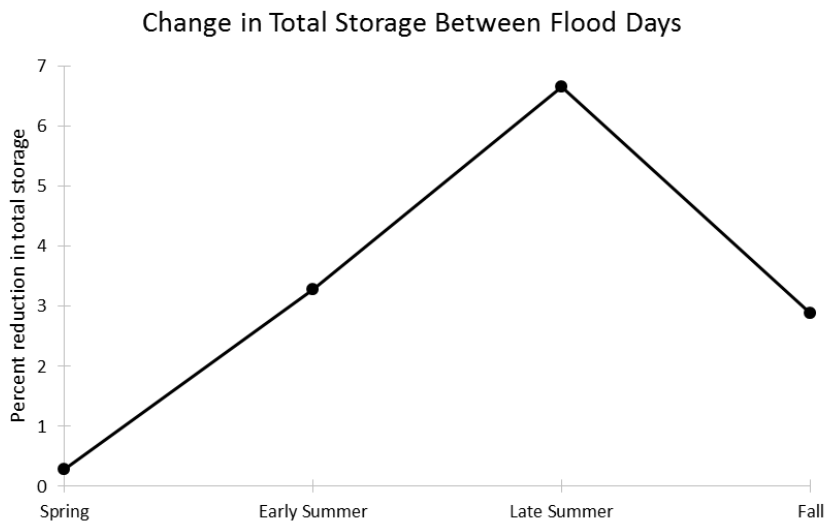


Figure C-5: Total percent of flood water stored on the first day of flooding minus the total volume of flood water stored on the second day for each flood with the exception being the Winter flood when outlet flows were not measured.